TRANSPORTATION RESEARCH RECORD 1003

International Symposium on Mechanical Properties of Special Concrete

TRB
TRANSPORTATION RESEARCH BOARD
NATIONAL RESEARCH COUNCIL
WASHINGTON, D.C. 1984

Transportation Research Record 1003
Price $8.20
Editor: Julia Withers
Compositor: Harlow A. Bickford
Layout: Theresa L. Johnson

modes
1 highway transportation
2 public transportation
3 rail transportation
4 air transportation
5 other

subject areas
32 cement and concrete
40 maintenance

Transportation Research Board publications are available by ordering directly from TRB. They may also be obtained on a regular basis through organizational or individual affiliation with TRB; affiliates or library subscribers are eligible for substantial discounts. For further information, write to the Transportation Research Board, National Research Council, 2101 Constitution Avenue, N.W., Washington, D.C. 20418.

Printed in the United States of America

Library of Congress Cataloging in Publication Data
National Research Council. Transportation Research Board.
International Symposium on Mechanical Properties of Special Concrete (1984: Washington, D.C.)
International Symposium on Mechanical Properties of Special Concrete.

(Transportation research record; 1003)
Part of the 63rd annual meeting of the Transportation Research Board held in Washington, D.C. Jan. 16-20, 1984.
1. Concrete–Mechanical properties–Congresses. 2. Reinforced concrete, Fiber–Mechanical properties–Congresses. I. National Research Council (U.S.). Transportation Research Board. Annual Meeting (63rd: 1984: Washington, D.C.) II. Title. III. Series.
TE7.H5 no. 1003 380.5 s 85-11564
[TA440] [625.8'4]
ISBN 0-309-03812-X ISSN 0361-1981

Sponsorship of Transportation Research Record 1003

GROUP 2–DESIGN AND CONSTRUCTION OF TRANSPORTATION FACILITIES
Robert C. Deen, University of Kentucky, chairman

Concrete Section
Robert E. Philleo, Consulting Engineer, chairman

Committee on Mechanical Properties of Concrete
V. Ramakrishnan, South Dakota School of Mines and Technology, chairman
Milton D. Anderson, John A. Bickley, Theodore R. Cantor, James T. Dikeou, Kurt H. Gerstle, Charles W. Josifek, Paul Klieger, Peter A. Kopac, H. S. Lew, V. M. Malhotra, Vernon J. Marks, Bryant Mather, Edward G. Nawy, Sandor Popovics, Owen Richards, John P. Roebuck, Jr., Ernie Schrader, Raymond J. Schutz, S. P. Shah, Michael M. Sprinkel, Rodney J. Stebbins, Peter C. Tatnall

William G. Gunderman, Transportation Research Board staff

The organizational units, officers, and members are as of December 31, 1983.

Contents

Addresses of Authors

Barnaby, Douglas, Department of Transportation Products, Quazite Corporation, 5515 Gasmer, Houston, Tex. 77035
Chynoweth, Gary L., Colbert Construction, Inc., P.O. Box 957, Sheffield, Ala. 35660
Dikeou, James T., Department of Business Development, Quazite Corporation, 5515 Gasmer, Houston, Tex. 77035
Fowler, David W., Department of Civil Engineering, University of Texas at Austin, Cockrell Hall 5.200, Austin, Tex. 78712
Jeniec, John D., Great Southwest Corporation, 1321 U.S. Highway 19 South, Clearwater, Fla. 33516
Josifek, Charles W., Carbon Steel Division, Ribbon Technology Corporation, 825 Taylor Station Road, P.O. Box 30758, Gahanna, Ohio 43230
Kobayashi, Tadashi, College of Engineering, Nihon University, Koriyama, Fukushima-ken 963, Japan
Macadam, David, Department of Civil Engineering, Cockrell Hall 5.200, University of Texas at Austin, Austin, Tex. 78712
MacDonald, C. N., Dow Corning Corporation, P.O. Box 1592, Midland, Mich. 48640
Meyer, Alvin H., Department of Civil Engineering, Cockrell Hall 5.200, University of Texas at Austin, Austin, Tex. 78712
Morgan, D. R., Manager, Materials Engineering Division, Hardy Associates (1978) Limited, 4052 Graveley Street, Burnaby, British Columbia V5C 3T6, Canada
Nawy, Edward G., Department of Civil Engineering, Rutgers–The State University, Busch Campus, Piscataway, N.J. 08854
Ohama, Yoshihiko, Department of Architecture, College of Engineering, Nihon University, Koriyama, Fukushima-ken 963, Japan
Paxton, James, North Pacific Division Laboratory, U.S. Army Corps of Engineers, 220 North West 8th Avenue, Portland, Oreg. 99209
Ramakrishnan, V., Department of Civil Engineering, South Dakota School of Mines and Technology, Rapid City, S. Dak. 57701-3995
Schrader, Ernest, 1255 Magnolia Drive, Walla Walla, Wash. 99362
Smith, Kevin, Department of Civil Engineering, Cockrell Hall 5.200, University of Texas at Austin, Austin, Tex. 78712
Stebbins, Rodney J., Rocky Mountain Chemical Company, 8701 Bay Pointe Drive, Tampa, Fla. 33615

Plastic and Steel Fiber-Reinforced Concrete Applications

C. N. MacDONALD

ABSTRACT

The designed properties of concrete for the use of steel or plastic fiber reinforcement are discussed. The reasons for using fiber reinforcement are cited from experience and case histories at chemical plants in various locations in the United States. The implementation techniques and applications are about repairs and original work with fiber-reinforced slabs, grade beams, and equipment and tower foundations. The benefits of using fiber reinforcement were realized in scheduling, economy, ease of placement, volume constraints, fire resistance, modulus of rupture, fatigue strength, skid resistance, durability, repairability, joint spacing, and deflection control. Histories have shown savings of 10 percent or more on projects bid against alternate designs with conventional reinforcement. Superplasticizer was vital in most cases to ease placement of the steel fiber-reinforced concrete. Field changes in some cases allowed no design changes to the concrete, and the performance has been better than expected with no adverse effects. These applications have highlighted the successful uses of plastic and steel fiber-reinforced concrete. However, there are risks from the lack of material design information that challenge the normal concrete codes and practices for design.

Fiber-reinforced concrete (FRC) is considered by many to be a new and challenging composite material. However, enthusiasm for trying a new material can either subside or soar by hearing of experiences and case histories. Most articles about fibers in concrete begin with a discussion of earlier efforts using straw in mud (1). Most of those earliest details are lost, except for one. Remember that Pharoah wanted to punish Moses by denying him straw necessary in the mud for making bricks. Even with this history, the use of fibers as reinforcement in concrete is still a new and exciting challenge and sometimes needs some defending. Examples of the enthusiasm and faith necessary for proper material applications of fiber reinforcement in concrete are imparted in this paper.

It has been suggested that the U.S. Department of Defense was the initiator of interest in fiber-reinforced concrete in the late 1950s. Regardless of the historical responsibility, most of the market from that time has consisted of individual fibers from glass and sheet steel by-products or scrap. These were commonly known as fiberglass and steel shavings. The introduction of these fibers into the concrete became a problem due to handling, balling, and uneven dispersion. The benefits in performance of the concrete were not significant enough in most cases to warrant the additional effort. Because proper design, manufacture, and construction of concrete already necessitates ample direction, the addition of fibers became just another problem to avoid.

Since 1975 the markets and applications of FRC have opened up considerably from the introduction of new technology fibers. In many cases, these fibers have displaced the old by overcoming the mix introduction problems and significantly improving performance. However, additional effort is still required for proper control. The technology has definitely not yet matured, but enough information is available for wisely choosing the proper application of FRC and then using this experience as a basis for yet further refinements.

PRODUCTS

The two fiber materials discussed in this paper are polypropylene plastic and high strength steel. Plastic fibers were available in different lengths depending on maximum aggregate size (2,3). The pre-mix fibers were collated or grouped into a bundle resembling a cigarette filter. The mechanical mixing action of the concrete unraveled this filter into a weak "hair net," which further mixing tore into individual fibers.

Steel fibers are available in different lengths depending on maximum aggregate size and design requirements (4,5). The "premix" fibers supplied by one manufacturer are available in two conditions: separate and individual fibers and those fibers collated and held together by weak glue. The availability of the fibers in these two conditions made a difference for mixability, handling, and batching operations for the job applications.

Collated fibers were chosen as much easier to handle and introduce into the mix by hand than the individual fibers. The collation and glue disappeared and the fibers were uniformly dispersed in the matrix from the mechanical shearing and mixing action of the batcher. However, some difficulty was encountered with too much glue on occasions, and balls of collated fibers were found. When these balls were broken apart or if the bag of collated fibers was shaken to ensure individual collated bundles, there were no problems with dispersion.

The single fibers were not used as they were expected to be more difficult to handle and more difficult to introduce into the mix. Single fibers have been observed to be much more prone to mechanically interlock and ball together before mix introduction (6).

The preferred way for mix addition depended on the job site conditions. The collated fibers could be added in bulk at the plant or on the site. Because some of the literature on single fibers indicates that fibers are best added by sprinkling or by a measured addition rate, this additional equipment, manpower, and scheduling problem was avoided by using collated fibers.

Fibers were introduced in two ways: (a) at the batch plant with mixing done en route and (b) at the job site with a specified time for mixing. The choice of where mixing occurred was determined by scheduling, safety, and ensuring the quality of the concrete before the fibers were introduced.

The steel fiber concrete usually had similar amounts of aggregate and sand, with a high cement content. The reason for these mix proportions was to ensure the bonding, locking, and contact of the fibers in the concrete matrix.

No modification of the mix for workability was necessary according to both the plastic and steel fiber manufacturers. The plastic fiber manufacturers acknowledged a loss in slump due to the fiber. However, their reasoning for not modifying the mix was that the loss in slump would be 1.5 to 2.5 in. (3.8-6.4 cm) but the real loss in workability would only be about 0.5 in. (1.3 cm). The significance of this 0.5-in. (1.3-cm) difference was evidently of concern to their marketing department.

The steel fiber manufacturers also acknowledged a loss in slump but hesitated to recommend another product to cure an "ill" of their product. The usual loss in slump was about 2 to 3 in. (5 to 7.6 cm).

The project engineer's concern has been with the quality of the concrete, which, in most cases, has always been a direct function of the amount of water. Experience showed that when a finisher saw a low slump concrete, it made no difference to him whether the link between slump and workability was apparent or real, the water was usually added. For this reason, the slump and water content needed to be determined and fixed with no field adjustment allowed except by special approval. The desired slump was first obtained with the understanding that there would be a subsequent loss in slump after the fibers were introduced.

The generally accepted key to fiber performance in concrete has been bonding and dispersion in the matrix. The use of a superplasticizer easily overcame the problem of water addition by providing flow, workability, and the ensured cement dispersion in the matrix. The superplasticizer improved the bonding and performance of the fibers because of the improved contact with the other materials by easier mixing, dispersion, and less working into position. The less working into position ensured that the fibers were positioned homogeneously and were not moved out of a plane due to the insertion of a tool through the matrix. The finished plastic or steel fiber concrete appeared "hairy" from a very close examination of most applications.

PROPERTIES

As always, the mechanical performance objectives of a material needed to be cost-optimized, and fiber-reinforced concrete was no different than any other material considered in a project application.

Some properties are presented in Table 1 as a summary of comparisons between fiber-reinforced and conventional nonfiber concrete. These properties are, from application experience, supported by actual testing and field observation of performance since 1979. The exact values of these properties are cited and compared in other technical literature. However, the relative values are important in material selection.

TABLE 1 Property Comparison Index[a]

Property	Plastic FRC	Steel FRC
Compression	1.05	1.15
Flexure	1.10	1.35
Impact	>1.00	100.00
Toughness	5.00	20.00
Fatigue	>1.00	1.90
Permeability	<1.00	<1.00
Durability	>1.00	>1.00

[a]Non-FRC concrete has an assumed index of 1.00.

DESIGN

Structural design using FRC was based on well-defined purposes for the application. Several related project objectives always influenced the material and property selection best suited for the particular application. Summaries of design features using FRC compared to non-FRC for these three project issues, cost, schedule, and performance, are given in the following sections. The information has been obtained by reasoning and from experience with more than $2 million in work on various projects within chemical plants in the United States. The applications were for slabs, grade beams, and equipment and tower foundations.

Cost

- Steel fibers added $50 per cubic yard ($65 per cubic meter) of concrete material.
- Plastic fibers added $10 per cubic yard ($13 per cubic meter) of concrete material.
- Superplasticizer for workability added $5 per cubic yard ($6.50 per cubic meter) of concrete material.
- Concrete volume was reduced because of reduced sections from improved strength properties.
- Temperature and shrinkage reinforcement was eliminated.
- Some load carrying or strength reinforcement was spaced wider or eliminated by using steel fibers.
- Thinner slab thicknesses because of improved strength properties allowed a reduced amount or less expensive fill material.

Schedule

- Smaller volume amounts of concrete material were used as a result of improved strength properties and therefore allowed: (a) greater surface area for unit volume and therefore faster placement, (b) smaller forms and easier removal or repositioning for faster setup, (c) less excavation time for faster job starts, and (d) reduced access time for trucks, eliminating placement crew waits.
- Superplasticizer speeded up placement and eased workability.
- Superplasticizer reduced or eliminated time spent positioning reinforcement before and after FRC placement.

Performance

- Greater reliability and assurance about reinforcing placement especially with slabs on grade when compared with welded wire fabric.
- Dependence on many individual fibers instead of a few bars.
- More homogeneous behavior and action due to dispersion of reinforcement throughout section.
- Increased joint spacing and less sawing for slabs.
- Higher ultimate strength.
- Better textured surface from fibers at surface for adhesion of coatings, patches, or repair.
- Less piece fracturing or fragmentation resulting in easier removal or modifications to slabs for inserts.
- More ductility to resist unspecified or unanticipated loads.

- More skid or slip resistance due to the texture of the concrete from the fibers at the surface controlled more or less by finishing.
- Extended performance life rather than replacement due to load carrying after initial cracking.
- Less displacement, chipping, and spalling due to more homogeneous reinforcing.
- Availability of a more homogeneous corrosion-resistant material and less micro cracking with reduced permeability. A corrosive exposure to fibers in concrete results in the loss of fibers at that specific location. This is due to their discrete size, orientation, and non-connection to the rest of the concrete beyond the immediate location of corrosive exposure.

The analysis for design using FRC required in many cases the artistic engineering balance between project objectives and the material properties. This may appear intuitively obvious for all structural materials following form and function. However, many of the problems were with finding the material properties of FRC. Not enough empirical or analytical data were available (7).

As an example, consider the design requirement for ACI 318-77 for temperature and shrinkage steel reinforcement. The concepts of reinforcing and bonding are from a surface area, mass, and cross-sectional area relationship. From this, a conventional slab design might allow an 8-in. (20.3-cm) thickness, two layers of wire fabric, and a 20-ft x 20-ft (6.1-m x 6.1-m) size for joint spacing. Steel fiber-reinforced concrete has performed as well as this conventional design with a 3.5-in. (8.9-cm) thickness and a 40-ft x 60-ft (12.2-m x 18.3-m) size for joint spacing. However, there are no formulas available to guide the engineer in comparing conventional concepts of reinforcing and bonding with the fiber design. Consequently, an empirical artistic approach was taken in most cases.

Because an increased joint spacing was possible with the steel FRC, special attention was paid to the joint design and materials used. The materials used to seal the joints needed in most cases to have good weatherability, be easy to install, and cure quickly. Field observation of the 3.5-in. (8.9-cm) thick slab showed excessive joint movement. Fortunately, the joint material chosen could withstand this extension and compression movement (8).

Fiber manufacturers have been extremely helpful for most common design properties. They also usually have some technical pioneers to consult with about what could be expected in various applications. However, because of the variability of concrete in general, FRC property tests are strongly recommended in the locale of the application because the expectations and test results were not always in agreement.

SPECIFICATIONS

Some specification information was available from the fiber manufacturer and other sources concerned about writing specifications (9). However, guide-, edit-, and delete-type specifications have not yet been generally available. Additional information for design, specification, and construction was obtained from national professional organization publications.

A "first" project seriously considering the use of FRC always appeared to cause uncertainty with everyone involved. Confidence was obtained by placing FRC in the project locale in a small noncritical performance application. This first-hand experience was usually after, or even rather than, a controlled laboratory example. The field experience was recorded with slides or video tape. These visual records were then used with samples and brochures from the fiber manufacturers. This experience, the recording of it, and other information was used in several ways for the benefit of the present and future project applications of FRC by the engineer, owner, concrete producer, and contractor. A simple example of an advantage to this approach was reduction of the uncertainty factor added on to a bid price by a contractor unfamiliar with FRC.

ACKNOWLEDGMENT

Dow Corning has supported this author's interest in fiber-reinforced concrete beyond what would normally be expected of an employer. Several people at Dow Corning and in the community have cooperated with a patient wait-and-see attitude concerning the many aspects of applying fiber reinforced concrete. The fiber manufacturers have contributed much with their field assistance and the resources of their technical pioneers.

REFERENCES

1. American Concrete Institute. State-of-the-Art Report on Fiber Reinforced Concrete. Concrete International Design and Construction, May 1982, pp. 9-30.
2. Fibermesh Company. Fibermesh. Chickamanga, Ga., 1983, 4 pp.
3. Forta Fibre, Inc. Forta Fibre® Fact-Data Sheet. Grove City, Pa., 1983, 4 pp.
4. Ribbon Technology Corporation. Technical Data for Xorex Steel Fiber Reinforcement for Concrete. Gahanna, Ohio, 1983, 4 pp.
5. Bekaert Steel Wire Corporation. The Miracle in the Mix, Dramix® Steel Fibers. Niles, Ill., 1982, 12 pp.
6. V. Ramakrishnan, T. Brandshaug, W. Coyle, and E. Schrader. A Comparative Evaluation of Concrete Reinforced with Straight Steel Fibers and Fibers with Deformed Ends Glued Together into Bundles. American Concrete Institute Journal, May-June 1980, pp. 135-153.
7. M.A. Ghalib. Moment Capacity of Steel Fiber Reinforced Small Concrete Slabs. American Concrete Institute Journal, July-Aug. 1980, pp. 147-157.
8. Dow Corning Corporation. Installation Guide for Dow Corning® 888 Silicone Highway Joint Sealant. Midland, Mich., 1983, 16 pp.
9. A. Koller. The Magic in the Mix--Fiber Reinforced Concrete. The Construction Specifier, Construction Specifications Institute, Alexandria, Va., Dec. 1982, pp. 44-55.

Superplasticized Fiber-Reinforced Concretes for the Rehabilitation of Bridges and Pavements

V. RAMAKRISHNAN

ABSTRACT

The most critical problem facing the highway industry is the rehabilitation of its distressed structures, particularly concrete bridge decks and pavements. Various forms of distress have occurred in some of the surfaces and different rehabilitation procedures can be very costly. There is a need to determine the most effective and the most economically advantageous means to rehabilitate the damaged concrete bridge decks and pavements. An investigation sponsored by the U.S. Department of Transportation has been completed at the South Dakota School of Mines and Technology to develop a tough, high-strength, high-density, durable concrete for bridge deck construction; and a medium-strength, flowing, structural concrete through the use of superplasticizers and steel fibers. The study was conducted in two phases. The first investigated the basic properties of concrete made with superplasticizers through the use of experimental mixtures conforming to the requirements dictated by statistically valid factorial designs, so that analysis of variance can be used in the evaluation. The second phase extended the findings into an evaluation of superplasticized concrete containing steel fibers. The study has been completed and the significant results are presented in this paper. The addition of the special type of steel fibers (with deformed ends and glued together into bundles with a quick water soluble adhesive) to superplasticized concrete greatly increased its ductility, toughness, impact resistance, ultimate flexural strength, post-crack load-carrying capacity, and shock resistance. The fiber-reinforced superplasticized concrete also had higher freeze-thaw durability and lower permeability. These improvements were achieved without a reduction of workability or the usual balling of steel fibers in the plastic concrete. Therefore, the fiber-reinforced superplasticized concrete is an almost ideal material for the rehabilitation of bridge decks and highway pavements, and for construction of other concrete structures.

The causes of concrete deterioration are many and varied. In general, concrete not properly designed, prepared, installed, finished, or cured is more susceptible to those deleterious influences that cause the concrete to deteriorate and spall and the reinforcing to rust and lose section. This, in turn, reduces the structural sufficiency and ultimately results in failure. Corrosion of reinforcing steel is the major cause of deterioration in bridge decks, beams, caps, columns, abutments, wing walls, and underdecks. Due to increasing heavy traffic, use of de-icing salts, freeze-thaw cycles, studded tires, and various other fatigue, surface deterioration and failures are beginning to show up on the bridge decks and pavements. Rehabilitation of bridges is one of the most critical problems facing the highway industry. Therefore, there is a need to find the most effective and most advantageous methods to rehabilitate the distressed concrete bridge decks and pavements.

The author was given a contract by the U.S. Department of Transportation to develop a tough, high-strength, high-density, durable concrete for bridge deck construction and a medium-strength flowing structural concrete through the use of superplasticizers and steel fibers (1). The study was conducted in two phases. In the first phase, an extensive investigation of superplasticized concretes (both flowing concrete and high-strength concrete) was completed (2,3), and the second phase extended the findings into evaluation of superplasticized concretes with new types of steel fibers. Highlights of this research are presented in this paper.

SUPERPLASTICIZED CONCRETE

Concrete having desirable properties in the hardened state is normally made with a low water-cement ratio and with the least possible amount of cement paste in the mix. Such a concrete usually has a low slump and requires intensive and careful compaction such as the high-density, low-slump concrete used in the Iowa Method of bridge deck resurfacing. In order to produce concrete of the same quality but requiring less vibration, very effective plasticizers, known as superplasticizers, have been developed for making flowing and self-compacting concrete. Superplasticizers are added to concrete to cause a vast increase in its workability to allow a large reduction in mixing water, and thus produce high-strength concrete. Such a change in concrete properties would result in reduced placement costs or reduction in the cement requirement. A well-designed mix with superplasticizer will have good flowability and sufficient cohesiveness and would not cause bleeding or segregation or strength reduction either during or after placing of the concrete.

The introduction of superplasticizers has opened up new possibilities for the use of concrete in construction, particularly for bridge-deck repair and resurfacing, pavement rehabilitation, and construction of other highway facilities.

EFFECTS OF SUPERPLASTICIZERS ON FRESH CONCRETE

The results reported in this paper are based on the work done by the author using the following two types of superplasticizers: sulfonated naphthalene formaldehyde condensate and sulfonated melamine formaldehyde condensate. The results obtained have established certain real advantages, economical as well as technical, that can be gained by the controlled and proper use of these admixtures (1-4). Compared to the corresponding normal concrete, the concrete with the addition of superplasticizer has good flowability, excellent cohesiveness, less bleeding, no segregation, better pumpability, and lower pumping pressure. The entrained air content of fresh superplasticized concrete decreases with time.

Superplasticized concretes exhibit large increases in workability (slump). Because slump loss is an inherent property of concrete, this increase in slump is of short duration, and within 30 to 60 min, the concrete loses its increased workability. The rate of loss of slump depends on the type of superplasticizer, its dosage rate, temperature of the concrete, the humidity, and the type of cement. Figure 1 shows typical slump loss with time curves for a particular mix with different concrete temperatures. The increase in temperature increases the rate of slump loss. The mixes made at lower temperatures had higher initial air contents and high slumps whereas mixes made at higher temperatures had very low air contents and low slumps.

Although useful trends can be deduced from such visual examination of the slump loss curves, more quantitative parameters are needed. Two such parameters that have been found useful are "slump window" and "total working time." "Slump window" is defined as the time taken for the slump to decay from 76 mm to 25.4 mm and would be useful to those interested in slipform operations in which high slumps could not be tolerated. The "total working time" is defined as the time needed for the slump to go from the initial value to 25.4 mm. These two parameters are plotted in Figure 1.

The rapid loss of workability with time is considered a serious drawback. A delay in the discharge of concrete from truck mixer could cause stiffening to the point of unworkability and loss in air content thus affecting the desired air-void system. However, this disadvantage can be minimized or mitigated by retempering (adding additional dosages of superplasticizer and air entraining agent). The large increase in workability and the desired air content can be maintained for several hours by the addition of a second and third dosage as shown in Figure 2. The second and third dosages used were less than the initial dosage. The slump after initial mixing was 220 mm, whereas the slump after the first and the second retempering was 191 mm. The rate of slump loss was low and the time taken to reach a workable slump of 51 mm after each retempering was 3.5 hr. Overdosing of superplasticizer should be avoided because this can cause segregation.

EFFECT OF SUPERPLASTICIZERS ON THE PROPERTIES OF HARDENED CONCRETE

With the addition of superplasticizers, water reductions of up to 20 percent can be achieved in the manufacture of concrete. This causes an increase in mechanical properties such as compressive strength, flexural strength, and modulus of elasticity. This increase in strength is generally proportional to the reduction in the water-to-cement ratio. The ability of superplasticizers to reduce water and achieve very high strengths is of special importance for the concrete repair and rehabilitation work where high early strengths are needed. In some cases, the concretes with superplasticizers had shown higher strengths at earlier ages than the reference concretes, indicating an increased rate of strength development at early ages.

The study has shown that the shrinkage of superplasticized concrete is equal to or less than the shrinkage of reference concrete. The concrete with the superplasticizers has approximately the same creep as the reference concrete. The study has shown that the addition of superplasticizer does not affect the relationship between the accelerated strength and 28-day compressive strengths. The modified boiling test, ASTM C684, was the accelerated strength test used in the study.

In cold regions, the resistance of concrete to freeze-thaw cycling is important. Therefore, for concretes used in the cold regions, an air entraining admixture is added to entrain air bubbles of the required sizes. These air bubbles provide the satisfactory freeze-thaw durability of the concretes. An extensive investigation has shown that the concretes with superplasticizers have adequate freeze-thaw durability in spite of the larger bubble sizes found

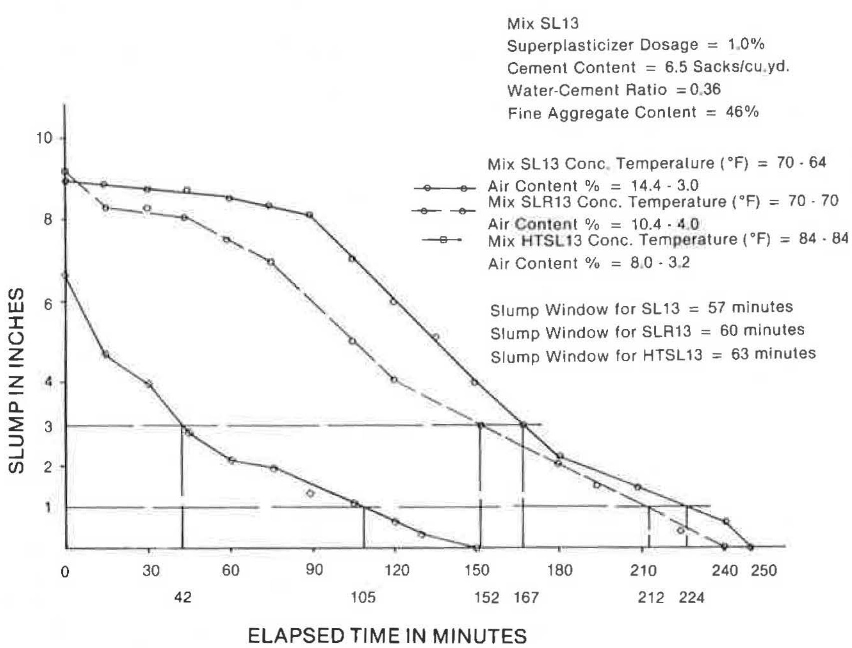

FIGURE 1 Slump versus time.

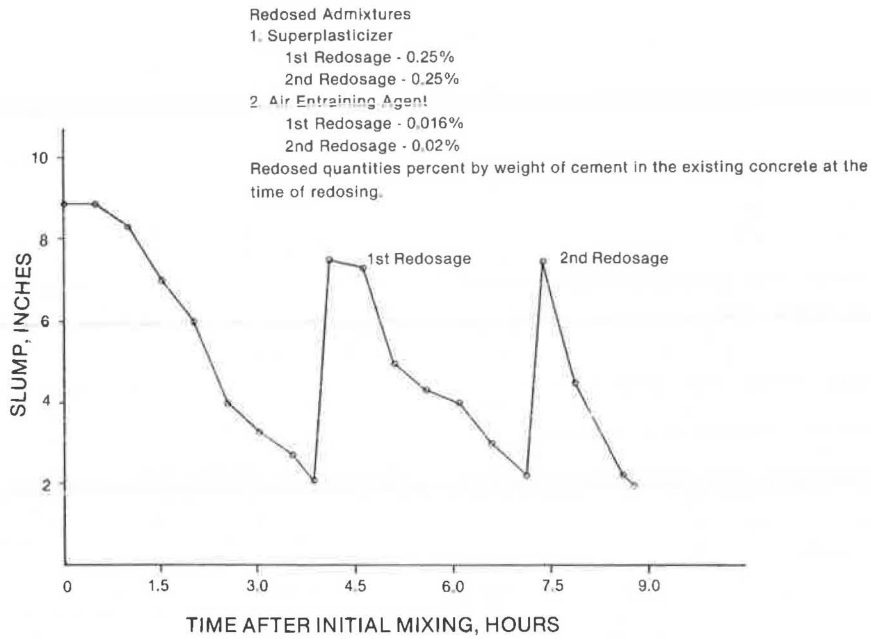

FIGURE 2 Slump-time-retempering study for Mix RTP13.

in some concretes. The superplasticized concretes had performed equally well in the de-icer scaling test recommended by ASTM.

In general, the study has shown that with the addition of superplasticizers, it is possible to produce a very highly workable concrete, which is known as flowing concrete, without any detrimental effects either in the plastic or in the hardened states. It is also possible to produce extra high-strength concretes (80 to 100 MPa) with a low water-cement ratio (0.25 to 0.28) and high workability.

SUPERPLASTICIZED FIBER-REINFORCED CONCRETE

High-strength concrete is being increasingly used in the repair and rehabilitation of bridges (particularly overlays), buildings, and other reinforced and prestressed concrete structures. One major drawback of high-strength concrete is that it is brittle and leads to a sudden and explosive type of failure. The failure will be catastrophic, particularly in structures that are subjected to earthquakes, blast, or suddenly applied loads. An ideal solution to overcome this serious disadvantage of high-strength concrete is to add steel fibers in the concrete. It is well-established (4-7) that the addition of steel fibers greatly increases the ductility, energy absorption capacity, and ultimate strain capacity of the concrete. Fiber reinforcement considerably increases the ultimate flexural strength, the post-crack load-carrying capacity, impact resistance, shear and torsional strength, fatigue strength, shock resistance, and failure toughness. However, the main problems associated with fiber concrete are fiber balling and inadequate workability. Balling of fibers in the mixer prevents uniform distribution and also causes problems when the concrete is placed. Fiber balling and consequent inadequate mix workability imposes an upper limit beyond which increase in strength and other properties are no longer realized when using conventional mixing procedures.

To remedy the problem of fiber balling, a new type of fiber (several fibers with hooked ends glued together side by side with water soluble adhesive) were used with successful results, and a superplasticizer was used to increase workability adequately. The addition of fibers and superplasticizers proved to be an ideal combination to produce high-strength ductile concrete.

The hooked fibers used in this project are glued together side by side into bundles with a water-soluble adhesive. These fibers are made from low carbon steel wires, and have a nominal length of 52 mm and a diameter of 0.5 mm. The bundling of fibers creates an artificial aspect ratio (the ratio of length to diameter of the wires) to approximately 30 when introduced to the mix. When the glue is dissolved by the water in the mix, the fibers will be separated as individual fibers with an aspect ratio of 100. These hooked fibers are commercially known as Dramix.

The basic properties of superplasticized fiber-reinforced concretes were investigated through the use of 47 experimental mixes conforming to the requirements dictated by statistically valid factorial design so that analysis of variance could be used in the evaluation. Using a statistical model (the central Rotatable Composite Factorial Design), four major factors--water-cement ratio, cement content, fiber content, and superplasticizer dosage--were investigated. The statistical analysis determined the effect of these factors and their mutual interactions on the different response variables workability (slump, vebe time, and flow table spread), plastic unit weight, compressive strength, and flexural strength. The developed prediction equations were used to construct a set of curves for a variety of levels of the four independent variables to readily obtain the estimate of compressive strength, flexural strength, slump, flow table spread, and vebe time (1).

For the same water-cement ratio, an increase in superplasticizer dosage caused considerable increase in slump and air content. With higher cement content (390 kg/m^3) and higher superplasticizer dosage (1.2 percent), it was possible to achieve up to 200 mm of slump at low water-cement ratios (0.30) without any segregation. The measured slumps for superplasticized fiber-reinforced concrete was slightly less when compared to the values of superplasticized concrete without fibers.

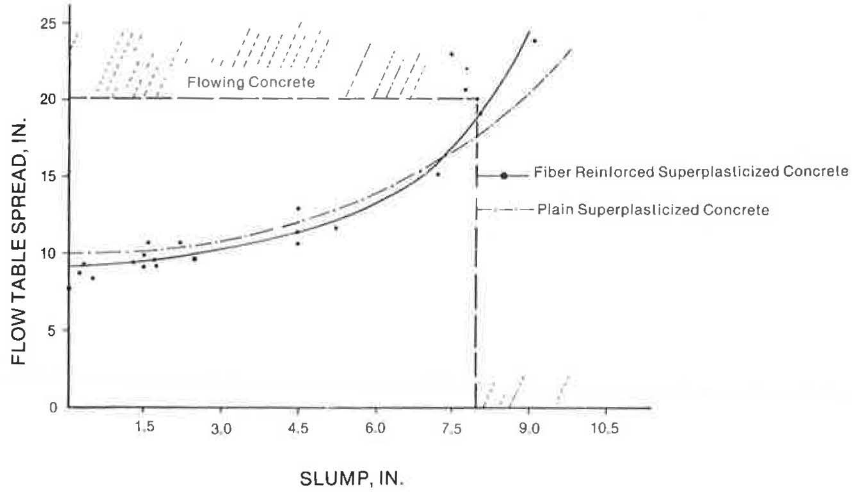

FIGURE 3 Relationship between slump and flow table spread.

The hooked fibers performed well during mixing because no balling occurred in almost all the mixes except for mixes with zero slumps and high fiber contents, even though the fibers were charged to the mixer all at one time along with the aggregates. This must be taken as the consequence of low aspect ratio created by the collating of the fibers. It took approximately 1.5 min for the glue to dissolve and for the fibers to separate. Of the workability tests commonly used, the slump test is the most sensitive indicator of change because the range covered is so large. However, the flow table test conditions are closer to the real placing situation and, consequently, a more realistic indicator of workability for flowing concrete than the slump test. The relationship between slump and flow table spread for plain and fiber-reinforced superplasticized concrete is shown in Figure 3. These two curves show only a small difference between them; the relationship between slump and flow table spread is approximately the same for both superplasticized concretes, with and without fibers.

Concrete with superplasticizer added and having a slump of 200 mm (7.9 in.) or greater and a flow table spread within the range 510 to 620 mm is classified as a flowing concrete. Flowing concrete should not exhibit excess bleeding or segregation. Other terms used to describe the flowing concrete are: self-compacting concrete; flocrete; soupcrete; and liquid, fluid, and collapsed-slump concrete. This study has shown that it is possible to produce flowing fiber-reinforced concrete.

Unlike those for plain superplasticized concretes, the measured vebe times were quite high for superplasticized fiber-reinforced concretes. For superplasticized fiber-reinforced concrete mixes with zero slumps, vebe times were approximately in the range of 10 to 28 sec, whereas for superplasticized concretes without fibers, they were in the range of 7 to 10 sec.

The increase in fiber content from 32.63 kg/m^3 to 56.36 kg/m^3 had negligible effect on the slump and flow table spread. However, an increase in fiber content caused an increase in vebe time. Slump and flow table tests are used to measure the workability of concrete based on the flowability character of concrete. Consequently, an increase or decrease in fiber content did not have much influence on the results attained from these tests. Vebe time is used to measure the workability of concrete, based on the energy needed to compact the concrete. The energy requirement for plain superplasticized concrete mixes is less than for superplasticized fiber-reinforced concrete. In the case of superplasticized fiber-reinforced concrete mixes, the energy needed appears to be proportional to the fiber content in the concrete.

The slump of the concrete had a greater influence on the air content than the air-entraining agent used. For concrete with zero slump, an increase in air-entraining agent from 0.2 percent to 0.8 percent caused no appreciable increase in air content. For zero slump concrete, it was never possible to achieve an air content of 6 percent, even with a very high dosage of air-entraining agent (0.8 percent by weight of cement).

Figure 4 shows that for a constant quantity of air-entraining agent (0.4 percent), the air content increases from 4.2 percent to 7.4 percent with an increase in slump from 0.0 mm to 38.0 mm. The same phenomenon is true for other dosages of air content. With a constant dosage of air-entraining agent (0.2-0.25 percent), the air content increased from 3.8 percent to 9.6 percent for an increase in slump from 0 mm to 152.4 mm, and for a constant dosage of from 0.1 percent to 0.15 percent, the air-content increased from 3.8 percent to 9.2 percent when the slump increased from 0 mm to 229 mm.

Based on the statistical analysis, two typical mixes, Mix 1 and Mix 26 were selected for intensive study. Mix 1 had a low water-cement ratio (0.3), high cement content (474 kg/m^3), and medium workability, and it will be suitable for bridge deck overlays and for constructions where high-strength and highly impermeable concretes are needed. Mix 26 had a medium water-cement ratio (0.4) medium cement content (363 kg/m^3), and high workability, and it will be suitable for general structural work and for construction of highway pavements. For these concretes, all the fresh concrete as well as the hardened concrete properties were determined (1).

The initial setting time for Mix 26 corresponding to a penetration resistance of 3.45 MPa was 8 hr 45 min and the final setting time corresponding to a penetration resistance of 27.5 MPa was 10 hr 50 min. The corresponding initial and final setting times for Mix 1 were 7 hr 59 min and 10 hr 36 min.

The slump loss study had shown that there was adequate total working time (0.5-1.5 hr) for fiber-reinforced superplasticized concretes. The retempering study had shown that after each stage of mixing, the concrete had good workability and maintained it for more than an hour (depending on the superplasticizer dosage), especially after first retempering.

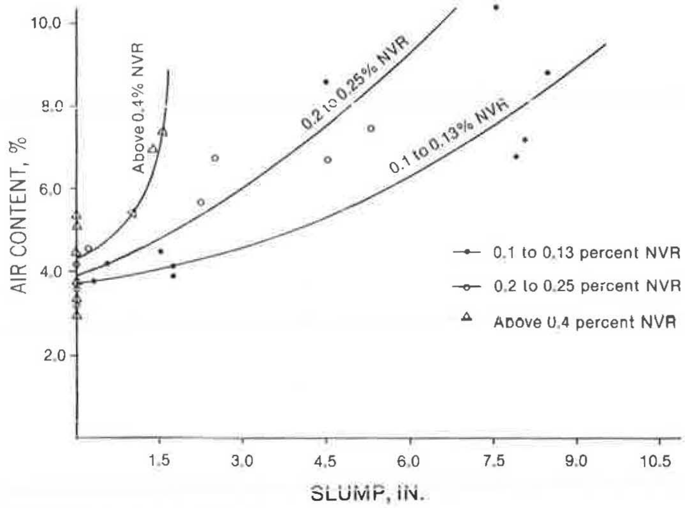

FIGURE 4 Relationship between slump, air-entraining agent, and air content.

There was a substantial loss in entrained air during retempering; however, the air content could be increased by adding an air-entraining agent at each stage of retempering.

Hardened Concrete Properties

Compressive Strength

The analysis has shown that for the same water-cement ratio and superplasticizer dosage, concretes with a higher cement content showed higher strength, and an increase in superplasticizer dosage caused an increase in compressive strength. An increase in fiber content caused no appreciable change in compressive strength.

Flexural Strength

When all other factors were the same, an increase in fiber content caused an increase in ultimate flexural strength. However, the increase in flexural strength was only about 10 percent for an increase in fiber content from 36.63 kg/m^3 to 56.36 kg/m^3. The flexural strength values varied in the same way as compressive strength values, with respect to variation in all factors, except in the case of fiber content. For a given compressive strength, the corresponding flexural strength was greater for superplasticized fiber concrete when compared to plain superplasticized concrete.

A significant difference in the performance of plain superplasticized concrete and superplasticized fiber-reinforced concrete was found in the static flexural test. The hooked fibers had proved their ability as crack arrestors. The cracks were prevented from propagating until the composite ultimate stress was reached. The mode of failure was simultaneous yielding of the fibers and the matrix. During the test, one could actually hear the popping sound of the fibers failing in tension and not because of the bond failure. It appears obvious that the deformed ends contributed significantly to the increase in bond between fiber and matrix. The significance of good bond can be observed from the typical load deflection curves (Figure 5). The curves indicate a ductile behavior. These curves also show the advantage of fiber-superplasticized concrete versus nonfiber-superplasticized concrete in obtaining higher flexural strength, higher toughness, and high energy absorption qualities.

Toughness Index

The toughness index is a measure of the amount of energy required to deflect the 102 x 102-mm beam a given amount, compared to the energy required to bring the beam to the point of the first crack. It is calculated as the area under the load-deflection curve up to 1.9 mm, divided by the area under the load-deflection curve of the fibrous beam up to the first crack strength (proportional limit, defined as first deviation from linear).

In general, the toughness index for the fiber-reinforced superplasticized concrete varied greatly depending on the position of the crack and the distribution of fibers. An increase in fiber content caused an increase in toughness index; the toughness index increased from 4.75 to 6.5 for an increase in fiber content from 32.63 kg/m^3 to 56.36 kg/m^3. All specimens made of plain superplasticized concrete failed immediately after the first crack and, consequently, the toughness index for these specimens is equal to 1.

Impact Strength

The fiber-reinforced concrete showed a tremendous ability to absorb impact loading. The measured impact resistance at various ages for the selected concretes are shown in Figure 6. Concrete containing 44.5 kg/m^3 steel fibers had 10 times greater impact resistance at 28 days than its corresponding concrete without fibers.

The relationships between compressive strength and other properties such as tensile strength, flexural strength, pulse velocity, dynamic modulus of elasticity, and static modulus of elasticity were determined based on the regression analysis (1). For compressive strengths varying from 13.8 to 55 MPa, there was an approximate linear relationship between the compressive strength and other properties. For both concretes with and without steel fibers, higher early strengths were achieved with the addition of superplasticizer.

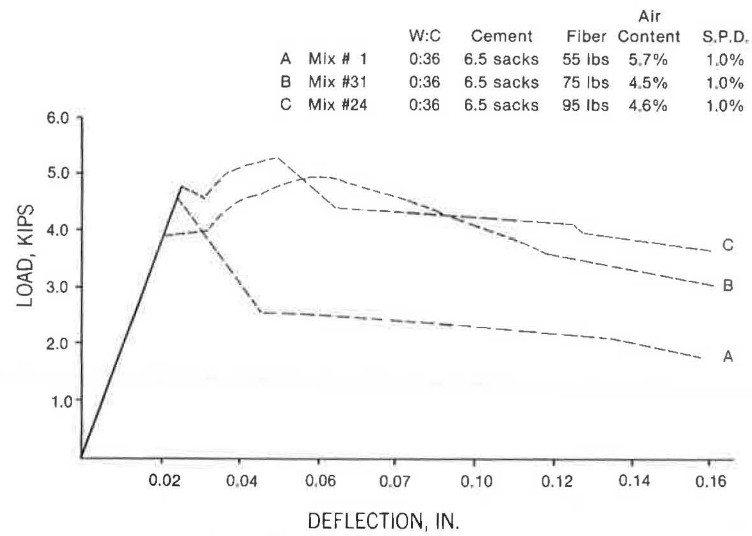

FIGURE 5 Comparison of load deflection curves for mixes with different fiber contents (7-day).

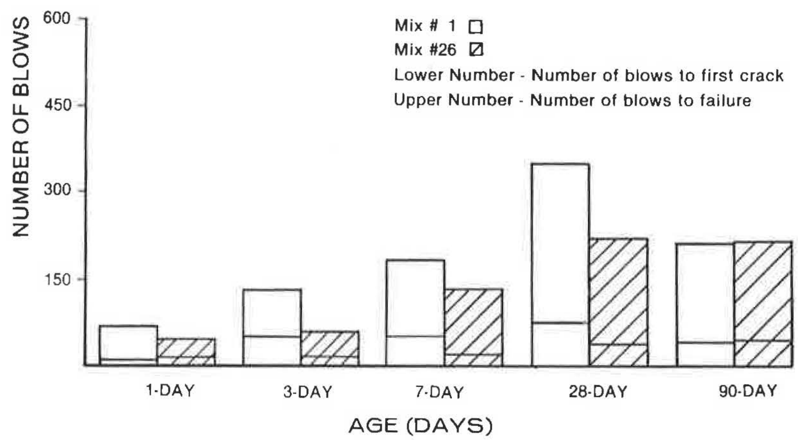

FIGURE 6 Impact resistance with age.

Shrinkage and Creep

The shrinkage and specific creep strains increased with an increase in the water-cement ratio and the concrete that exhibited higher shrinkage also had higher creep. The total shrinkage strains measured at the end of 566 days were 42.9×10^{-5} and 49.85×10^{-5}, respectively, for low (0.3) and medium (0.4) water-cement ratio concretes. The total specific creep strains measured at the end of 375 days were 45.6×10^{-6} and 58.6×10^{-6} (in./in./psi), respectively, for low and medium water-cement ratio concretes. These creep and shrinkage strains are much lower than those obtained for the normally used structural concretes.

The fiber-reinforced superplasticized concretes had less shrinkage and comparable creep than that of the corresponding superplasticized concrete without fibers.

Thermal Conductivity

The thermal conductivity of the concrete specimens was measured with a guarded hot box apparatus. The use of steel fibers appeared to have very little effect on the thermal conductivity of superplasticized concrete. For Mix 1, the plain mix had an average thermal conductivity of 0.659 Btu/hr-ft-°F (0.975 g cal m/hr m^2 °C) and the mix with fiber had an average value of 0.613 Btu/hr-ft-°F (0.907 g cal m/hr m^2 °C). This is a 7.5 percent difference. This shows that the plain concrete was a slightly better heat conductor. For Mix 26, the plain mix had an average thermal conductivity of 0.625 Btu/hr-ft-°F (0.925 g cal c/hr m^2 °C) and the mix with fiber had an average value of 0.665 Btu/hr-ft-°F (0.984 g cal mhr m^2 °C); this is a 6.4 percent difference. In this case, the concrete with fibers was a slightly better heat conductor.

The measured thermal conductivity values are lower than those obtained for conventional structural concretes made with limestone aggregates.

Chloride Permeability

The migration of sodium chloride solution (8 percent solution) into superplasticized concrete cylinders at room temperature was investigated. The superplasticized concretes offered a slightly greater resistance to chloride penetration at 50 mm depth, compared to regular concretes without superplasticizer (2).

Resistance to De-Icing Chemicals

The resistance to scaling when exposed to de-icing chemicals (4 percent calcium chloride solution) was determined as per the recommendations of ASTM C672. At every 5-cycle interval, each specimen was evaluated for damage for a total of 50 cycles. The observed rating of scaling resistances for the two concretes (Mixes 1 and 26) are given in Table 1. The high cement content concrete showed no scaling at the air contents tested. The medium cement concrete showed very slight scaling at the end of the 50 cycles. The resistance to scaling when exposed to de-icing chemicals improved with lower water-cement ratio and higher cement content. Some rusting of the exposed fibers was observed on all the beams, but this rusting was found only at the surface. The fibers inside the beams showed no signs of rusting.

TABLE 1 Scaling Resistance to 4 Percent Calcium Chloride Deicing Solution by ASTM Ratings

	Mix by Specimen Number							
	26C		1C		26D		1D	
Cycle	1	2	1	2	1	2	1	2
0	0	0	0	0	0	0	0	0
5	0	0	0	0	0	0	0	0
10	0	0	0	0	0	0	0	0
15	0	0	0	0	0	0	0	0
20	0	0	0	0	0	0	0	0
25	0	0	0	0	0	0	0	0
30	0	0	0	0	0^+	0^+	0	0
35	0	0	0	0	0^+	0^+	0	0
40	0^+	0^+	0	0	0^+	0^+	0	0
45	0^+	0^+	0	0	0^+	0^+	0	0
50	0^+	0^+	0	0	½	½	0	0

The high resistance to de-icer scaling of Mix 1 resulted from a greater impermeability of this concrete. This greater impermeability resulted from higher cement content, which caused lower water absorption. As compared to concrete without steel fibers, it can be stated that the addition of fibers did not adversely affect the de-icer scaling resistance.

Freeze-Thaw Durability

The durability of both concretes (Mixes 1 and 26) subjected to rapid freezing and thawing was evaluated as per ASTM C666-77, Procedure A, "Rapid Freezing and Thawing in Water." All specimens were tested at approximately 30-cycle intervals, for a total of 300 cycles for any weight change, pulse velocity, and dynamic modulus. At the conclusion of 300 cycles, all beams were also tested for flexural strength and moisture absorption. For the moisture absorption test, the specimens were kept immersed in water for 30 min. The specimens were then taken out, surface water wiped with an absorbing paper, and the specimens were weighed accurate to 1 gram. These specimens were placed in an oven at a temperature of 105°C ± 5° for 48 hr. The moisture absorption is taken as the difference in weight of the wet and dry specimens divided by the weight of the dry specimen.

Durability

For both concretes, except for Mix 26D, the calculated durability factors were greater than 98.25 percent, whereas ASTM C494-77 sets the minimum durability factor at 80 percent. The higher cement-content concrete showed a higher durability even though the air content was less than for the medium cement-content concrete.

For the concrete with low air content (3.8 percent) and medium cement content (362.5 kg/m^3), Mix 26D, there was slight scaling after 300 cycles of freeze-thaw, and the reduction in dynamic modulus was much higher than for concretes with higher air contents but having the same cement and water contents. The calculated durability factors for these specimens were not satisfactory. It is evident that for superplasticized concretes with low air contents even when steel fibers are added, there will be deterioration due to freeze-thaw cycles. It is therefore recommended that a minimum of 6 percent air content should be used for superplasticized fiber-reinforced concretes.

Flexural Strength

The high-cement-content concrete showed an increase in flexural strength after 300 cycles of freeze-thaw as compared to the 14-day flexural strength, whereas the freeze-thaw specimens of the medium-cement-content concrete with higher air contents showed the same flexural strength after 300 cycles of freezing and thawing as compared to the 14-day flexural strength. However for medium cement concretes with lower air contents (Mixes 26D and 26F), there was a considerable reduction in their flexural strengths after 300 cycles of freeze-thaw when compared to their 14-day flexural strengths.

Weight Loss

The loss of weight at different freeze-thaw cycles was more for the concretes with medium cement content than for the concretes with high cement content.

Moisture Absorption

In all concretes, there was an increase in the water absorption after they were subjected to 300 cycles of freeze-thaw showing that there is an apparent deterioration or increase in internal microcracking due to freezing and thawing. This appears to be true for concretes with or without fibers, with high or low strengths, high or low cement contents, high or low water contents, and high or low air contents. However, higher cement and air contents reduce the damage considerably. Both reference and freeze-thaw specimens made from the high-cement-content concrete showed lower water absorption than those of the medium-cement-content concrete. The percentage difference of water absorption between freeze-thaw and reference specimens is less for the high cement-content concrete.

There appears to be a relation between the water absorption and the durability factor. Concretes with higher water absorption coefficients showed lower durability. Therefore, a simple determination of the water absorption coefficients for different concretes might give a qualitative evaluation of their durabilities.

Pulse Velocity

The change in pulse velocity followed the same pattern as the change in dynamic modulus for almost all the specimens. In this investigation, the pulse velocity determination was used as an alternate test for verifying the observations based on the transverse resonant frequency readings.

A comparison of concretes with and without steel fibers had shown that the concretes with steel fibers had higher freeze-thaw durability, higher pulse velocity, and lower moisture absorption than their corresponding concretes without fibers and having the same air content.

Air-Void Characteristics

For the selected concretes (Mixes 1 and 26), the air-void characteristics of the hardened concretes were determined using the Linear Traverse Method as described in ASTM C457-71 with modifications to suit the use of a minicomputer. Four specimens (two from each mix) were studied (1).

Two specimens showed very good air-void characteristics. All the air-void parameters, as well as the distribution of the chord intercepts, were satisfactory. One specimen showed air-void characteristics slightly outside the recommended parameters, but the results were still acceptable. The last specimen showed low specific surface due to larger air bubbles in the concrete. This specimen also had high air content. Larger air bubbles and high air content had only reduced the strength in the concrete. The distribution of the chord intercepts for the two last specimens was acceptable, but they lacked some smaller air bubbles. However, all four concretes had highly satisfactory resistance to rapid freeze-thaw cycles and their durability factors were above 94 percent.

CONCLUSIONS

Substantial improvement in workability with consequent reduction in placement costs or a considerable saving in cement content is the realistically achievable advantages through the use of superplasticizer for whatever purpose conventional concrete is being used. Superplasticized concretes with low water-cement ratios and high early strengths are particularly suitable for concrete repair and rehabilitation of bridges and other structures.

The addition of the special type of steel fibers (with deformed ends and glued together into bundles with a quick water-soluble adhesive) to superplasticized concrete greatly increases its ductility, toughness, impact resistance, ultimate flexural strength, post-crack load-carrying capacity, shear and torsional strength, fatigue strength, and shock resistance. This is achieved without a reduction of workability or the usual "balling" of steel fibers. Therefore, the fiber-reinforced superplasticized concrete is an almost ideal material for the rehabilitation of concrete structures.

ACKNOWLEDGMENTS

Grateful acknowledgment is expressed to William V. Coyle (co-principal investigator of the project) and Peter A. Kopac, project monitor, for their help and valuable suggestions. The author is thankful to all the graduate research assistants for their help rendered during the experimental work. The author gratefully acknowledges the financial support of the Office of University Research, U.S. Department of Transportation (Contract No. DOT-RC92035) and C.W. Josifek of the Bekaert Steel Wire Corporation, Chicago.

REFERENCES

1. V. Ramakrishnan, W.V. Coyle, and P.A. Kopac. Steel Fiber Reinforced Superplasticized Concretes for Rehabilitation of Bridge Decks and Highway Pavements. Final Report CDT-822. South Dakota School of Mines and Technology, Rapid City, July 1982, 375 pp.
2. V. Ramakrishnan, W.V. Coyle, and P.A. Kopac. Superplasticized Concretes for Rehabilitation of Bridge Decks and Highway Pavements. Report DOT/RSPA/DPB-50/81/3, Office of University Research, U.S. Department of Transportation, Jan. 1981.
3. V. Ramakrishnan, W.V. Coyle, and P.A. Kopac. Supplement to Phase One Interim Report--Superplasticized Concretes for Rehabilitation of Bridge Decks and Highway Pavements. Report CDT-821. South Dakota South of Mines and Technology, Rapid City, July 1982.
4. V. Ramakrishnan, T. Brandshaugh, W.V. Coyle, and E.K. Schrader. A Comparative Evaluation of Concrete Reinforced with Straight Steel Fibers and Fibers with Deformed Ends Glued Together into Bundles. American Concrete Institute Journal, Vol. 77, No. 3, 1980, pp. 135-143.
5. V. Ramakrishnan. Performance Characteristics of Steel Fiber Reinforced Superplasticized Concrete. Proc., Symposium L, Materials Research Society, University Park, Pa., 1980, pp. 145-148.
6. V. Ramakrishnan, W.V. Coyle, L.F. Dahl, and E.K. Schrader. A Comparative Evaluation of Fiber Shotcretes. Concrete International, Design and Construction, Vol. 3, No. 1, 1981, pp. 59-69.
7. V. Ramakrishnan, W.V. Coyle, P.A. Kopac, and T.J. Pasko. Performance Characteristics of Steel Fiber Reinforced Superplasticized Concrete. SP68-29. American Concrete Institute, 1981, pp. 315-334.

Epoxy-Bonded, Steel Fiber-Reinforced Thin Cementitious Overlay at Orlando International Jetport, Florida

RODNEY J. STEBBINS, CHARLES W. JOSIFEK, and JOHN D. JENIEC

ABSTRACT

The reasons for selecting an epoxy-bonded, steel fiber-reinforced, cement/fly ash, superplasticized thin overlay are discussed. Each project field application procedure from existing concrete preparation through project completion is also discussed. A total of 40,000 ft^2 was applied from 1.5 in. to 3 in. thick with no signs of delamination or visible cracking evident after testing at 90 days' maturity. To date, this is the largest project of its type in the state of Florida.

The structure that received the repairs is best described as an elevated cast-in-place structure that receives light-to-heavy vehicular traffic. The areas repaired (4 each of 10,000 ft^2) were the baggage unloading areas for major airlines. The experience gained on this project should provide assistance for future design, specifications, and construction for thin concrete overlays on suspended and elevated structures.

The project was accomplished in two phases. Phase 1 (10,000 ft^2) was completed in fall 1982. Phase 2 (30,000 ft^2) was implemented and completed in the fall of 1983 after testing Phase 1 for delaminations and cracking at 28 and 90 days, visual inspections, and chain dragging through fall and winter 1982, and spring and summer 1983.

PROJECT AREA AND DESCRIPTION OF PHYSICAL REQUIREMENTS

Orlando International Jetport is a recently constructed facility located south of Orlando, Florida. Four individual areas each measuring approximately 10,000 ft^2 required an application of thin overlay to correct or to reduce vibrations to the structure caused by small tractors pulling hard rubber-wheeled carts (used to transport baggage from the airplanes to the baggage unloading areas) rapidly over drain "crickets" that are cast into the floor. The anticipated structural deflection did not occur, thus requiring the engineer to modify the drainage crickets during construction from an original two-column pattern to a one-column pattern. Because the drains had been set at the designed elevation, the drainage angles became very pronounced. When the tractors and towed carts traveled the waves of crickets, they caused pronounced and unacceptable vibrations throughout the structure. The tractors and carts have hard rubber tires but do not have shock absorbers.

REPAIR DESIGN

Scarification to below-the-top reinforcing and placing new concrete was considered. However, it was dismissed due to the cost and customer inconvenience. An asphalt overlay was considered. However, it was dismissed as being a temporary repair. Rapid-setting concrete products were considered and were dismissed due to their lack of history in very thin cementitious overlay applications. A fear of high shrinkage and cracking was instrumental in dismissing these types of products. Epoxy mortars were considered for the complete overlay. However, economics dictated that this was not feasible.

The best solution for an overlay would require the following:

1. Positive bond to existing concrete,
2. Ability to place from 0 in. to 3 in. of thick concrete,
3. No crack propagation,
4. No delamination,
5. No excavation or demolishing of existing concrete,
6. Minimal construction time,
7. A reasonable dust-free environment to protect machinery and baggage, and
8. Mutual occupancy (contractor/airlines).

Steel fiber-reinforced concrete was selected. It has the ability to be placed easily, resist crack propagation, and it can be placed as thin as 1.5 in. thick without tremendous problems provided a good mix design is provided to the contractor. An epoxy (fresh to existing concrete) binder was selected through the results of slant-shear testing that would satisfy the positive bond and delamination requirements. Epoxy-bonded steel fiber-reinforced concrete as a composite system satisfied all of the foregoing needs except that the thinnest it could safely be applied was 1.5 in.

An epoxy mortar (epoxy and graded silica sand) was specified to be used from 1.5 in. to 0 in. Originally, feathering to zero was not allowed. The contractor was required to saw 0.5 in. deep and excavate an area 18 in. wide to provide a key. Subsequent testing proved the key was not necessary and the contractor was allowed to "featheredge" the mortars.

MIX DESIGNS AND PRODUCTS

Epoxy Fresh Concrete Binders

Products considered acceptable for this project were required to meet the following physical properties.

Physical Properties (Unmixed) at 25°C (77°F)
Component A (Resin)

- Weight per gallon, lb = 10.4±1
- Viscosity = 2,000-2,600 centimeters per second (cps)
- Specific gravity = 1.236-1.260
- Shelf life (closed containers) = 2 yr

Component B (Catalyst) at 25°C (77°F)

- Weight per gallon, lb = 8.3+0±0.1
- Viscosity = 150-180 cps
- Specific gravity = 0.984-1.008
- Shelf life (closed containers) = 2 yr

Physical Properties (Mixed) at 25°C (77°F)

- Weight per gallon, lb = 10.0
- Viscosity = 1,900-2,300 cps
- Specific gravity = 1.18-1.22
- Solids by weight = 100%
- Pot life = 26-32 min
- Mixing ratio =
  By weight--A = 84%; B = 16%
  By volume--A = 81%; B = 19%

Must Conform to ASTM C881-78, Type II Application = 12-15 mil

Concrete Substrate Temperatures

	86°F (30°C)	68°F (20°C)	32°F (0°C)
Contract time	1.5 hr	3 hr	18 hr
Bond strength	(ASTM C 882)	1,500 psi	

Epoxy Mortars

Physical Properties (Unmixed) at 77°F (25°C)
Component A (Resin)

- Weight per gallon, lb = 9.3±0.1
- Viscosity = 500-700 cps
- Specific gravity, gr/cc = 1.116±0.012
- Shelf life (closed containers) = 2 yr

Component B (Catalyst)

- Weight per gallon, lb = 8.2±0.1
- Viscosity = 150-250 cps
- Specific gravity, gr/cc = 0.984±0.012
- Shelf life (closed containers) = 2 yr

Physical Properties (Mixed) at 77°F (25°C)

- Weight per gallon, lb = 9.08±0.1
- Viscosity = 350-500 cps
- Specific gravity = 1.089±0.012
- Solids by weight = 100%
- Pot life = 20-25 min
- Mixing ratio =
  By weight--A = 80%; B = 70%
  By volume--A = 78%; B = 22%

Compressive: ASTM C109-75

- Age: at 25°C (77°F) = 7 days
- Compressive strength, psi = 10,000

Tensile: ASTM C190-72

- Age: at 25°C (77°F) = 7 days
- Tensile strength, psi = 1,090
- Must conform to ASTM C881--Type III

Mortar Mix Design

- Combined A and B = 16.69 lb
- Silica 20/30* = 50.09 lb
- Silica 30/65* = 50.09 lb
- Total weight per ft^3 = 116.87 lb
- Aggregate/resin ratio = 6/1

*The Standard Sand Company, Tampa, Florida.

Steel Fiber-Reinforced Concrete

Mix design for SFRC/yd^3

- Cement = 540 lb, Type I FM and MC (ASTM C150)
- Fly ash = 165 lb, Type F FM and MC (ASTM C618)
- Coarse aggregate = 1,323 lb, PM and MC Broco (ASTM C33)
- Fine aggregate = 1,433 lb, Jahna-Clearmont (Silica) (ASTM C33)
- Admixture = 54 oz, WRDA 79--Type D (ASTM C494)
- Admixture = 4 oz, WRDA 19--Type F (ASTM C494)
- Water = 282 lb
- Steel fibers = 100 lb, 2-in. corrugated
- Slump = 3-6 in.
- Air = 2-4%
- Unit weight = 142 lb
- Water-cement + fly ash = 0.40
- Field sampling = ASTM C172 and C31
- Strength testing = ASTM C94
- Laboratory testing = ASTM C39 and E329

Test Results

Epoxy Mortar Compressive Strength, psi--ASTM C109:

Days	No. 1	No. 2	No. 3	No. 4
3	8,100	8,500	9,400	4,250
7	8,525	9,250	9,550	5,000
28	10,000	10,000	10,500	6,625

Compressive Concrete Strength without Steel Fibers, psi--ASTM C39:

Days	No. 1	No. 2	No. 3	No. 4
3	5,447	5,200	5,412	5,412
7	5,766	5,695	6,615	5,730
28	6,200	7,782	7,711	7,888

Flexural Strength of Concrete Specimen with corrugated deformed steel fibers, psi--ASTM C293:

Days	No. 1	No. 2	No. 3
3	834	751	801
7	1,068	959	1,008
28	1,240	1,651	1,118

CONSTRUCTION PROCEDURES

Surface preparation is most important to assure bond. Steel wheel-cutter type machinery was used on the first 10,000 ft^2 with satisfactory results. The only undesirable feature was the time required for the preparation. The customer's baggage conveyor equipment precluded sand-blasting the concrete.

The surface needed to be textured or roughened to the extent that no laitance (cement paste) was evident and that the sand-aggregate particles were visible. Care was taken to prevent traffic or contamination on prepared surfaces. The remaining 30,000 ft^2 were prepared using a steel shot-blaster. This equipment allowed the contractor to prepare the concrete surface with considerably more speed than with the steel wheel-cutting type equipment mentioned previously.

THIN OVERLAY

Where the overlay was thinner than 1.5 in., the epoxy mortar was placed to the final grade with 1.5-in. wood forms lined with construction plastic to prevent the epoxy from sticking to the wood-forming materials. The mortars were sloped to the existing floor a distance from the form of about 2 ft. Initially, the contractor was required to saw into the existing concrete 0.5-in. deep and remove about a 12-in. wide section for the length of the epoxy mortar repair. However, after testing of the epoxy mortar in place, the engineer allowed the contractor to place the remainder of the areas without removing any material.

EPOXY MORTAR MIXING

The contractor mixed the epoxy mortars as follows:

1. Mix the A component.
2. Pour the B component into the A component mixture and mix until streak-free.
3. Pour in the 30/65 silica and mix until a homogenous mass is evident (maximum 2 min).
4. Pour in the 20/30 silica and mix until all particles are coated.

A 0.75-in. variable-speed drill motor was used with a Jiffy blade mixer. (Paddle mixtures cause segregation and do not blend the materials properly.) Plastic pails (5-gal size) were used to mix the epoxy mortars. Before placing the mortars, 10 to 15 mil of the mortar resin (neat and without aggregates) was painted on the concrete to prevent starvation of the mortar bond line. The mortar (epoxy with aggregates) was mixed and poured in place for screeding with a 2 x 4 board screed. No troweling was required.

The final finish was completed when loose 20/30 silica sand was broadcast into any standing pools or wet areas of mixed resin. This allowed the contractor to provide a nice blend of texture from the epoxy mortar to the concrete at the 0-in. line. Within 2 to 4 hours the forms could be stripped, and the fresh concrete bonder and the steel fiber-reinforced concrete could be placed using the epoxy mortar (at the 1.5-in. thick side) as a screed edge.

FRESH CONCRETE BINDER

The fresh concrete binder was mixed in 5-gal quantities by pouring the premeasured B component into the A component pail and mixing with the Jiffy mixer until streak-free. The binder was then poured in strips on the prepared concrete surface and squeegied to a thickness of approximately 0.015 in. (15 mil = 107±ft^2/gal).

Before the binder became "stringy" or "tack-free," the fresh concrete was placed right on the epoxy binder. No mixing of the epoxy and concrete was required. Had the epoxy been allowed to become stringy or tack-free, another application of 15 mil before 24 hr had passed would provide the originally desired results.

STEEL FIBER-REINFORCED CONCRETE (SFRC)

Elevations

The finished elevation was established with the use of pipe (screed rails) and threaded chairs. All final elevations were carefully established with a transit before placing the epoxy binder and SFRC.

Concrete

The mix design was provided by the manufacturer and the concrete was delivered to the project in transit trucks batched to a 2-in. slump. Superplasticizer was introduced into the transit truck before the fibers. The fibers were poured from bags into the transit mixer and mixed for 5 min. The SFRC was dumped into a 3-yd bottom dump bucket, craned up one story, and dumped into motorized Georgia Buggies, driven to the screed and placed. The superplasticizers allowed the concrete mix to be fluid enough with a slump of 8 in. to allow easy placing, screeding, and finishing. No balling of the fibers was evident. A vibrating screed machine mounted on standard 2 x 8-in. boards was used.

Internal vibration was not performed due to the depth of the overlay. No problems were encountered by the contractor in providing the owner/engineer a well-consolidated SFRC overlay mainly as a result of a combination of steel fiber and mix design selection, coarse and fine aggregate, gradation, cement/fly ash content, superplasticizer, and quality cement finisher personnel.

CURING

Hydration was carefully monitored because of fairly high cement content, depth of overlay, warm days, and warm substrates. The contractor elected to blanket the overlay with burlap, apply trickling water for curing, and to cover the burlap with construction plastic sheets. The water curing continued for 3 to 5 days.

EVALUATION

The first 10,000-ft^2 overlay has been in place more than 1 yr with the subsequent 30,000-ft^2 area in place for more than 120 days. To date, there is no evidence of delaminations or visible cracks. It is sufficient to state that the project is successful and that thin SFRC overlays can be placed easily and effectively yielding a "Monolithic Composite." All tests indicated that the anticipated results were achieved and that all specifications were easily met. The contractor completed each phase of construction ahead of schedule.

CONCLUSIONS

1. Thin (1.5-in.) overlays can be accomplished without complications by usual contractor personnel.
2. Epoxy mortars can be used as an effective material to overlay concrete from 0 in. to 1.5 in. without special aggregates or concern.
3. Epoxy-bonded SFRC overlays are an effective and economically feasible solution to resurfacing of suspended slabs for vehicular traffic.

ACKNOWLEDGMENTS

The following gentlemen provided their valuable expertise to the contractor, engineer, and material suppliers, and their contributions were instrumental in making the project a success: Milton D. Anderson, David W. Fowler, David R. Lankard, V. Ramakrishnan, John P. Roebuck, and R.M. Broley.

Low-Temperature Curing of Polymer Methacrylate Polymer Concrete

TADASHI KOBAYASHI and YOSHIHIKO OHAMA

ABSTRACT

In recent years, polymethyl methacrylate polymer concrete (PMMA-PC) has been used extensively in the field of construction works. It is needed because it will harden within 1 hr at low temperatures. A basic investigation of the low-temperature curing characteristics of workable PMMA-PC is the focus of this paper. PMMA-PC and its binder are prepared with various binder formulations, and the working life of the binder and the peak exotherm time and compressive strength of PMMA-PC are examined under various low-temperature conditions. The working life of the binder and the peak exotherm time of PMMA-PC decrease with an increase in promoter and cross-linking agent contents and a rise in test temperature. The contents of the binder with the desired working life at low temperatures less than 0°C can be estimated by using a nomograph prepared in this investigation. The peak exotherm time of PMMA-PC can be predicted from the working life of the binder. In conclusion, the optimum binder formulations are recommended for the low-temperature applications of PMMA-PC, which hardens and develops a high compressive strength of about 500 kg/cm^2 in the range of 0°C to -20°C within approximately 1 hr.

Recently, polymethyl methacrylate polymer concrete (PMMA-PC) has been widely used for various construction works, such as the repair and restoration of concrete structures, because of its good workability and high early strength development. For its applications during winter, in cold districts, in the repair of cold stores, and so forth, the development of the high early strength is required at low temperatures, and, in many cases, the construction time is quite limited (1). This investigation was conducted to make clear the low-temperature curing characteristics of PMMA-PC.

PMMA-PC and its binder were prepared with variation of cross-linking agent and promoter contents, and the working life of the binder and the peak exotherm time and compressive strength of PMMA-PC were investigated under various low-temperature conditions in order to obtain the optimum binder formulations that give a high early strength at temperatures less than 0°C. The results of this investigation are presented in this paper.

MATERIALS

Binder System

The binder system used was methyl methacrylate (MMA) monomer, together with polymethyl methacrylate (PMMA) as a thickening agent, trimethylolpropane trimethacrylate (TMPTMA) as a cross-linking agent, 50 percent dicyclohexyl phthalate powder of benzoyl peroxide (BPO) as an initiator, and N,N-dimethyl-p-toluidine (DMT) as a promoter. The basic properties of MMA, PMMA, and TMPTMA are given in Table 1.

TABLE 1 Basic Properties of MMA, PMMA, and TMPTMA

Material for Binder	Molecular Weight	Specific Gravity (20 °C)	Viscosity (20 °C ,cP)
MMA	100.12	0.94	0.85
PMMA	ca. 250,000	1.19	—
TMPTMA	338	1.06	13.0

Filler and Aggregates

Commercially available calcium carbonate (heavy grade) was used as a filler. Hatsukari crushed andesite for coarse aggregate and Abukumagawa river sand for fine aggregate were employed. Their properties are given in Table 2. The water contents of the filler and aggregates were controlled to be less than 0.1 percent.

TABLE 2 Properties of Filler and Aggregates

Type of Filler or Aggregate	Size (mm)	Specific Gravity (20°C)	Water Content (%)	Organic Impurities
Calcium carbonate	$<2.5 \times 10^{-3}$	2.70	<0.1	Nil
Crushed	10 - 20	2.51	<0.1	Nil
andesite	5 - 20	2.51	<0.1	Nil
River	1.2 - 5	2.46	<0.1	Nil
sand	<1.2	2.46	<0.1	Nil

TESTING PROCEDURES

General Conditions for Tests

The tests, except for the viscosity of binder, were carried out at temperatures of 0°C, -10°C, and -20°C. Before the tests, all the materials were stored at the respective test temperatures. The formulations of the binder and the mix proportions of PMMA-PC are given in Tables 3 and 4.

Test of Working Life of Binder

About 100 g of binder was tested for working life according to JIS K 6833 (General Testing Methods for Adhesives). The time elapsed from the addition of the initiator to the spinning of the binder was observed as the working life of the binder.

TABLE 3 Formulations of Binder

Formulation No.	Formulation by Weight			
	MMA + PMMA	TMPTMA	BPO (as solids)	DMT
1	95	5	2.0	1.0
2				2.0
3				3.0
4				5.0
5	90	10		1.0
6				2.0
7				3.0
8				5.0
9	80	20		1.0
10				2.0
11				3.0
12				5.0

TABLE 4 Mix Proportions of PMMA-PC

Materials			Weight Percent
Binder	MMA + PMMA + TMPTMA		10.00
Filler	Calcium Carbonate		10.00
Aggregate	Crushed Andesite	Size, 10-20 mm	15.02
		5-10 mm	15.02
	River Sand	Size, 1.2-5 mm	9.91
		< 1.2 mm	40.05

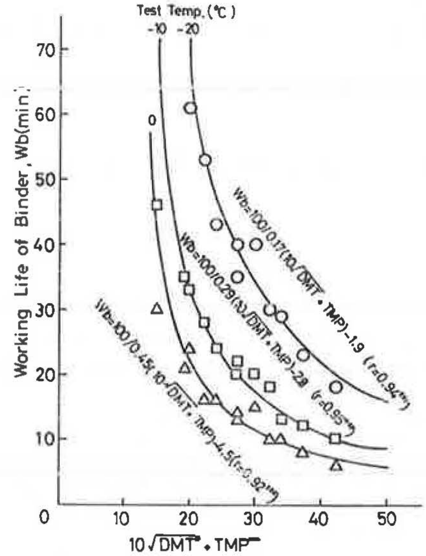

Note; * DMT content (%), ** TMPTMA content (%), *** Coefficient of correlation.

FIGURE 1 Effects of DMT and TMPTMA contents and test temperature on working life of binder (with BPO content 2.0%).

Test of Peak Exotherm Time of PMMA-PC

About 500 g of fresh PMMA-PC mixed according to JIS A 1181 (Method of Making Polyester Resin Concrete Specimens) was tested for peak exotherm time. The exotherm temperature was determined by chromel-alumel thermocouples embedded in PMMA-PC. The time elapsed from the addition of the initiator to the attainment of the maximum exotherm temperature of PMMA-PC was observed as the peak exotherm time of PMMA-PC.

Compressive Strength Test of PMMA-PC

In accordance with JIS A 1181, PMMA-PC was mixed, and then cylindrical specimens 7.5 x 15 cm were molded. After molding, the specimens were cured according to the following methods: (a) 1-hr, 2-hr, 4-hr, 24-hr, 3-day, and 7-day cures at casting temperatures (0°C, -10°C, and -20°C); and (b) 24-hr cure at each casting temperature plus 24-hr, -20°C cure. The specimens were tested for compressive strength in accordance with JIS A 1182 (Method of Test for Compressive Strength of Polyester Resin Concrete).

TEST RESULTS AND DISCUSSION

The effects of DMT and TMPTMA contents and test temperature on the working life of binder are shown in Figure 1. The working life of the binder tends to shorten with increasing DMT and TMPTMA contents, irrespective of the test temperature. The working life of the binder is also markedly affected by the test temperature and lengthens with a fall in the test temperature. The working life of the binder at -20°C is 2 to 3 times longer than that at 0°C. From Figure 1 it is observed that a close correlation exists between the factor ($10\sqrt{\text{DMT content}}$ + TMPTMA content) and working life of PMMA-PC regardless of the test temperature. Consequently, this empirical relationship can be expressed by

$$Wb = 100/[(0.014t + 0.44)(10\sqrt{DMT} + TMP) - (0.13t + 4.4)] \qquad (1)$$

where

Wb = working life of the binder,
t = test temperature,
DMT = DMT content, and
TMP = TMPTMA content.

By using this relationship, a nomograph for the DMT and TMPTMA contents of the binder with the desired working life can be prepared as shown in Figure 2. The validity of this nomograph is limited in the range of the binder formulations given in Table 3. In addition, the procedure to estimate the DMT and TMPTMA contents of the binder with the desired working life at different ambient and materials temperatures less than 0°C by applying this nomograph is explained in the example that follows.

Example

It is desired to calculate the DMT and TMPTMA contents of a binder with a working life of 30 min at materials and ambient temperatures of -20°C. In Figure 2, a straight line perpendicular to the y axis is drawn from point a of Wb = 30 min, and point b on the intersection of the straight line, and the curve denoting Wb at -20°C is obtained. Then a straight line perpendicular to the x axis is drawn from point b, and the two DMT contents are estimated on the intersections, c and d, of the straight line, and the curves denoting DMT at TMP = 20 percent and 10 percent, respectively, as follows:

DMT contents (DMT) at TMPTMA contents (TMP) 20% and 10% = 1.5% and 5.0%, respectively (2)

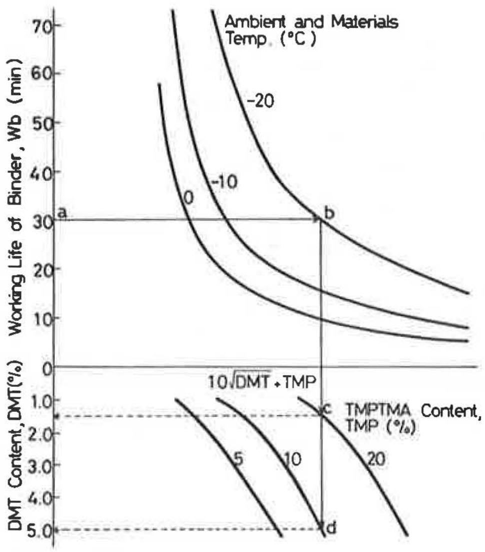

FIGURE 2 Nomograph for DMT and TMPTMA contents of binder (with BPO content 2.0%).

If necessary, the working life of PMMA-PC can be predicted from that of its binder by using the empirical equation, Wc = 2.29Wb + 2.33 (where Wc is the working life of PMMA-PC), which was proposed by the authors' previous study (2). The effects of DMT and TMPTMA contents and test temperature on the peak exotherm time of PMMA-PC are shown in Figure 3. Like

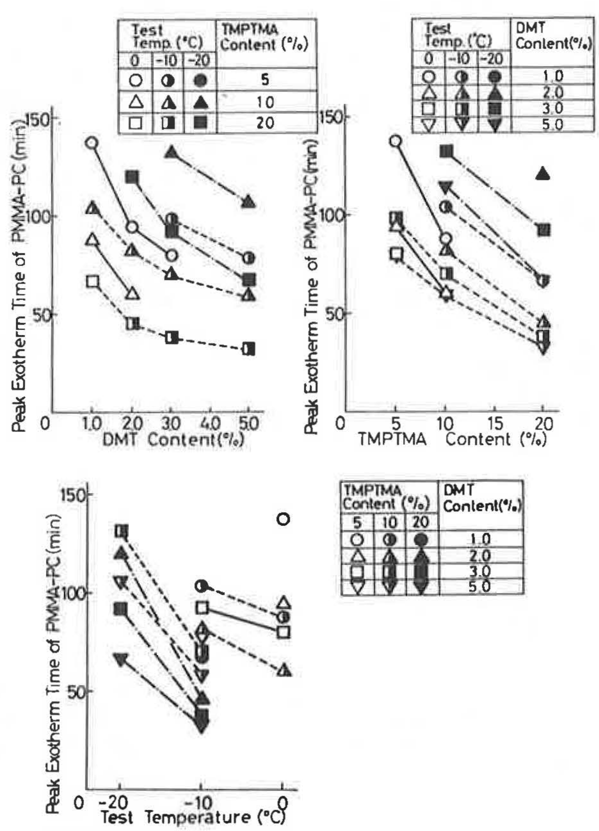

FIGURE 3 Effects of DMT and TMPTMA contents and test temperature on peak exotherm time of PMMA-PC.

the working life of the binder, the peak exotherm time of PMMA-PC decreases with increasing DMT and TMPTMA contents and rising test temperature.

It can be observed from Figure 4 that a reliable positive correlation exists between the working life of the binder and the peak exotherm time of PMMA-PC, regardless of the formulations of the binder and test temperature. This empirical relationship can be expressed by

$$Pc = 3.8\ Wb - 1.6 \quad (3)$$

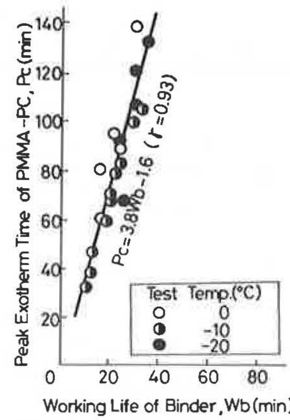

FIGURE 4 Working life of binder versus peak exotherm time of PMMA-PC.

where Pc and Wb are the peak exotherm time of PMMA-PC, and the working life of the binder, respectively. From the preceding relationship, the peak exotherm time of PMMA-PC can be predicted by determining the working life of the binder. Probably the peak exotherm time of PMMA-PC gives a measure to determine the time that is required before demolding precast products or to cure after repairing works.

Figure 5 shows the relation between the DMT content and compressive strength of PMMA-PC. An increase in the DMT content raises the compressive strength of PMMA-PC, regardless of the test temperature. PMMA-PC, when provided an additional cure at 20°C for 24 hr after curing at each casting temperature, shows a higher compressive strength than the one cured at 0°C, -10°C, or -20°C for 24 hr. This tendency is especially remarkable at a casting temperature of -20°C. The explanation for this probably is that the polymerization of unreacted monomer remaining in the binder is accelerated by rising cure temperature.

Figure 6 shows the relation between the TMPTMA content and compressive strength of PMMA-PC cast at -20°C. Irrespective of curing method, the effect of the TMPTMA content on the compressive strength of PMMA-PC is hardly recognized.

Figure 7 shows the strength development of PMMA-PC after the peak exotherm time. After the peak exotherm time, the compressive strength of PMMA-PC is elevated with additional curing time at low temperatures of 0°C and -20°C, and tends to become constant within about one day.

On the basis of the foregoing data, considering the use of the prepackaged method from a viewpoint of the simplified applications of PMMA-PC, the appropriate formulations of the binder with a good balance of performance and economy may be recommended (Table 5). By applying these formulations of the binder, PMMA-PC has a peak exotherm time of approximately 1 hr and compressive strengths of about

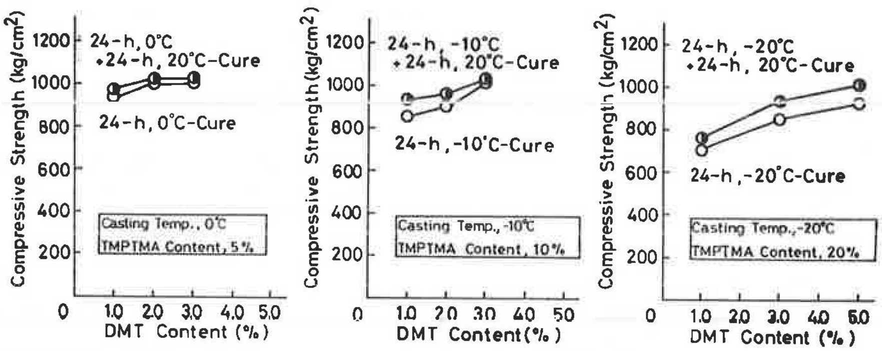

FIGURE 5 DMT content versus compressive strength of PMMA-PC.

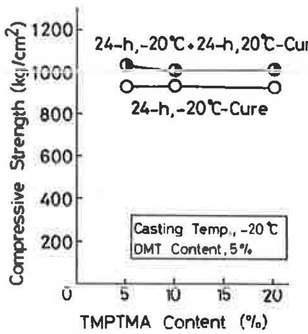

FIGURE 6 TMPTMA content versus compressive strength of PMMA-PC cast at 20°C.

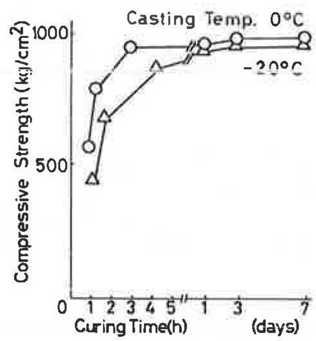

FIGURE 7 Strength development of PMMA-PC after peak exotherm.

TABLE 5 Recommendable Formulations of Binder for PMMA-PC Cast at Low Temperatures

Ambient and Materials Temperatures (°C)	Formulation by Weight			
	MMA + * PMMA	TMPTMA	BPO (as solids)	DMT
0 ~ -10	90	10	2.0	2.0~3.0
-20	80	20	2.0	5.0

Note; * MMA : PMMA = 90 : 5 (By Weight).

500 kg/cm² at the peak exotherm time, and 900 kg/cm² or higher in a 1-day cure even when the ambient and materials temperatures are in the range of 0°C to -20°C. The compressive strength of PMMA-PC cured at such low temperatures is much the same as that of a 1-day -20°C 50% R.H.-cured one.

It is evident from these test results that PMMA-PC is promising as a concrete material for construction works in cold districts because of its superior strength developed in low-temperature curing.

CONCLUSIONS

The working life of the binder and the peak exotherm time of PMMA-PC decrease with an increase in DMT and TMPTMA contents and a rise in test temperature. The relation between the working life of the binder and the DMT and TMPTMA contents can be expressed by Equation 1. By using a nomograph prepared on the basis of this equation, the DMT and TMPTMA contents can be estimated for the desired working life of the binder at different ambient and materials temperatures. The relationship between the working life of the binder and the peak exotherm time of PMMA-PC can also be expressed by Equation 2. From this relationship, the peak exotherm time can be predicted by determining the working life.

Irrespective of curing method, the compressive strength of PMMA-PC increases with a rise in DMT content, but the effect of TMPTMA content on the compressive strength is hardly recognized.

By applying the optimum formulations of the binder suggested in Table 5, PMMA-PC has a peak exotherm time of approximately 1 hr and compressive strengths of about 500 kg/cm² at the peak exotherm time and 900 kg/cm² or higher in a 1-day cure even when the ambient and materials temperatures are in the range of 0°C to -20°C. It is obvious from these results that PMMA-PC is promising as a concrete material for construction works at low temperatures.

REFERENCES

1. D.W. Fowler, A.H. Meyer, and D.R. Paul. Low Temperature Curing of Polymer Concrete. Polymers in Concrete, Proc., Third International Congress on Polymers in Concrete, Vol. 1, College of Engineering, Nihon University, Koriyama, Japan, 1982, pp. 421-434.
2. Y. Ohama and T. Kobayashi. Working Life of Polymethyl Methacrylate Concrete and Its Control. Journal of the Society of Materials Science, Japan, Vol. 32, No. 358, 1983, pp. 215-221.

Evaluation of Rapid-Setting Concretes

DAVID MACADAM, KEVIN SMITH, DAVID W. FOWLER, and ALVIN H. MEYER

ABSTRACT

Rapid-setting materials are becoming widely available. Transportation agencies have a strong need for materials that will set rapidly yet provide a durable repair especially in urban areas. There are eight categories of rapid-setting concretes, and these possess a wide range of characteristics and properties. A survey of state transportation departments indicated that there are several preferred properties and characteristics of rapid-setting materials. A test program was conducted to evaluate test procedures for these materials and to determine the properties of a range of rapid-setting concretes. The results of this test program are summarized in this paper.

Rapid-setting repair materials have been in wide demand for the repair of portland cement concrete pavements and bridge decks. High traffic volumes in urban areas require materials that will cure rapidly yet provide adequate strength and durability.

Many types of repair materials are available:

- Portland cement,
- Other chemical-setting cements,
- Thermo-setting materials,
- Thermoplastics,
- Calcium sulfate,
- Bituminous materials,
- Composites, and
- Additives used to alter mix characteristics (1).

Many of the materials are proprietary and the formulations are not made available. Some are suitable only for temporary repairs, and others are designed for permanent repairs. Some can be used only in hot weather, and some can be used only in dry conditions.

A survey was conducted in Texas and nine other states to determine the desired characteristics and properties. Setting time, durability, and ease of mixing, placing, and finishing were considered to be the most important characteristics. Bond strength, flexural strength, and shrinkage were selected as the most important properties (2).

A test program has been conducted to evaluate test methods for rapid-setting materials and to evaluate selected rapid-setting materials. A summary of the results of this program follows.

MATERIALS

1. Magnesium phosphate (MPH). The magnesium phosphate material is packaged as a mortar mix; that is, fine aggregate is included. The material is water-activated and may be extended by the addition of coarse aggregate.

2. Magnesium polyphosphate (MPPH). The magnesium polyphosphate concrete is packaged as a two-component mortar mix. The dry magnesia component is activated by the liquid phosphate component. The mix may be extended by the addition of coarse aggregate.

3. Gypsum-modified portland cement (GPC). This mixture of gypsum (calcium sulfate) and portland cement is packaged neat and water-activated. Sand is added to obtain a mortar. Both sand and coarse aggregate are added to the material to obtain a concrete mix.

4. Modified portland cement (MPC). This modified portland cement is packaged as a mortar mix and is water-activated. The modifiers are proprietary. It may be extended by the addition of coarse aggregate.

5. Accelerated concrete. The accelerated concrete consists of portland cement concrete used in combination with an accelerating admixture. The concrete mix contains Type III cement with a low water-cement ratio (0.45) and a high cement content (7-sack mix). A high-range water reducer is added to improve workability when required. Accelerators used include: calcium chloride ($CaCl_2$), calcium nitrite [$Ca(NO_2)_2$], calcium nitrate [$Ca(NO_3)_2$], and sodium thiocyanate (Na SCN).

EVALUATION TESTS

Compressive Strength

Mortar Cubes

The mortar cube compressive strength test was run according to ASTM C109-80 "Compressive Strength of Hydraulic Cement Mortars" for the accelerated concrete mixes. For the prepackaged rapid-setting materials, the composition of the mortars was according to manufacturers' recommendations. The specimens were cast in 2 x 2 x 2-in. steel molds.

Cylinders

The compression cylinders were made and tested according to ASTM C39-81 "Compression Strength of Cylindrical Concrete Specimens." Specimens were cast in cardboard molds and capped to provide a smooth loading surface. Specimens containing 0.375-in. aggregate were 3 in. x 6 in. whereas specimens containing 0.75-in. aggregate were 6 in. x 12 in.

Modulus of Elasticity

The modulus of elasticity of the rapid-setting materials was determined according to ASTM C469-65 "Static Modulus of Elasticity of Concrete in Compression." A compressometer was attached to 7-day compression cylinders to determine strains.

Flexural Strength

The flexural strength of 2 in. x 2 in. x 12-in. beams was determined according to ASTM C78-75 "Flexural Strength of Concrete." The beams spanned 6 in. and were loaded at one-third points. Mixes containing 0.375-in. coarse aggregate were used.

Set Time

Gilmore Needle

Set times for the rapid-setting materials were determined according to ASTM C266-77 "Time of Setting of Hydraulic Cement by Gilmore Needles." Mortar mixes proportioned according to manufacturers' recommendations were used to form 3-in.-diameter x 0.5-in.-thick pats.

Penetration Resistance

The penetration resistance set time was performed according to ASTM C403-80 "Time of Setting of Concrete Mixtures by Penetration Resistance" for accelerated concretes. Mortar mixes were used for the packaged rapid-setting materials.

Peak Exotherm

Peak exothermic temperature was used to estimate set times of packaged rapid-setting materials. A thermocouple was used to measure the temperature at the center of 3-in. x 6-in. and 6-in. x 12-in. cylindrical specimens.

Bond

Direct Shear Bond

For the direct shear bond test, a 5 x 5 x 0.5-in. layer of rapid-setting mortar was cast onto a 5 x 5 x 1-in. cured portland-cement concrete plate. The bond surface of the PCC plate was troweled smooth and roughened by wirebrushing. Direct shear was then applied to the bond plane until failure.

Flexural Bond

The flexural bond strength of rapid-setting concrete to PCC was determined by casting a 2 x 2 x 6-in. section of rapid-setting concrete against a 2 x 2 x 6-in. cured PCC prism. The resulting 2 x 2 x 12-in. specimen was loaded at one-third points of the 6-in. span until failure.

Sandblast Abrasion

The abrasion resistance test was run according to ASTM C418-76 "Abrasion Resistance of Concrete by Sandblasting." Seven-day mortar specimens of 5 in. x 5 in. x 0.5 in. were used.

Length Change

The length change test was carried out according to ASTM C157-80 "Length Change of Hardened Cement Mortar and Concrete." For rapid-setting concretes, both 1 x 1 x 0.25-in. mortar specimens and 2 x 2 x 0.25-in. concrete specimens were used. For accelerated concretes, 2 x 2 x 11.25-in. concrete specimens were used. For the rapid-setting mortar and concrete specimens, measurement of length change was started immediately after removal of specimens from forms, approximately 1 hour after casting.

Freeze-Thaw Resistance

The freeze-thaw resistance test was run according to ASTM C666-80 "Resistance of Concrete to Rapid Freezing and Thawing." Concrete specimens of 3 x 3 x 16-in. were tested. Specimens were cured 7 days at the start of testing. Specimens were frozen and thawed in water at a rate of 4 cycles per day.

TEST VARIABLES

1. Temperature. For ambient temperatures of 40, 75, and 110°F, flexural strength, cylinder compressive strength, and set times were determined for all materials.
2. Aggregate type, size, and quantity. Concrete mixes with variable (a) type of aggregate (siliceous or limestone), (b) size of aggregate (0.375 in. or 0.75 in.) and (c) quantity of aggregate (coarse aggregate weight to total concrete weight ratios of 0.10, 0.20, and 0.30) were tested for cylinder compressive strength. These tests were performed on packaged rapid-setting materials only.
3. Type of cement. For accelerated concretes, the brand of Type III cement was examined as a variable. Flexural strength, cylinder and mortar cube compressive strength, and set times were determined.

TEST RESULTS

Compressive Strength

The effects of test variables on rapid-setting materials and accelerated concretes were determined from the relationship between compressive strength and time. Compressive strength versus time curves for accelerated concretes at ambient temperatures of 40, 75, and 110°F are shown in Figure 1. All accelerators tested are plotted for 75°F. The most rapid strength gain occurred in mixes containing calcium chloride and calcium nitrite.

Compressive strength versus time curves for the rapid-setting materials at 40, 75, and 110°F are shown in Figures 2-4. At all temperatures, the magnesium phosphate and magnesium polyphosphate exhibited the most rapid strength gain at early times.

In Figure 5, compressive strength versus time relationships for rapid-setting concrete mixes with varied quantities of coarse aggregate are shown. Mixes with ratios of coarse aggregate weight to total concrete of 0.10, 0.20, and 0.30 were evaluated. For all materials, the compressive strength was increased by reducing the percentage of coarse aggregate. The increase in strength was most dramatic in the magnesium phosphate material.

The effect of size and type of aggregate on compressive strength of rapid-setting materials is shown in Figure 6. In general, the mixes containing 0.375-in. limestone aggregate achieved higher strength.

Modulus of Elasticity

The modulus of elasticity and 7-day cylinder compressive strengths for rapid-setting materials are given in Table 1.

Flexural Strength

The effect of temperature on flexural strength was determined for rapid-setting materials and accelerated concretes. In Figure 7, flexural strength versus time curves for accelerated concretes are shown for temperatures of 40, 75, and 110°F. All accelerators tested are shown for 75°F. Mixes containing calcium chloride and calcium nitrite exhibited the most rapid strength gain. Only curves for mixes

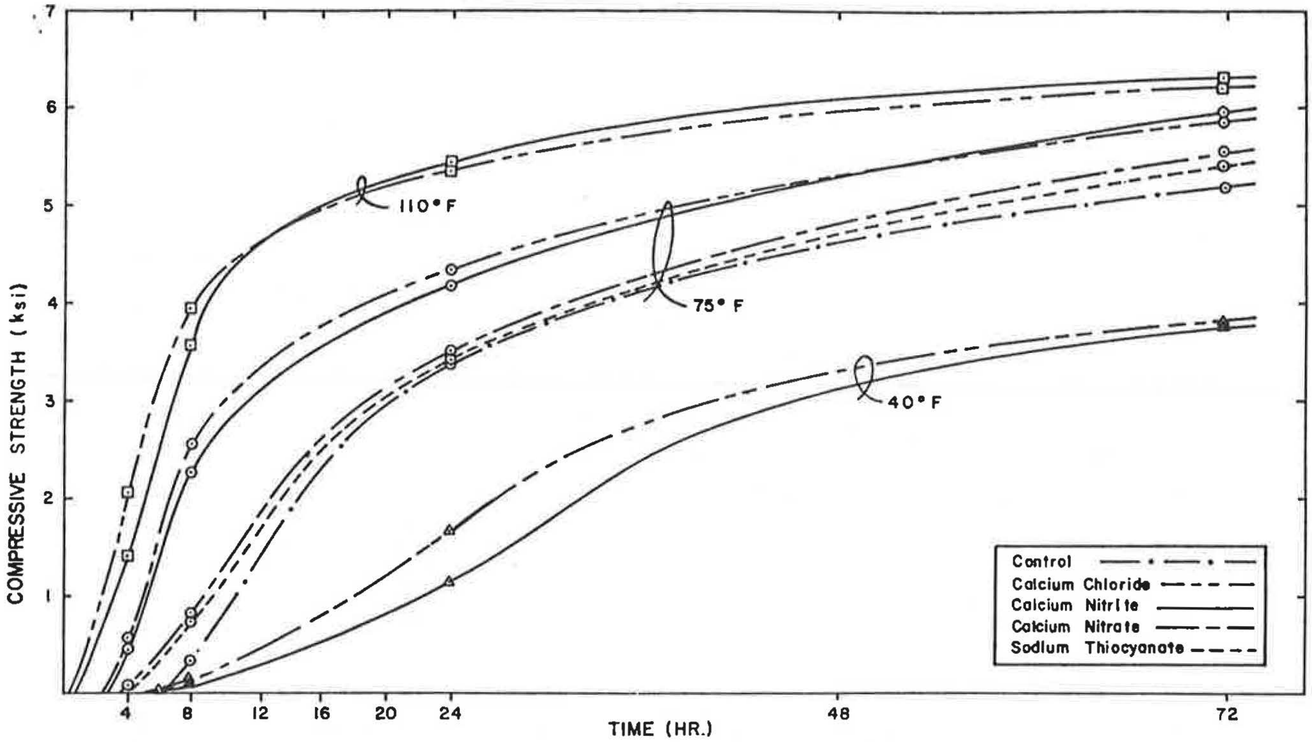

FIGURE 1 Compressive strength of accelerated concrete as a function of time and ambient temperature.

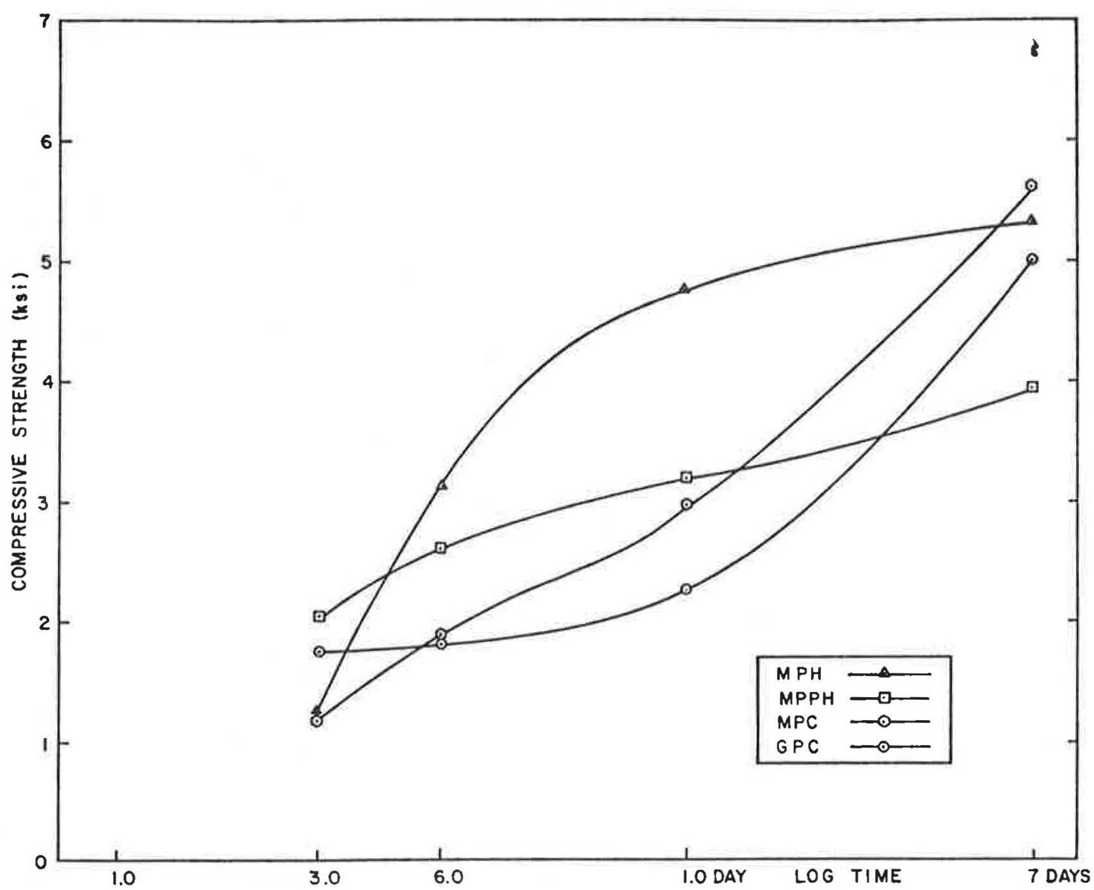

FIGURE 2 Compressive strength of rapid-setting concretes as a function of time at ambient temperature of 40° F.

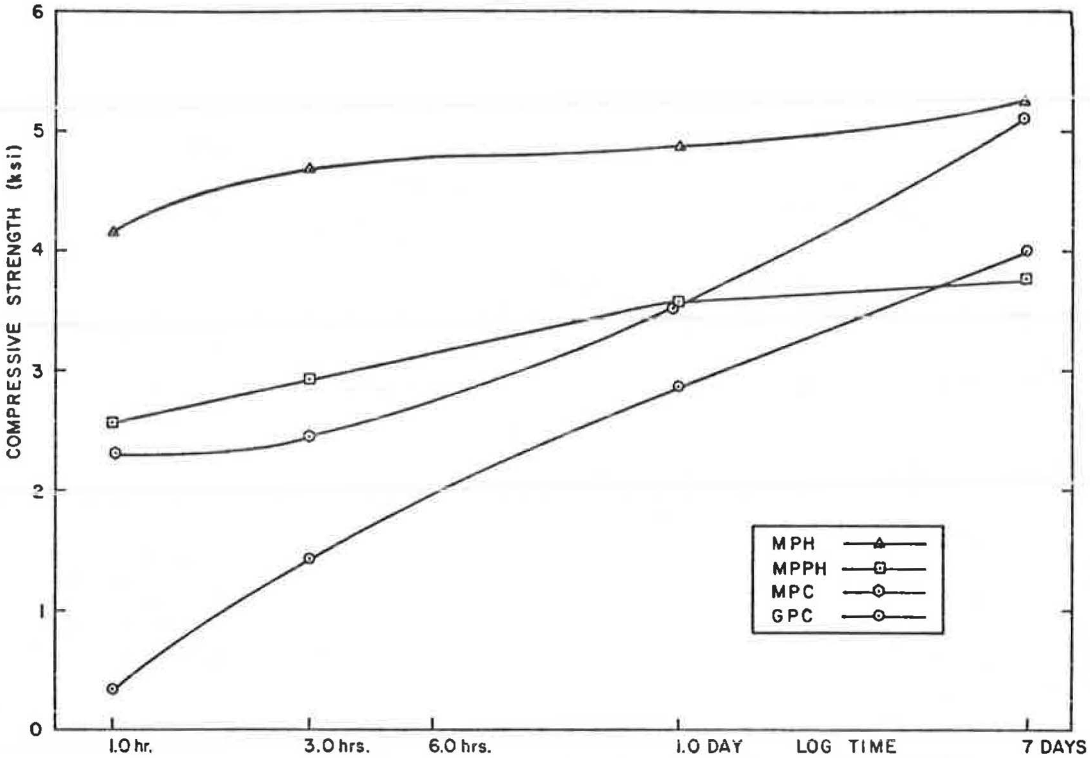

FIGURE 3 Compressive strength of rapid-setting concretes as a function of time at ambient temperature of 75°F.

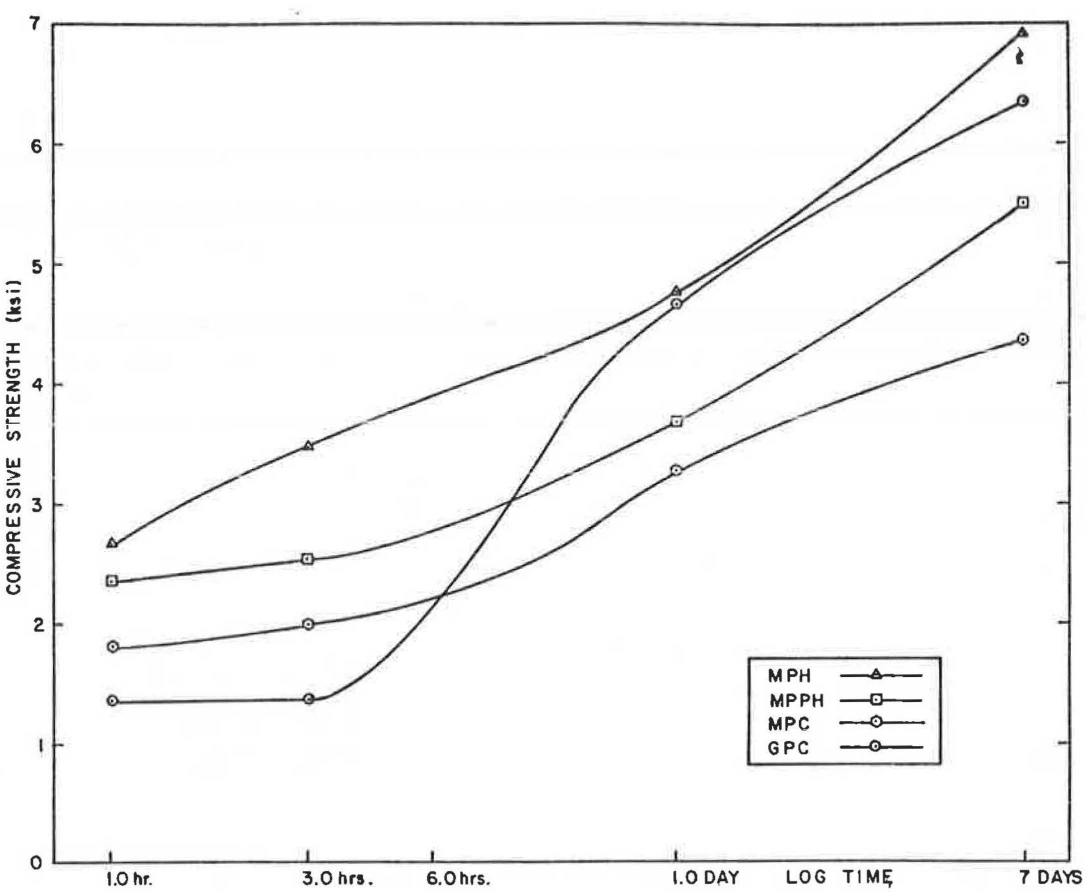

FIGURE 4 Compressive strength of rapid-setting concretes as a function of time at ambient temperature of 110°F.

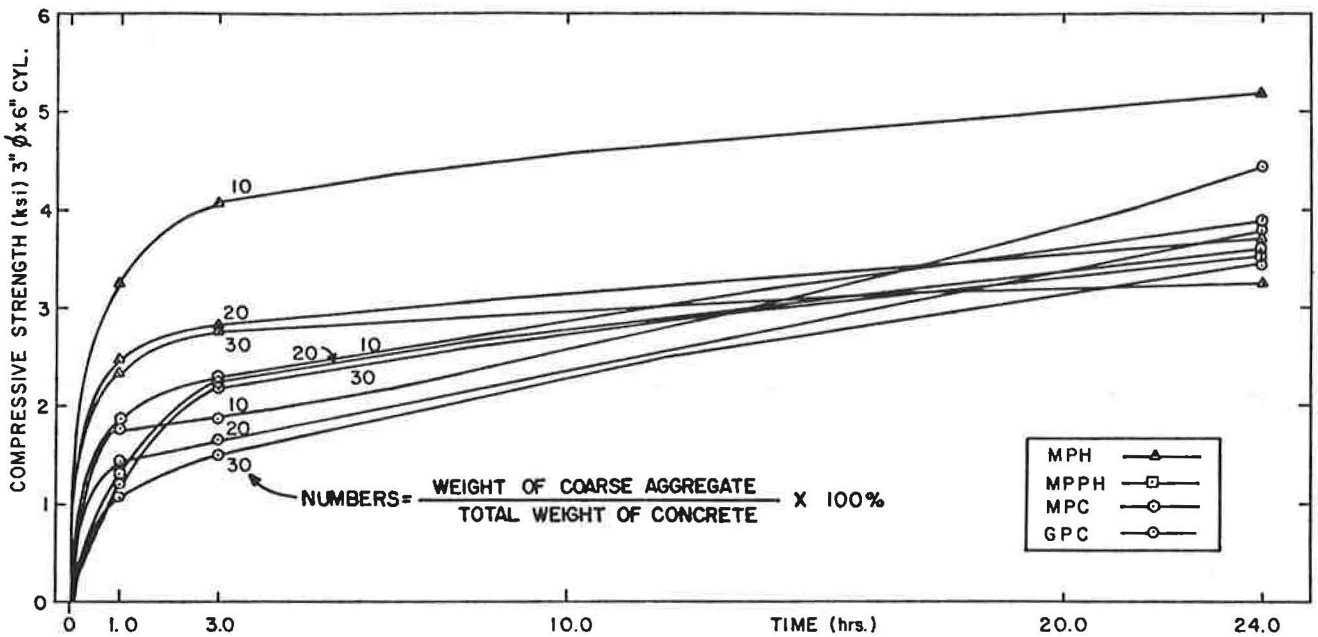

FIGURE 5 Compressive strength of rapid-setting concrete mixes with varied quantities of coarse aggregate.

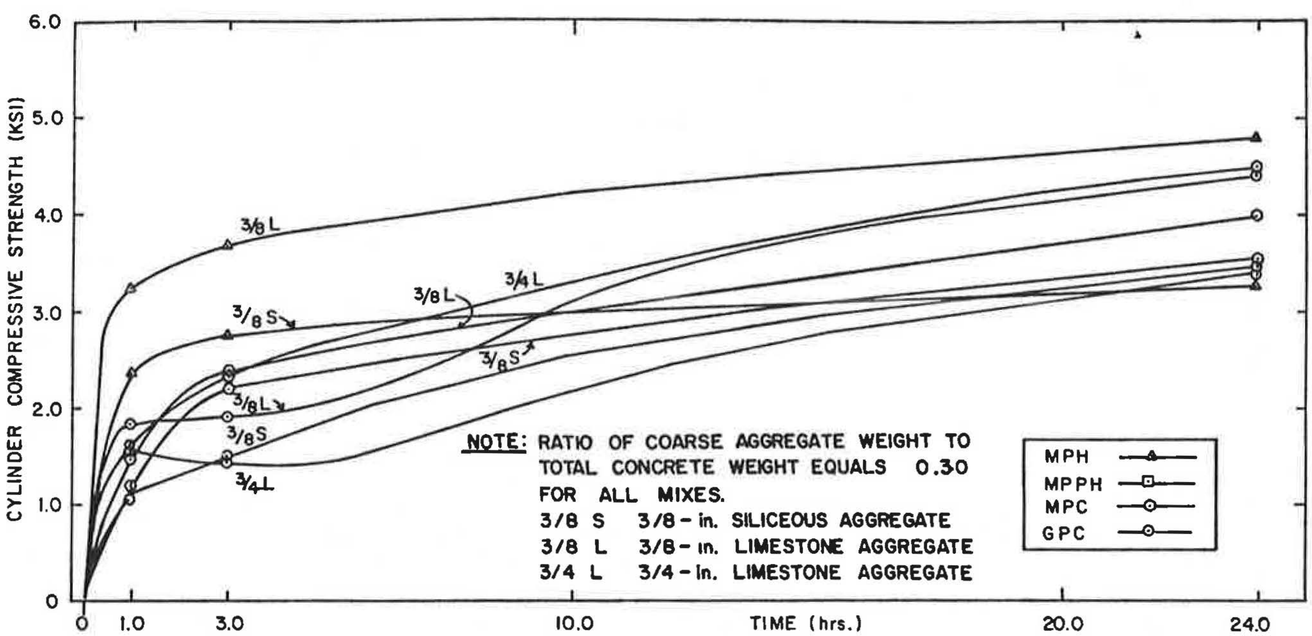

FIGURE 6 Compressive strength of rapid-setting concrete mixes with varying types of coarse aggregates.

TABLE 1 Compressive Strength and Modulus of Elasticity at Age of 7 Days

Material	Average 7-Day Compressive Strength (psi)	Average Modulus of Elasticity (1×10^6 psi)
Magnesium phosphate	5,230	4.51
Magnesium polyphosphate	3,730	6.41
Gypsum-based portland cement	4,000	4.75
Modified portland cement	5,100	3.97

using these accelerators were plotted for 40°F and 110°F.

Flexural strength versus time curves for the rapid-setting materials at 40°F, 75°F, and 110°F are shown in Figure 8. At 75°F and 110°F, the magnesium phosphate and magnesium polyphosphate exhibited the most rapid strength gain. At 40°F the gypsum-based portland cement and the modified portland cement had higher 6-hr strengths.

Set Time

Initial and final set times for accelerated concretes, determined by penetration resistance, are

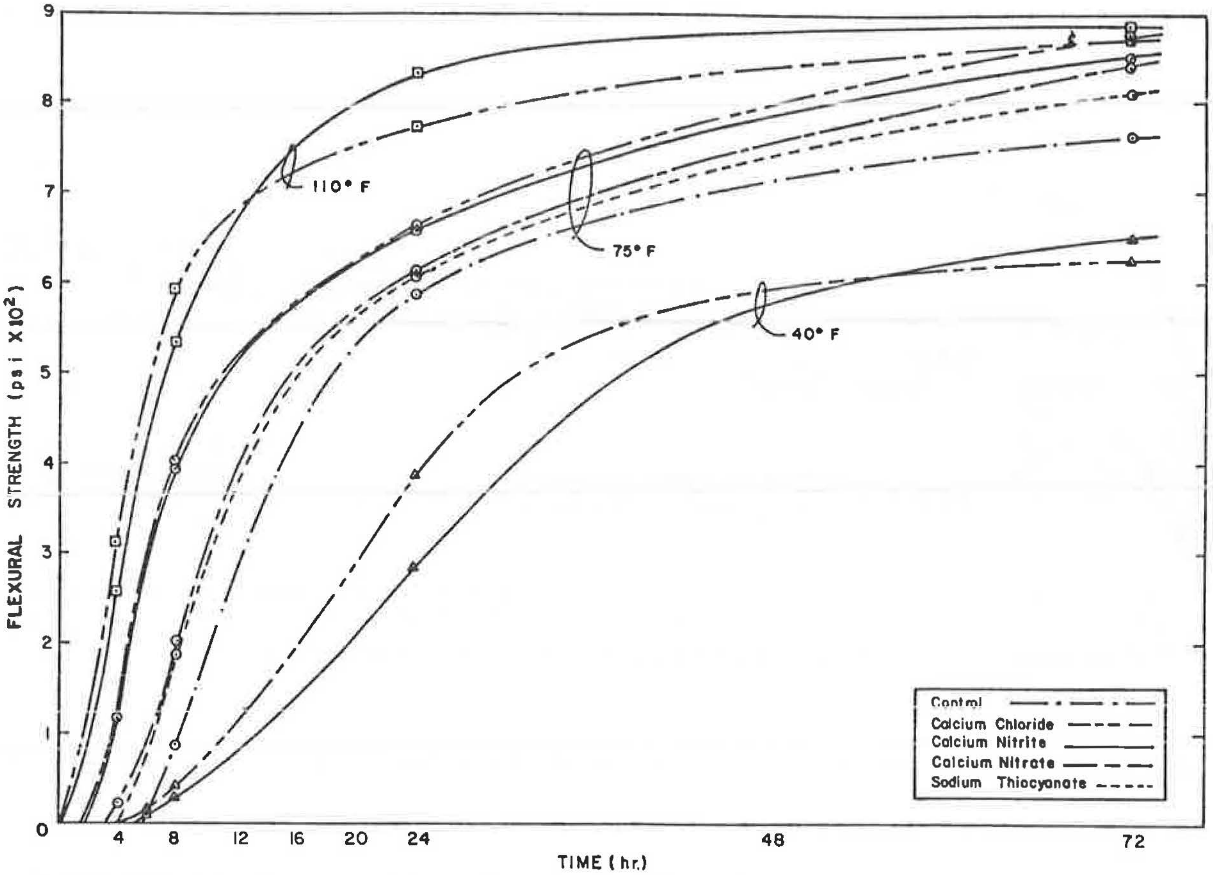

FIGURE 7 Flexural strength of accelerated concrete as a function of time and ambient temperature.

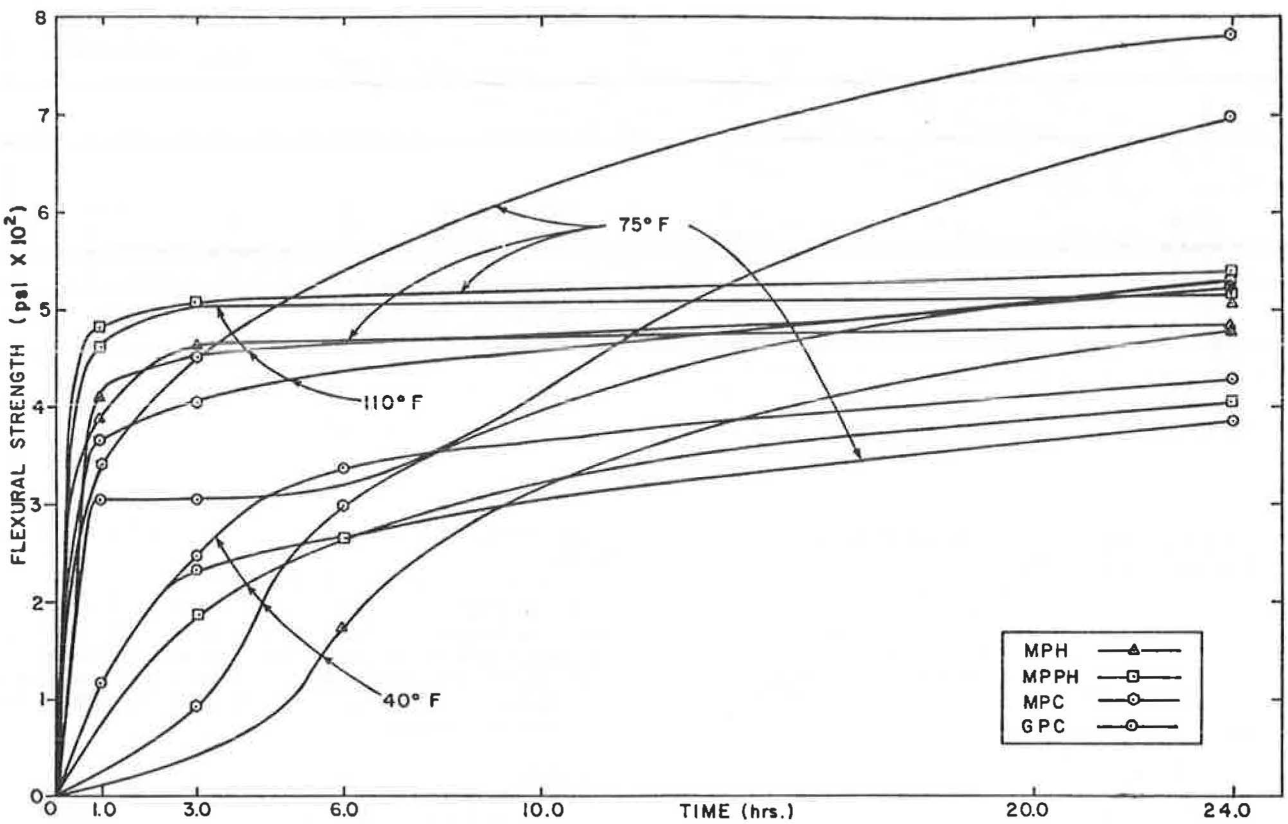

FIGURE 8 Flexural strength of rapid-setting concretes as a function of time and ambient temperature.

shown in Figure 9. Set times were determined at ambient temperatures of 40°F, 75°F, and 110°F. Calcium chloride and calcium nitrite provide the most rapid setting at all temperatures.

In Figure 10, the set times for the rapid-setting materials determined using the Gilmore needle are shown for temperatures of 40°, 75°, and 110°F. At all temperatures, the magnesium phosphate and magnesium polyphosphate set most rapidly. However, at higher temperatures these materials set too rapidly to allow adequate placing and finishing.

Bond

Direct shear bond and flexural bond tests have been performed on the magnesium phosphate and gypsum-based portland cement. The flexural bond strength of the magnesium phosphate was greater than that of the gypsum-based portland cement. The results were reversed for the direct shear bond test. The results appeared inconsistent and are not presented.

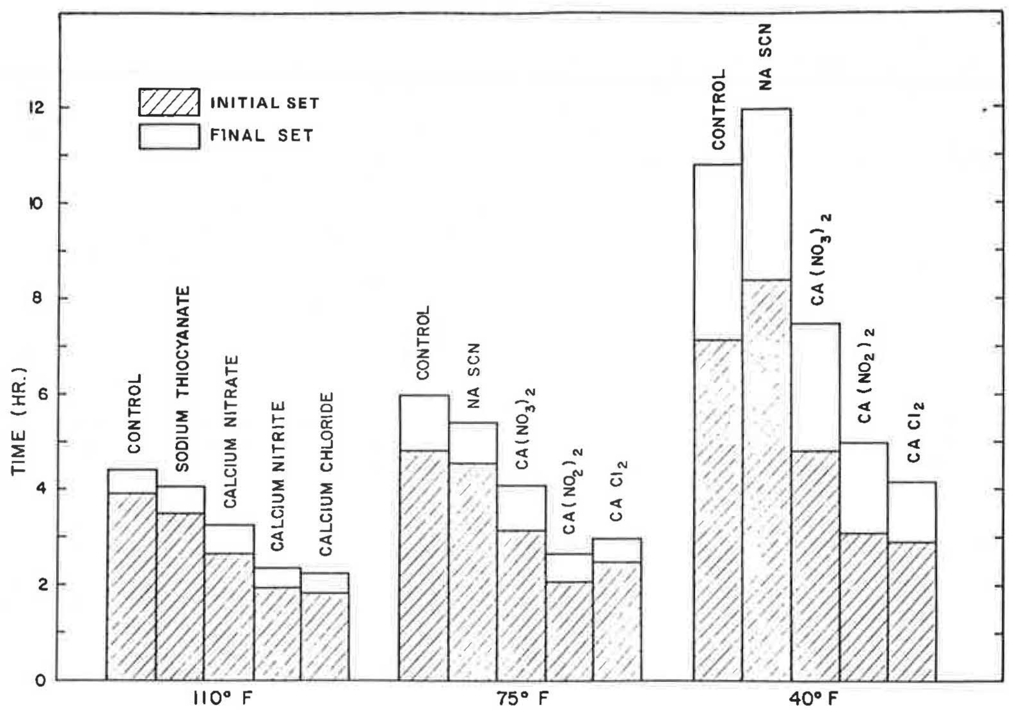

FIGURE 9 Set time of accelerated concretes by penetration resistance for various ambient temperatures.

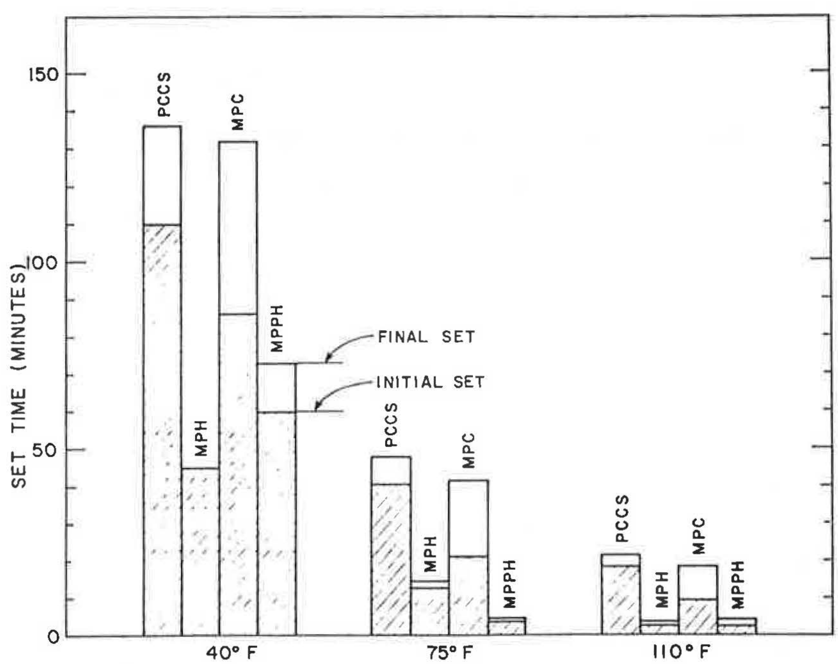

FIGURE 10 Set time of rapid-setting concretes by Gilmore needles for varying ambient temperatures.

Sandblast Abrasion

Sandblast abrasion coefficients are given in Table 2. The abrasion loss for the rapid-setting materials was significantly greater than that of the accelerated concretes.

Length Change

Change in length versus time relationships for the rapid-setting concretes are shown in Figure 11. The beams contain 0.375-in. siliceous coarse aggregate with a 0.30 ratio of coarse aggregate weight to total weight of concrete. The modified portland cement exhibited the most severe shrinkage. The gypsum-based portland cement expanded slightly.

In Figure 12, change in length versus time curves for accelerated concretes are shown. Most concretes exhibited expansion during the 7-day moist-curing period. The initial rate of shrinkage was greater for the accelerated concretes than for the control specimen.

TABLE 2 Sandblast Abrasion Coefficients

Material	Average Abrasion Coefficient (cm^3/cm^2)
Magnesium phosphate	0.164
Gypsum-based portland cement	0.117
Modified portland cement	0.007
Calcium chloride accelerated concrete	0.011
Calcium nitrite accelerated concrete	0.012

Freeze-Thaw

Results from the freeze-thaw tests on the rapid-setting materials are shown in Figure 13. Both the magnesium phosphate and the magnesium polyphosphate performed poorly with failure occurring at less than 100 cycles. The modified portland cement outperformed the other materials.

CONCLUSIONS

1. For evaluation of mechanical properties of the rapid-setting concretes and accelerated concretes, cylinder compressive strength, modulus of elasticity, and flexural strength appeared most appropriate.
2. The working time of the rapid-setting concretes was best evaluated using the Gilmore needle test. The set times of the accelerated concretes were best determined using the penetration resistance test.
3. The performance of both the rapid-setting concretes and the accelerated concretes appeared to be best evaluated using both the freeze-thaw resistance test and the shrinkage test.
4. The mortar cube compressive strength test, the peak exotherm test, the bond tests, and sandblast abrasion test appeared least appropriate in evaluating these materials.
5. In the evaluation of accelerated concretes, calcium chloride and calcium nitrite exhibited the most rapid strength gain in all tests performed.

In general, the magnesium phosphate and the magnesium polyphosphate display higher early strength

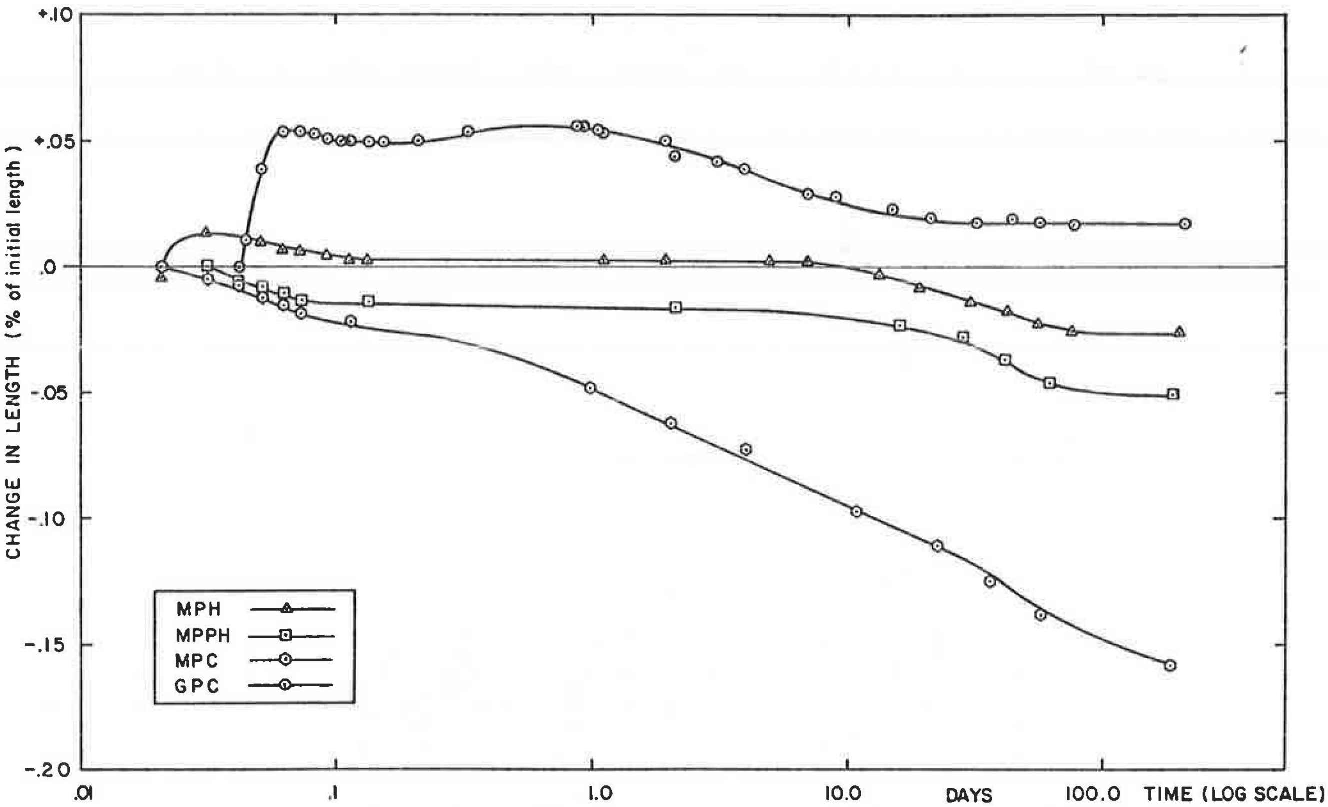

FIGURE 11 Change in length of rapid-setting concrete beams.

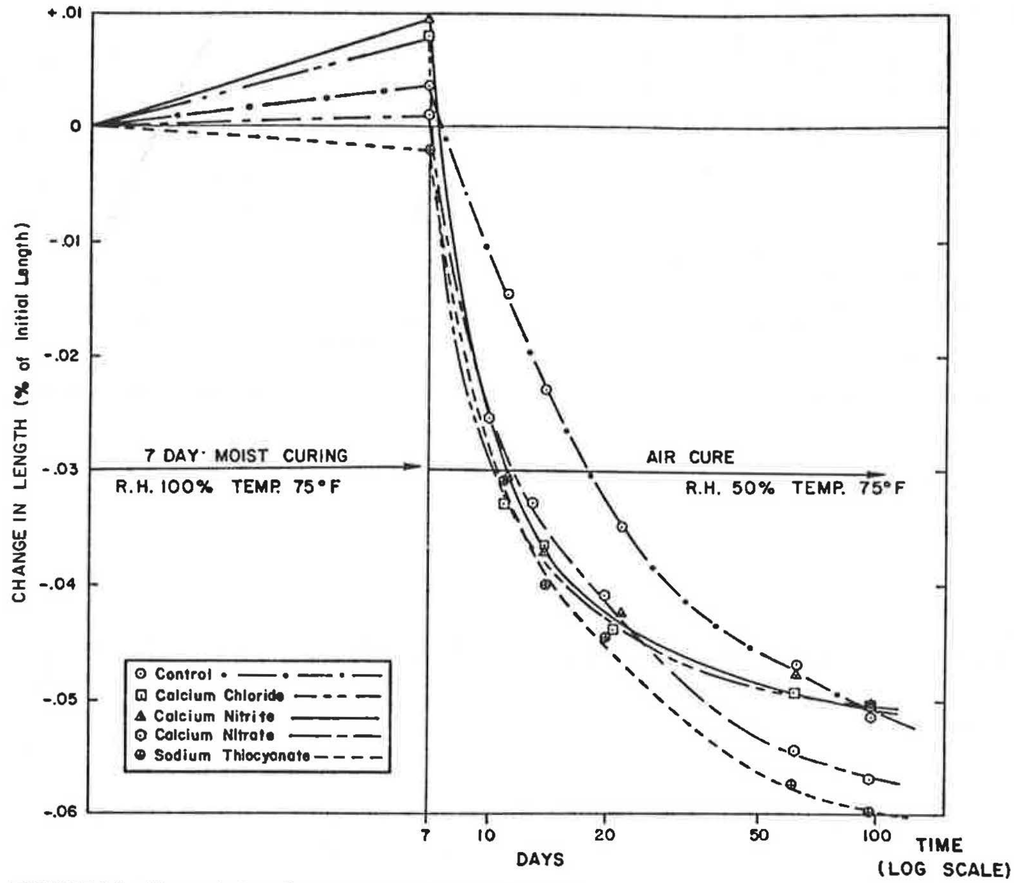

FIGURE 12 Change in length of accelerated concrete beams.

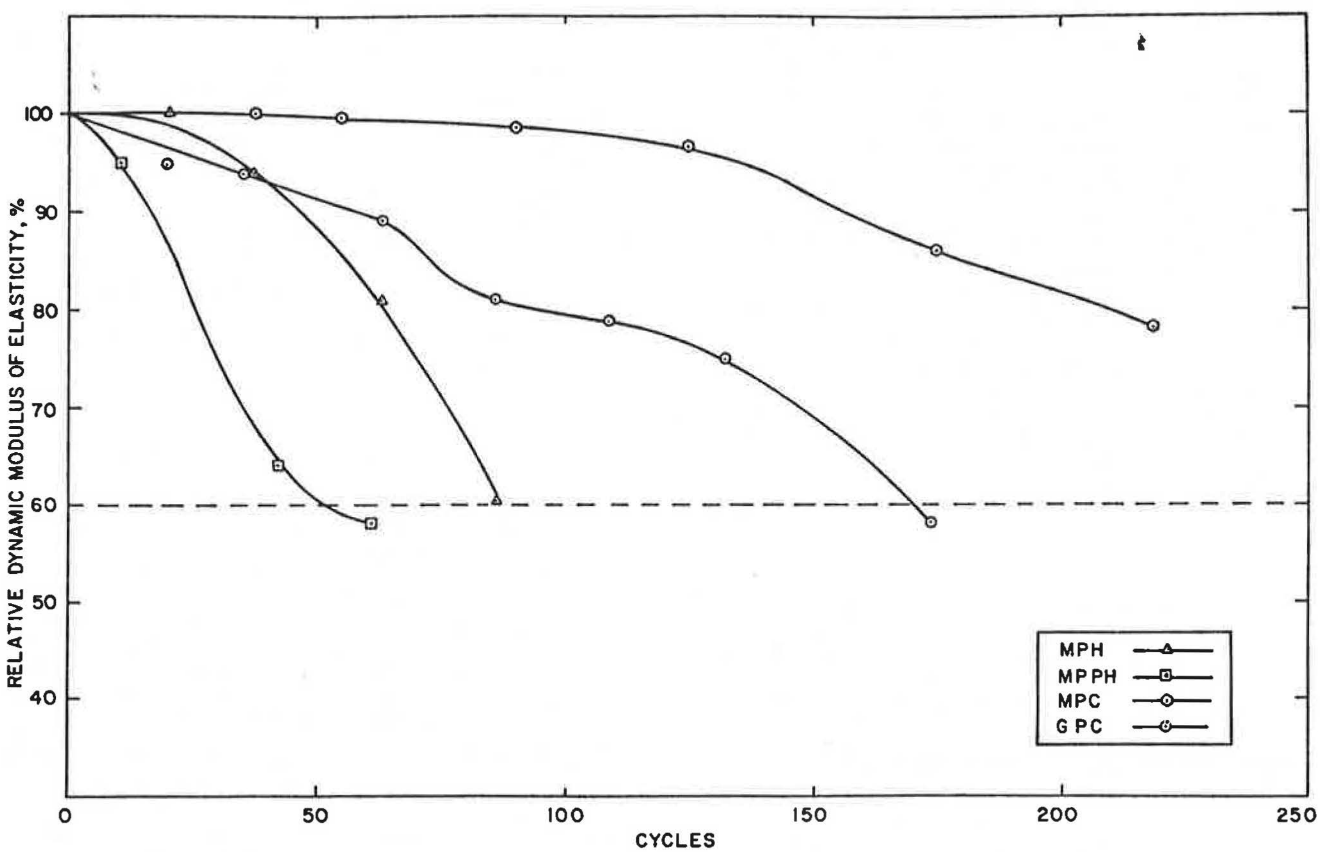

FIGURE 13 Change in dynamic modulus of rapid-setting concretes as a function of freeze-thaw cycles.

gains. However, these materials do not allow reasonable working time at higher temperatures. The freeze-thaw performance of the modified portland cement and the gypsum-modified portland cement was significantly better than for the magnesium phosphate and the magnesium polyphosphate.

ACKNOWLEDGMENTS

The authors wish to acknowledge the support provided by the Texas Department of Highways and Public Transportation and the Federal Highway Administration, U.S. Department of Transportation, for the funding of this research.

REFERENCES

1. P.E. Irick. Rapid-Setting Materials for Patching of Concrete. In NCHRP Report 45. TRB, National Research Council, Washington, D.C., 1977, 13 pp.
2. G.P. Beer, D.W. Fowler, A.H. Meyer, and D.R. Paul. Results of a Survey on the Use of Rapid-Setting Repair Materials. Research Report 311-1. Center for Transportation Research, The University of Texas, Austin, Dec. 1982.

The opinions expressed are those of the authors and not necessarily of the sponsoring agencies.

Shear Transfer in Two-Layer Composite Systems

EDWARD G. NAWY

ABSTRACT

Experiments were conducted to evaluate the shear transfer capacity of two-layered systems using polymer-modified concrete as the top layer. The experimental program was designed to verify the general theory of shear transfer mechanism for concrete and to evaluate the necessary constants of the theoretical expressions. The general theory presented covers structural members with (a) no shear reinforcement, (b) moderate shear reinforcement, and (c) high shear reinforcement. Four groups of specimens were tested. Group A specimens were used to investigate the relation between intrinsic bond shear transfer capacity and the strength of the composite materials. Group B specimens contained various amounts cast monolithically using ordinary concrete to serve as control specimens. Group C contained control specimens made up of totally cast-in-place concrete with no cold joints. Group D contained control specimens made up of cast-in-place concrete over precast concrete.

The problem of shear transfer in concrete structures arises when shearing loads must be transmitted across a definite and often weak plane. Typical situations are encountered in corbels, nonmonolithic joints in concrete, and composite elements where concrete is cast in place over a precast member.

Since the early 1950s, several researchers have studied this problem. It is generally recognized that the shear transfer capacity in concrete elements can be attributed to any of the following: friction at the shear plane, interlocking action of the aggregates, dowel action of any reinforcement, and bond forces (apparent cohesion) at the shear plane. However, there continues to be a great deal of debate regarding the relative importance of the various parameters.

Of the many expressions for shear transfer capacity (1-12), the simplest and most widely used has been that based on the shear friction hypothesis of Birkeland and Birkeland (1). This expression with minor modification (9) has been incorporated in the American Concrete Institute (ACI) code. Although the expression is useful in estimating shear transfer capacities, its very formulation ignores "apparent cohesion" (bond) and dowel action resistance.

This paper is a condensation of "Shear Transfer in Concrete and Polymer Modified Concrete Members Subjected to Shearing Loads" (2), which deals with the shear capacity of the normal concrete-polymer modified concrete interface. A general theory on the shear transfer mechanism is also presented correlating with the tests (13,14). The discussion covers any two-layered system.

A THEORY OF SHEAR TRANSFER MECHANISM FOR CONCRETE

It is hypothesized that the total shear transfer capacity in a concrete element is made up of: intrinsic bond shear resistance, ΔV_b; shear friction resistance, ΔV_f; aggregate interlock resistance, ΔV_i; and dowel resistance, ΔV_d.

Consider an element subjected to a shearing load (Figure 1). Initially, all shear resistance is provided by intrinsic bond. After cracking has started and some slip has occurred, resistance is developed through friction, aggregate interlock, and dowel action. Shear transfer through friction is due purely to the surface shear resistance to slip. Aggregate interlock is due to the interlocking action of the aggregates at the failure plane. Dowel action shear resistance is a result of the steel reinforcement as shown in part b of Figure 1.

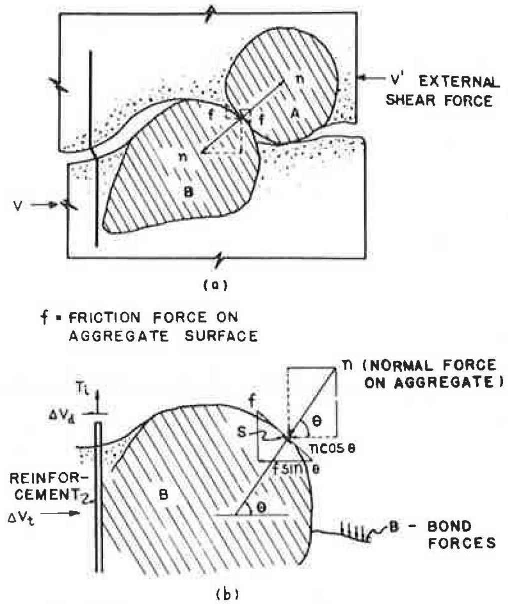

FIGURE 1 Idealized shear resisting forces [shear resistance through friction (f sin θ), aggregate interlock (n cos θ), and dowel action V_d].

Summing up the resistances in the horizontal direction gives

$$V_t = \Delta V_b + \Delta V_f + \Delta V_i + \Delta V_d \tag{1}$$

and the nominal shear transfer capacity becomes

$$\upsilon_t = [\int_A \Delta V_t]/A \tag{2}$$

where A is area of the shear plane. (Note: a list of notations used in the equations appears at the end of this paper.)

By idealizing concrete mass as brittle material containing micro-cracks, it has been shown that bond shear strength is an intrinsic property of any given concrete (13). The resistance due to bond can be represented by $\nu_b = BdA$, where B is strength per unit bond area.

If n' is the total number of bars, and T_f is the load transferrable by dowel action per bar, the expression for the total dowel force from Dulacska (4) modified such that the shear reinforcement is taken normal to the fracture plane yields a total dowel force.

$$n'T_f = [4A_s'/\pi] \{[1 - (f_s/f_y)^2]\ 1.51\ f_c'/f_y\}^{1/2} \tag{3}$$

The shear stress over the cross-sectional area bw of the failure plane is $\nu_d = (n'T_f)/bw$. If $\bar{\rho} = n'A_s'/bw$ = steel ratio for shear transfer reinforcement, then:

$$\upsilon_d = [4\bar{\rho} f_y/\pi] \{[1 - (f_s/f_y)^2]\ 1.51 f_c' f_y\}^{1/2} \tag{4}$$

where ν_d represents dowel action shear resistance. This expression incorporates the condition that as the tension force in the shear reinforcing steel approaches the yield point, ν_d tends to become zero.

For friction and aggregate interlock, the contribution of the surface frictional force to transfer strength (Figure 1) is expressed as

$$\upsilon_f = f \sin\theta \tag{5}$$

where f is frictional force on the surface. The contribution due to aggregate interlock is

$$\upsilon_i = n \cos\theta \tag{6}$$

where n is normal force per unit area. If T_i = tension force in the steel per unit area = $\bar{\rho} f_s$, summing forces in the direction n gives

$$\upsilon_n = (\bar{\rho} f_s + BdA) \sin\theta - \upsilon_d \cos\theta$$

Frictional force f = μ_n where μ is the coefficient of friction between the aggregate and the cement mortar surrounding it.

Recollecting terms and integrating these forces over the surface area of the aggregates and dividing by the cross-sectional area of the failure plane, the resistance ν_f due to friction and ν_i due to aggregate interlock can be defined as follows:

$$\upsilon_f = \mu[(\bar{\rho} f_s + Bk_1)\pi/4 - 1/2\ \upsilon_d]\, k_2 + \mu(\bar{\rho} f_s + Bk_1)k_3 \tag{7}$$

$$\upsilon_i = [\bar{\rho} f_s + Bk_1)/\pi - 1/2\upsilon_d]\, k_2 \tag{8}$$

where

k_1 = ratio of bond area to total shear area,
k_2 = ratio of projected area of aggregates to total shear area,
$k_3 = 1 - k_1 - k_2$, and
B = bond shear strength for unit area.

The detailed derivation of Equations 7 and 8 can be found in Ukadike (13,pp.145-149).

Adding the various components of resistance and rearranging terms gives

$$\upsilon_t = Bk_1 + (4\bar{\rho} f_y/\pi)\{[1 - (f_s/f_y)^2]\ 1.51\ f_c'/f_y\}^{1/2}\{1 - k[1 + (\mu/2)]\} + (\bar{\rho} f_s + Bk_1)\{\mu k_3 + k_2\ \pi[(\mu/4) + 1]\} \tag{9}$$

Members with No Shear Reinforcement

When no shear reinforcement is provided (i.e., $\bar{\rho} = 0$) Equation 9 reduces to:

$$\upsilon_t = Bk_1 + Bk_1\ [\mu k_3 + k_2 \pi(\mu/4 + 1)] = C_o \text{ (a constant)} \tag{10}$$

This may be written as

$$C_o = Bk_1(1 + \mu') = \text{“apparent cohesion”} \tag{11}$$

where $\mu' = [\mu k_3 + k_2\pi(\mu/4 + 1)]$ = apparent coefficient of friction.

The term Bk_1 is the value of shear transfer capacity that would be developed if there were no coarse aggregates at the shear plane (i.e., in mortars). The other term, $Bk_1\mu'$, is due to aggregate interlock and friction forces made possible by the intrinsic bond force, which creates a compression on the failure surfaces. The factors $\pi/4$, $1/\pi$, and 1/2 reflect the shape of the aggregates (assumed spherical) in the concrete mix. The constants k_1 and k_2 depend on the concrete strength and aggregate ratio, respectively, as the definitions of k_1 and k_2 imply.

Members with Moderate Shear Reinforcements

If a moderate amount of shear reinforcement is provided (Figures 2 and 3), shear failure will be pre-

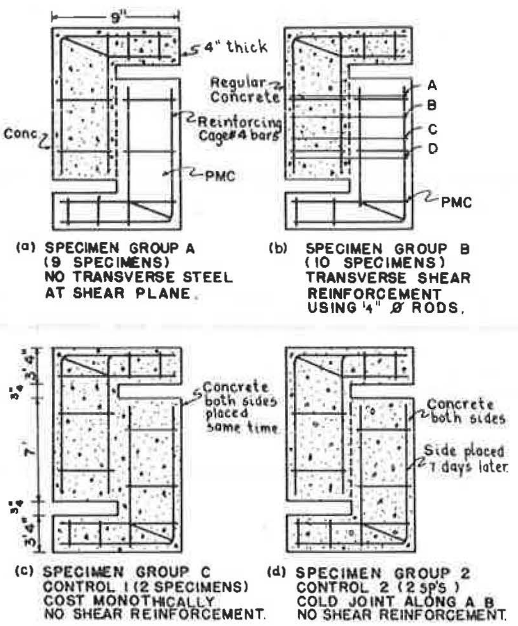

FIGURE 2 Test specimen groups.

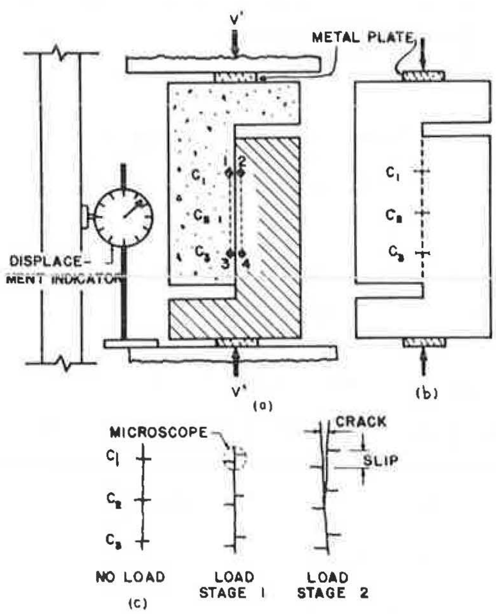

FIGURE 3 Instrumentation of L-prism specimens.

ceded by the yielding of the reinforcement, that is, $f_s = f_y$.

Therefore,

$$v_t = (Bk_1) + (\bar{\rho}f_y + Bk_1)\,[\mu k_3 + k_2\pi(\mu/4 + 1)] \tag{12}$$

Rearranging the expression and grouping constant terms yields

$$v_t = \rho f_y \times \mu' + C' \tag{13}$$

$$= I \times \mu' + C' \tag{14}$$

where $C' = (Bk_1)(1 + \mu')$ and $I = \bar{\rho}f_y$ (defined as shear reinforcing strength).

Experimental investigations show that the addition of shear reinforcement results in a rapid increase of v_t. This is because an increase in the value of I not only provides compression at the shear surface, but also inhibits cracking, with the new higher value of the apparent cohesion C' at $\bar{\rho} > 0$ as compared to apparent cohesion C at $\bar{\rho} = 0$.

Equation 13 is similar to that proposed by Hermansen and Cowan (8). Unlike the shear friction hypothesis, the expression accounts for the shear transfer capacity observed in shear tests where there has been no shear-reinforcing steel.

Members Having High Shear Reinforcement

If the shear reinforcing strength ($\bar{\rho}f_y$) is very high, the aggregates on the shear plane may be dislocated or sheared off as load is applied and k_1 and k_2 will equal 0. Shear transfer capacity will then only be due to friction and dowel action of reinforcement.

$$v_t = (4\bar{\rho}f_y/\pi)\left\{(1.51\, f_c'/f_y)[1 - (f_s/f_y)^2]\right\}^{1/2} + \bar{\rho}f_s\,\mu \tag{15}$$

For a given concrete cracking strength, as $\bar{\rho}$ increases, f_s decreases; thus for high values of I, $[1 - (f_s/f_y)^2]$ is almost equal to 1 and $\bar{\rho}f_s$ becomes a constant.

The expression, therefore, reduces to

$$v_t = GI + Q \tag{16}$$

where $G = 1.564\,(f_c'/f_y)^{1/2}$ and $Q = \bar{\rho}f_s\mu$.

If the aggregates are not dislocated, the concrete in the vicinity of the shear plane may fail as a result of the combined stresses (6), namely, direct compressive stress due to transverse steel tension and shear stress due to applied shear load.

EXPERIMENTAL INVESTIGATION

Experimental investigation was performed to verify the general form of the derived shear capacity expressions and to determine the values of the constant terms in them. The study dealt with composite elements of precast concrete and cast-in-place PMC. Similar ordinary concrete elements were used as control specimens. The details of the four groups of specimens A, B, C, and D are presented in Figure 2 and Tables 1 and 2.

Group A specimens were used to investigate the relationship between intrinsic bond shear transfer capacity and the strength of the composite materials (PMC and concrete). No transverse steel was used in these specimens. There were three types; the only variable among them was the strength of the PMC.

Group B specimens were for the purpose of verifying the shear transfer capacity expressions developed earlier. For this group, the PMC strength was set at 68.95 MPa (10,000 psi), the same as in specimen Group A, Type II. There were five types in this group, each having a different shear reinforcing strength.

Group C specimens were cast monolithically of ordinary concrete to serve as control specimens to give concrete shear strength. No shear transfer reinforcement was used.

Group D contained control specimens made up of cast-in-place concrete over precast concrete. They were designed to give the apparent cohesion of such elements, for the purpose of comparison with Group A specimens.

TABLE 1 Properties of "L" Prism Shear Tests

Designation: Grp (1)	Type No. (2)		Cylinder Compressive & Tensile Splitting Strengths (PSI): Concrete (Side 1) (3)	PMC (Side 2) (4)	Shear Reinforcing Strength I=pfy (PSI) (5)	Specimen Description (6)
A	1	i	5130 (546)	8120 (774)	-	Cold-Jointed Concrete/PMC Specimens (no transverse reinforcement), Only Intrinsic bond; PMC strength is only variable
		ii	5130 (546)	8120 (774)	-	
		iii	5130 (546)	8120 (774)	-	
	2	i	5130 (546)	10040 (1020)	-	
		ii	5130 (546)	10040 (1020)	-	
		iii	5130 (546)	10040 (1020)	-	
	3	i	5130 (546)	11640 (1222)	-	
		ii	5130 (546)	11640 (1222)	-	
		iii	5130 (546)	11640 (1222)	-	
B	1	i	5540 (562)	9820 (996)	286	Cold-Jointed Concrete/PMC Specimens with varying amount of reinforcing
		ii	5300 (553)	10300 (1000)	286	
	2	i	5540 (562)	9820 (996)	572	
		ii	5300 (553)	10300 (1000)	572	
	3	i	5540 (562)	9820 (996)	858	
		ii	5300 (553)	10300 (1000)	858	
	4	i	5540 (562)	9820 (996)	1073	
		ii	5300 (553)	10300 (1000)	1073	
	5	i	5540 (562)	9820 (996)	1375	
		ii	5300 (553)	10300 (1000)	1375	
C		i	5130 (546)	5130 (540) concrete	-	Monolithic Concrete Specimen
		ii	5540 (562)	5540 (362)	-	
D		i	5130 (546)	5300 (553) concrete	-	Cold-Jointed Concrete/Concrete; no reinforcement
		ii	5130 (546)	5300 (553)	-	

Instrumentation

To observe the behavior of the specimens under loading and determine the onset of failure, the slip and crack widths at the shear plane were measured. Slip was measured using three different methods (Figure 3). Demac discs were installed at positions 1, 2, 3, and 4 on each specimen such that positions 1-4 and 2-3 were about 4 in. apart. During the loading, the distances were measured with a 4-in. mechanical gauge. By subtracting the change in positions 1-4 from that of positions 2-3, the displacement due to other causes can be eliminated and the slip obtained as $1/2(\Delta_{2-3} - \Delta_{1-4})$ (13). A displacement indicator was also mounted on the loading platform as shown in Figure 3. The readings from the indicator, when corrected for other effects, give a second slip estimate. Three short horizontal lines were drawn at locations C_1, C_2, and C_3 across the shear plane. Slip was determined by measuring the vertical distance between the two displaced parts of each line (part c of Figure 3) by means of a microscope. Crack length was also measured.

RESULTS OF THE "L" PRISM SHEAR TESTS

Observed Behavior of Shear Test Specimens

During the course of the investigation, the following observations were made regarding the behavior of the specimens.

1. In Group A specimens, loading was not accompanied by much slip or cracking until quite close to the ultimate. There was no noticeable vertical strain or lateral bulging in either the PMC or the concrete halves of the specimens. When the cracks finally appeared, they ran parallel to the joint or diagonally into the regular concrete half, at an angle of 40 to 55 degrees. Examination of the failure surface showed that most of the cracking and separation had occurred in the ordinary concrete section near the shear plane.

2. Generally, Group B specimens behaved like those in Group A up to the occurrence of continuous cracks along the shear plane. After this stage, subsequent loading was accompanied by large increases in the crack width and the amount of slippage. Three of the 4 bars in specimens Bl_i and Bl_{ii} broke when the specimens were loaded beyond the yield strength. The failure surface showed considerable smoothing but it was not clear whether the smoothing occurred before or during loading to collapse. The cracks on the specimens having the largest reinforcing strength (I = 1,375 psi) were shorter in length and not as wide as the others.

3. In the case of Group C specimens, the first few load increments caused no visible signs of distress. At a load of about 68.95 MPa (10,000 psi), short diagonal cracks suddenly appeared on the surface, crossing the shear plane at an angle of 40 to 50 degrees, somewhat similar to the cracks that oc-

TABLE 2 Results of the "L" Prism Shear Tests

Test Designation (1)		Shear Reinforcing Strength PSI (2)	Ultimate Shear Transfer Capacity PSI (3)	Failure Mode (4)
A1	i	-	567	
	ii	-	547	
	iii	-	571	
A2	i	-	685	Cracking along composite plane; Some slipping and finally spearation of the composite sides
	ii	-	640	
	iii	-	620	
A3	i	-	985	
	ii	-	905	
	iii	-	955	
B1	i	286	855	Slipping along plane; steel yield
	ii	286	877	
B2	i	572	1193	As above
	ii	572	1071	
B3	i	858	1243	Slipping & probable steel yield
	ii	858	1191	
B4	i	1073	1392	As above with cracking
	ii	1073	1304	
B5	i	1375	1428	Extensive cracking; slipping; steel yield unlikely
	ii	1375	1324	
C	i	-	984	Diagonal Cracking; typical Shear Failure
	ii	-	944	
D	i	-	488	Cracking along shear plane; little slip separation of composite sides
	ii	-	500	

Ultimate Shear Transfer Capacity = Force (lbs)/bw
where b and w are the length and width of the shear surface, respectively

curred in Group A specimens. Failure was preceded by the formation of series of cracks across the concrete struts formed by the previous diagonal cracks. The exposed aggregates were uncracked. Cracking had occurred in the mortar surrounding the aggregates.

4. Control specimens in Group D behaved like those in Group A except that when cracks appeared, they ran mostly along the shear plane. Failure followed the formation of a continuous crack along the shear plane almost immediately. Even in this group, some cast-in-place concrete stuck to the older concrete at the failure surface.

Shear, Slip, and Crack Result

The ultimate strength results are given in Table 2. The values represent the average of three or two results. The slips determined by the three different methods described previously are plotted separately. The first, Series I, includes all the composite specimens having no shear reinforcement, that is, Groups A and D. PMC strength was the only variable. Series II includes all the composite specimens in which the PMC strength was constant and the only variable was the shear reinforcing strength.

Analysis of Series I Specimen Results

The plots of applied shear stress (τ) versus slip and τ versus maximum crack width (Figures 4 and 5) show that:

1. Concrete-PMC composite specimens undergo considerable slip before failure. In contrast, the concrete control specimens failed suddenly.
2. Ultimate shear transfer capacity increases with increasing PMC strength.
3. The slopes of the curves increase with increasing PMC strength.
4. The slip at yield appears to be almost constant at 0.5 mm (0.02 in.).
5. The shear transfer capacity of the specimens having a PMC strength of 82.74 MPa (12,000 psi) is about the same as that of the monolithically cast ordinary concrete specimens.

The polymer at the composite interface creates a bond between the precast concrete and the cast-in-place PMC. It has been shown that this bond is in the form of polymer fibers bridging the micro-cracks in the specimen (5). The existence of these fibers makes it possible for the composite specimens to undergo substantial slips before failure. They act as ties preventing separation of the composite parts.

As the quantity of polymer in the PMC mix increases, so does the number of such "ties." This, in turn, gives rise to a higher binding force and consequently to a higher shear transfer strength. Thus, the observed increase is really due to increased polymer content. The same phenomenon increases PMC strength in the same manner as improved mortar aggregate bond increases concrete strength (12).

The increase in polymer fiber ties also means that for a given crack width or slip, a higher shear

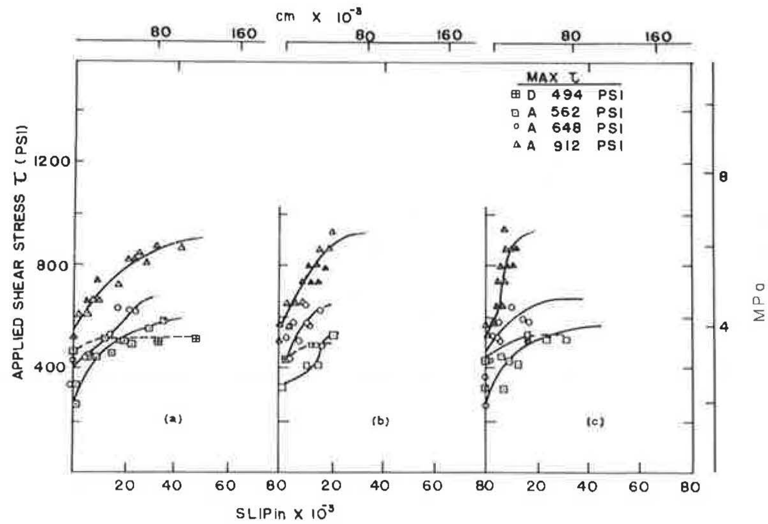

FIGURE 4 Applied shear stress τ versus slip for series I specimens (no shear reinforcement) (a) avg slip measure = 1/2 °Δ2-3 + Δ1-4]; (b) dial gauge measure; and (c) microscope measure.

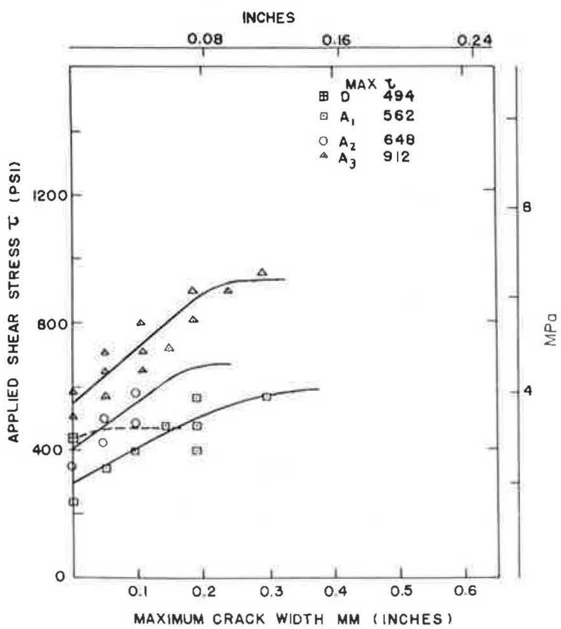

FIGURE 5 Applied shear stress τ versus crack width for Series I specimens.

stress can be withstood by those specimens that have higher strength PMCs. Thus arises the increase in slope with PMC strength.

The observed ultimate slip of 0.5 mm (0.02 in.) indicates that the polymer fibers have a certain yield length. Beyond this length, no further increase in fiber load and, consequently, shear transfer resistance can be obtained.

The similarity between the ultimate capacities of the monolithically cast control specimens and the high-strength PMC composite ones shows that the bond between PMC and precast concrete in the composite specimens was so strong that failure occurred in the concrete part instead of at the shear plane.

Analysis of Series II Specimen Results

Unlike those of Series I, each of the specimens in this group exhibited a yield plateau, undergoing slips of up to 2 mm (0.08 in.) before collapse. The specimens having shear transfer reinforcement had capacities increased with shear reinforcing strength (I). Figures 6 and 7 show that for a given maximum crack width and slip, an increase in I is accompanied by an increase in shear transfer resistance.

As the percentage of steel reinforcement is increased, the normal force exerted on the slip plane for a given crack width and slip increases. This results in higher shear transfer resistances for a given crack width or slip, as well as a higher shear transfer capacity with increasing I.

Visible cracks (by microscopy) appeared on these specimens between an applied stress of 429 to 643 psi. Failure in the heavily reinforced specimens was preceded by spalling of concrete near the exterior bars, suggesting the existence of high dowel forces.

Variation of Shear Transfer Capacity (ν_t) with Shear Reinforcing Strength (I)

The plots of ν_t versus I in Figure 8 show a form similar to that postulated earlier. Between the range $1.0 < I < 7.17$ MPa $(150 < I < 1{,}040$ psi), the relationship between ν_t and I is presumed linear. A least squares analysis of the data within this region gave the following results:

$$\upsilon_t = 0.609I + 711 \tag{17}$$

[The standard deviation in this expression is 336 Pa (48.8 psi).]

In Equation 17, 0.609 is the apparent coefficient of friction and 711 is the apparent cohesion (i.e., the maximum contribution to shear resistance due to bond).

It was observed that in specimens with $I > 1{,}040$ psi, failure was induced by high dowel forces. So, shear transfer capacity was due primarily to dowel action of reinforcement. For high shear reinforcement $I > 1{,}040$, given by Equation 16. The plot in Figure 8 for this range gives the expression:

$$\upsilon_t = 0.20I + 1{,}140 \tag{18}$$

For I = 0, the 68.95 MPa (10,000 psi) PMC composite specimens gave a strength of 648 psi. This is

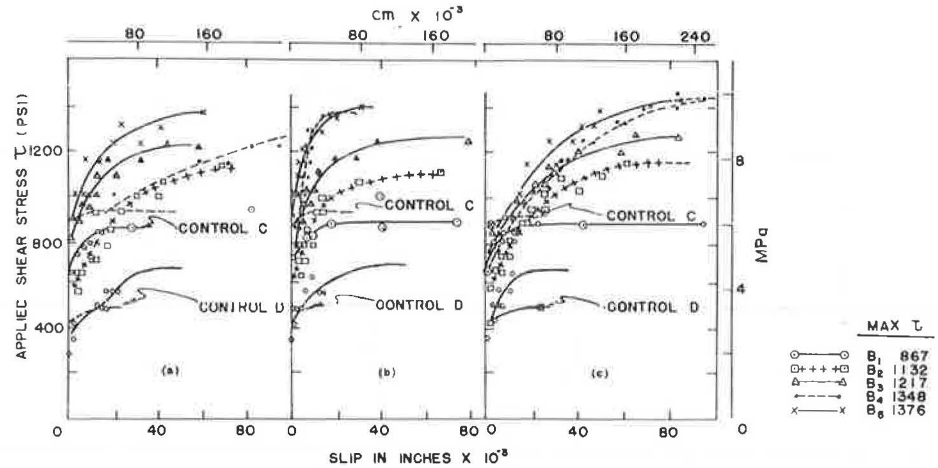

FIGURE 6 Applied shear stress t versus blip for Series II specimens (with shear reinforcement.

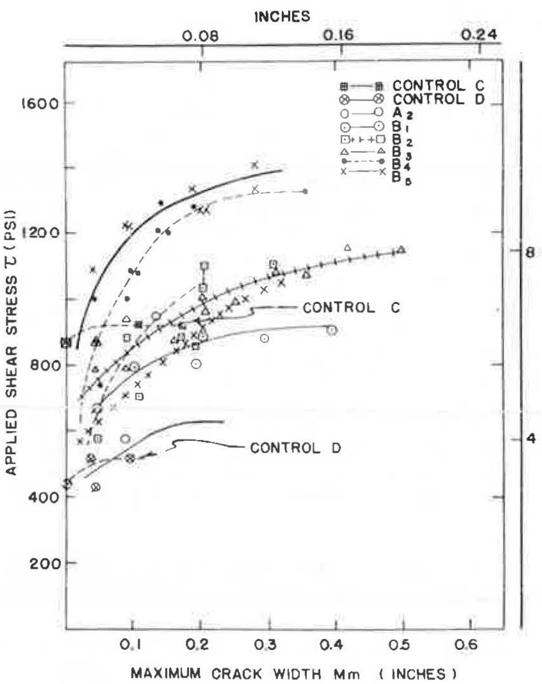

FIGURE 7 Applied shear stress τ versus maximum crack width for Series II specimens.

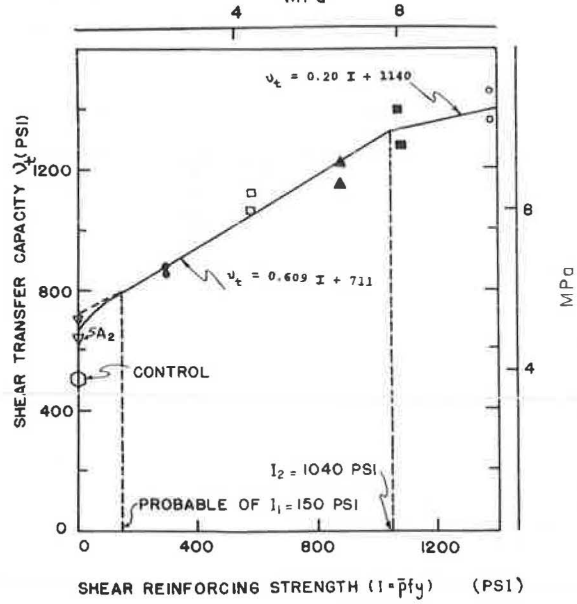

FIGURE 8 Shear transfer capacity v_t versus shear reinforcing strength $I = \bar{\rho}f_y$ for L-prism specimens.

TABLE 3 Comparison of ACI Shear Transfer Capacity Values with Those Given by Proposed Expressions

	Shear Transfer Capacity (psi)			
Shear Reinforcing Strength (I) (psi) (1)	Allowable by ACI Formula[a] $\mu = 1.0$ $\phi = 0.85$ (2)	By Hypothesis Equations 11, 13 (3)	$\frac{\text{Column } 3^b}{1.7}$ (4)	Failure Experimental Results (5)
0	0	648	381	647
100	85	648	381	-
286	243	885	520	867
572	486	1,059	622	1,132
858	729	1,233	725	1,217
1,073	(1,073) 800[a]	1,355	797	1,348
1,375	(1,375) 800[a]	1,415	832	1,376
1,500	(1,500) 800[a]	1,440	847	-

Note: 1 psi = 6.895 Pa.
ACI Formula $v_t = \phi\mu\bar{\rho}f_y$, namely $\phi\mu I$.
[a]Limit of 800 psi for concrete by ACI code 318-83.
[b]Values based on a safety factor of 1.7.

the resistance due to intrinsic bond. The range I = 0 to I = 150 psi is a transition stage where apparent cohesion increases with I.

The ACI code formula $\nu_t = \phi\rho f_y\mu < 800$ psi (μ = 1.4 - 0.8) basically ignores the apparent cohesion and presumably compensates for it by using high coefficient of friction values. When compared with experimental results (Table 3), it is observed that, initially, ACI values are unnecessarily conservative. But as I increases, the values obtained by the proposed shear transfer hypothesis as summarized in Equations 14 and 16 give allowable values comparable to the ACI limit of 800 psi, using a safety factor of 1.7 as in column 4 of Table 3.

CONCLUSIONS

The investigation has shown that the shear transfer capacity of concrete elements might be expressed as follows:

For $I = 0$ $\qquad v_t = C$

$I_1 < I < I_2$ $\qquad v_t = I\mu' + C'$

$I > I_2$ $\qquad v_t \approx GI + Q$

At any given value of I, the strength of the concrete under a condition of combined direct and shearing stresses gives the upper bound values for v_t.

The bond shear transfer capacity V_o' appears to increase with concrete or PMC strength. It varies from 495 psi for concrete on concrete composite element with $f_c' = 5{,}000$ psi, to 920 psi for a PMC on concrete element of PMC strength = 12,000 psi (82.7 MPa).

For a composite element of 10,000 psi PMC on 5,000 psi precast concrete, C = 650 psi; C' = 710; $\mu' = 0.609$; Q = 1,140 psi; G = 0.20; $I_1 = 150$ psi; and $I_2 = 1{,}040$ psi. On this basis, $v_t = 0.609I + 711$ for $150 < I < 1{,}040$ psi and $v_t = 0.20I + 1{,}140$ for $I > 1{,}040$.

ACKNOWLEDGMENT

This paper is the result of the continuing polymer research at Rutgers University under the direction of the author and is based on the doctoral thesis of Maurice M. Ukadike.

NOTATIONS USED IN EQUATIONS

A' = Area of shear surface (in.²),

A_s' = Area of steel shear transfer reinforcement (in.²),

C, C' = Apparent cohesion at $\bar{\rho} = 0$ and $\bar{\rho} > 0$, respectively (psi)

B = Bond force per unit area (psi)

$G = 1.564(f_c'/f_y)^{1/2}$ = A constant (dimensionless)

$I = \rho f_y$ = Shear reinforcing strength

k_1 = Ration of bond area to total shear area

k_2 = Ratio of projected area of aggregates to total shear area

$k_3 = 1 - k_1 - k_2$

P = Applied load (lb)

$Q = \bar{\rho} f_s \mu$ = A constant for high values of $\bar{\rho}$ (psi)

$\Delta V_b, \Delta V_d, \Delta V_f, \Delta V_i$ = Shear resisting loads due to bond, dowel action, friction, and aggregate interlock, respectively (lb)

ΔV_t = Total shear resisting load over the shear surface (lb)

$\bar{\rho} = A_s'/A$ = Ratio of steel shear reinforcement area to shear surface area

μ = Coefficient of friction

μ' = Apparent coefficient of friction

v_b, v_d, v_f, v_i = Shear resistance due to bond, dowel action, friction, and aggregate interlock, respectively (psi)

v_t = Total shear resistance (psi)

Δ_{i-j} = Change in distance between points i and j

τ = Applied shear stress (psi)

f_y = Yield strength of dowel reinforcement (psi)

f_c' = Cylinder compressive strength

b = Width of shear failure plane

n' = Number of dowels

T_f = Land transferred by dowel action per bar

V_n = Sum of forces in the direction of plane n

w = Length of shear failure plane

REFERENCES

1. P.W. Birkeland and H.W. Birkeland. Connections in Precast Construction. Proc., American Concrete Institute, Vol. 63, No. 3, March 1966, pp. 345-367.
2. E.G. Nawy and M.M. Ukadike. Shear Transfer in Concrete and Polymer Modified Concrete Members Subjected to Shearing Loads. Journal of Testing and Evaluation, Vol. 11, No. 2, March 1983, pp. 89-99.
3. B. Bresler and K.S. Pister. Strength of Concrete Under Combined Stresses. Proc., American Concrete Institute, Vol. 55, Sept. 1958, pp. 321-345.
4. H. Dulacska. Dowel Action of Reinforcement Crossing Cracks in Concrete. Proc., American Concrete Institute, Vol. 69, No. 12, Dec. 1972, pp. 754-757.
5. R.D. Eash and H.H. Shafer. Reactions of Polymer Latex with Portland Cement. In Transportation Research Record 542, TRB, National Research Council, Washington, D.C., 1975, pp. 1-8.
6. R.C. Fenwick and T. Paulay. Mechanisms of Shear Resistance of Concrete Beams. Journal of the Structural Division, ASCE, Vol. 94, No. ST-10, Oct. 1968, pp. 2325-2350.
7. W. Han-Chin. Dual Failure Criterion for Plain Concrete. Proc., ASCE, Paper 10996, Vol. 100, EM6, Dec. 1974, pp. 1167-1181.
8. B.R. Hermansen and J. Cowan. Modified Shear Friction Theory for Bracket Design. Journal of the American Concrete Institute, Feb. 1974, pp. 55-57.
9. J.A. Hofbeck, I.A. Ibrahim, and A.H. Mattock. Shear Transfer in Reinforced Concrete. Proc., American Concrete Institute, Vol. 66, No. 2, Feb. 1969, pp. 119-128.
10. A.H. Mattock and N.M. Hawkins. Research on Shear Transfer in Reinforced Concrete. Journal of the Prestressed Concrete Institute, Vol. 17, No. 2, March-April 1972.
11. R.M. White and M.J. Holley. Experimental Studies of Membrane Shear Transfer. Journal of the Structural Division, ASCE, Vol. 98, No. ST-8, Aug. 1972, pp. 1835-1852.
12. P. Nepper-Christensen and P.H. Nielsen Tommy. Modal Determination of the Effect of Bond Between Coarse Aggregate and Mortar on the Compressive Strength of Concrete. Proc., American Concrete Institute, Vol. 66, No. 1, Jan. 1969, pp. 69-72.
13. M.M. Ukadike. Durability Strength and Shear Transfer Characteristics of Polymer Modified Concretes for Concrete Structural Systems. Ph.D. thesis. Rutgers University, New Brunswick, N.J., May 1978, pp. 132-150.
14. E.G. Nawy, M.M. Ukadike, and J. Sauer. High Strength Field Polymer Modified Concrete. Journal of the Structural Division, ASCE, Vol. 103, ST-12, 1977, pp. 2307-2322.

Steel Fiber Shotcrete for Rehabilitation of Concrete Structures

D. R. MORGAN

ABSTRACT

Steel fiber-reinforced shotcrete (SFRS) was first introduced into North America in the early 1970s. Since that time, it has been used in numerous applications, mainly in new construction or lining rock slopes and underground openings in mines and tunnels. There has been relatively little use of this innovative material for rehabilitation of concrete structures. Some of the mix design, batching, mixing, and placing procedures that have been successfully used in numerous SFRS projects in British Columbia are reviewed. Physical properties of SFRS that make it particularly attractive as a rehabilitation material include its good bond characteristics, flexural strength, toughness, impact strength, fatigue resistance, and durability. These characteristics of SFRS are reviewed. Existing SFRS rehabilitation projects are briefly reviewed and suggestions are made for applications where SFRS could provide a viable alternative to conventional rehabilitation procedures.

Steel fiber-reinforced shotcrete (SFRS) was first used for structural applications in North America in the early 1970s. The early experimental work with this material was carried out by Battelle Laboratories in 1971. The first major practical application was SFRS lining of a tunnel adit at the Ririe Dam, Idaho, in 1973. Since that time, there has been considerable use of this new construction material in most of the world's industrialized nations. Henager (1) and Johnston (2) have summarized many of the applications of SFRS.

The largest volume of SFRS application has been found in support of underground openings. It has been extensively used in mining operations and for forming linings in various road, railway, and water tunnels. In British Columbia, SFRS has been used to: line several kilometers of new tunnels constructed through the Rocky Mountains by the British Columbia Railway in 1981-1983; rehabilitate deteriorating old tunnels on the Canadian Pacific Railway main trans-Canada line (used to control water flow and ice formation and stabilize rock scaling) (3); line exploratory adits in a slaking cretaceous shale; and line drainage tunnels in a rock slide area in two British Columbia hydroelectric projects (4). Large-volume applications of SFRS have been found in numerous rock slope stabilization projects (1,2).

It is apparent from reviewing the use of SFRS that its most successful applications are where it has been used in lieu of mesh-reinforced shotcrete. Morgan (5) has conducted a comparative evaluation of plain, mesh, and steel fiber-reinforced shotcrete and has demonstrated that SFRS can provide equivalent and, indeed, even superior performance to mesh-reinforced shotcrete.

There has been relatively little reported use of SFRS for rehabilitation of concrete structures. Some reported repair applications are detailed in the Applications section of this paper. SFRC mix design and materials are discussed and the main physical attributes that make SFRS an attractive material for rehabilitation of certain concrete structures are reviewed. Also presented is a discussion of those structures and structural elements to which SFRS may provide an economical and technically viable alternative to conventional rehabilitation procedures. Information in this paper is drawn from the experience of the author in successfully completed SFRS projects in British Columbia, Canada.

STEEL FIBER

SFRS is defined as a mortar or concrete containing discontinuous discrete steel fibers that are pneumatically projected at high velocity onto a surface (6). Steel fibers are available in a number of shapes, sizes, and metal types. A conventional numerical parameter describing a fiber is the aspect ratio of the fiber, defined as the fiber length divided by the equivalent fiber diameter. Typical aspect ratios range from about 30 to 150 for length dimensions of 5 to 75 mm (0.25 to 3 in.). Most successful shotcrete applications have, however, used fibers with lengths of 13 to 30 mm (0.5 to 1.2 in.). Many different types of fibers are commercially available. Fibers with round, rectangular, and crescent-shaped cross sections have been produced. Straight, crimped, deformed, hooked end, and a variety of other fibers have been used in shotcrete projects (1,2).

Ramakrishnan et al. (7) carried out a comparative evaluation of various types of fibers and found that hooked end fibers provided better physical properties than straight fibers for a given volume concentration of fiber. This is because of the better end anchorage provided by the hooked end fibers; that is, these fibers provide a higher effective aspect ratio than equivalent length straight fibers. Alternatively, lower volume concentrations of hooked end fibers are required for a given level of physical performance compared to shotcrete with straight fibers. Virtually all the major SFRS projects carried out in British Columbia have used a 30 mm-long x 0.4- or 0.5-mm-diameter and hooked-end fiber.

Concentrations of steel fiber used on construction projects have typically ranged from 0.6 to 2.0 percent by volume: 47 to 157 kg/m^3 (80 to 265 lb/yd^3) (1). Fiber concentrations in excess of 1.0 percent by volume 78 kg/m^3 (132 lb/yd^3) have generally been used with straight fibers; most of the tunneling and rock slope stabilization projects in British Columbia have used hooked end fibers at concentrations of 0.75 percent by volume: 59 kg/m^3 (99 lb/yd^3). Note that all these quantities refer to fibers added to the shotcrete mix; the volume concentration of fiber in the in situ shotcrete may be greater or smaller, depending on the degree of rebound of steel fiber relative to the other shotcrete materials. Henager (1) has reviewed the issue of rebound of SFRS at some length.

MIX DESIGN AND MATERIALS

Normal Type I portland cement has been used in most SFRS applications, although Type III high early strength cements have been used in tunnels and marine structures where high early strength development was important to resist the effects of blasting or wave action at an early age; Type V sulfate-resisting cements have been used in sulfate bearing soil or groundwater conditions.

Cement contents as batched have ranged from 390 kg/m^3 (658 lb/yd^3: the US 7 bag mix) to as much as 558 kg/m^3 (940 yd^3: the US 10 bag mix) in certain mortar mixes. Typical shotcrete mixes incorporating a 10-mm (0.375-in.) maximum size aggregate used in SFRS projects in British Columbia have contained 445 kg/m^3 (750 lb/yd^3: the US 8 bag mix) cement. It should be recognized that the cement content of the in situ shotcrete will always be higher than the as-batched cement content because of the higher degree of rebound of coarse aggregate and sand particles than cement. This is particularly true of shotcrete placed by the dry-mix process, shotcrete placed in thin layers [25 mm (1 in.) or less] and shotcrete sprayed overhead.

The American Concrete Institute (ACI) Standard Specification for Materials, Proportioning and Application of Shotcrete (8) lists three desirable combined aggregate gradation limits for shotcrete aggregates (see Table 2.2.1). Gradation No. 3 refers to a 20-mm (0.75-in.) maximum size aggregate gradation; this is seldom used in steel fiber shotcrete. Gradation No. 2 refers to a 10-mm (0.375-in.) maximum size aggregate gradation as shown in Figure 1. This is the gradation envelope most commonly used in SFRS projects in British Columbia. Generally, mixes are proportioned to the finer side of the gradation envelope for overhead applications (e.g., soffits of beams and slabs, arches and crowns of tunnels); to the middle of the gradation envelope for vertical applications (e.g., walls and columns); and to the coarser side of the gradation envelope for downward applications (e.g., canal linings, rock slopes, tunnel inverts).

The American Concrete Institute (ACI) Gradation No. 1 refers to a mortar mix containing no coarse aggregate. Mortar mixes have been successfully used in steel fiber shotcrete projects, but tend to require higher cement contents for equivalent strength performance because of the higher water demand of the mix (particularly in wet-mix shotcrete applications). These mixes tend to have higher porosity than mixes containing coarse aggregate as measured by boiled absorption and air voids (9). This is because of the higher water/cement ratio of the mix, as well as the reduced energy of consolidation compared to that imparted by coarse aggregate particles. Also, mortar mixes have a greater creep and shrinkage potential.

Most SFRS used in British Columbia has contained concrete sand and between 20 and 35 percent by mass of the total combined aggregates of 10- to 5-mm (0.357-in. to No. 4) coarse aggregate. Such aggregate would generally conform to the ACI Gradation No. 2 requirements. One commonly used premixed dry process SFRS mix is comprised of the following proportions by mass for a nominal cubic meter of shotcrete:

Mix	Kilograms	Pounds
Portland Cement, Type I	445	979
10-mm (0.375-in.) coarse aggregate	526	1,157.2
5-mm (No. 4) fine aggregate	1230	2,706
30 x 0.5-mm hooked-end steel fiber	59	129.8

Shotcrete accelerators are generally not required in SFRS and should only be used with extreme caution. Accelerators may be used in special circumstances (e.g., where shotcrete is subjected to blast vibrations, wave action, or traffic at an early age) but they should be free of corrosion-inducing chemicals such as chlorides, fluorides, sulfites, sulfides, and nitrates that could promote corrosion of the steel fibers.

BATCHING, MIXING, AND PLACING

There are two basic methods of applying SFRS: the dry process and the wet process. In the dry process, batching and mixing can be done in a variety of different ways. The cement, damp sand, and coarse aggregate can be mixed in a ready-mix concrete truck with the discrete steel fibers then being added to the truck. Alternatively, the shotcrete materials can be mixed in a central mix plant or mobile site

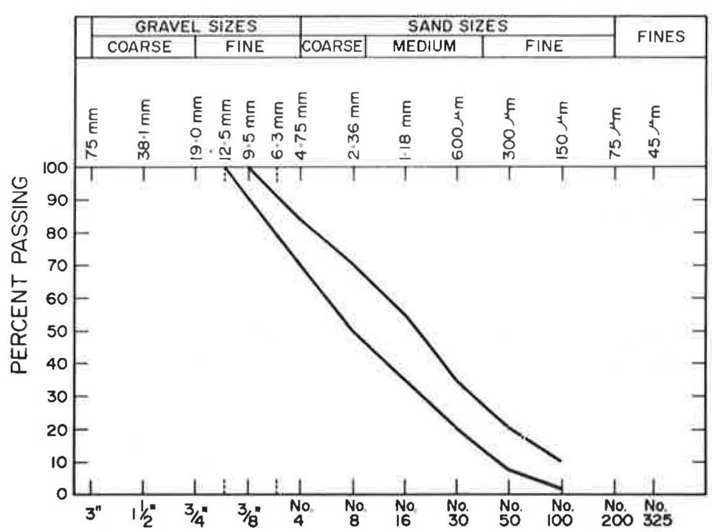

FIGURE 1 ACI 506.2-77, Table 2.2.1, Gradation No. 2.

batch plant (1,6). A variety of different techniques has been developed for adding the fibers. These include dispensing the fibers through a shaker or vibrating screen such that clusters of fiber are not dispensed into the shotcrete materials. Fibers have been discharged onto conveyor belts and fed in with the aggregates or added through special fiber dispensers (1,6).

The most widely used system in British Columbia, however, has been prebagged SFRS. The cement, completely dry aggregates, and steel fiber are weighed, batched, and mixed in a dry bag plant and then discharged into paper bags or bulk synthetic cloth bags. Paper bags have generally been supplied in 23-kg (50-lb) or 40-kg (88-lb) sizes. Bulk bin bags have been supplied with masses varying from 1134 kg (2,500 lb) to 1814 kg (4,000 lb). The dry materials are then discharged into a premoisturizer in which water is added to bring the moisture content of the SFRS into a 3 to 6 percent-by-mass range before discharge into the shotcrete pot.

Bulk bin bags have the advantage of requiring very little manpower; once supported above the premoisturizer hopper, they are essentially self-discharging. Bags with bottom opening spouts are also returnable. In mining and remote tunneling operations, however, it has generally been found more economical to use single-use bulk bin bags; the rate of attrition on supposedly returnable bags is high.

In volume placements of 10 m^3/hr (13 yd^3/hr) or more, it is generally more economical to use ready-mix or site-batched shotcrete. In the small volume and intermittent placement often encountered in rehabilitation of concrete structures, it is often more economical to use prebagged SFRS supply. Prebagged material is also technically preferable from a set-time-control perspective because the time of contact between cement and moisture before discharge into the shotcrete pot is kept to a minimum. Schutz (10) has shown that the set-time of shotcrete mixtures is markedly affected by the time of prehydration of the cement before shooting. For example, in plain shotcrete, he found that a 15-min prehydration period delayed final set of shotcrete by 2.5 hr. The effect was even more pronounced in shotcrete containing accelerators as shown in Figure 2.

Conventional dry process shotcrete equipment has been successfully used to place SFRS. Henager (1) lists various types that have been used for this purpose. Much of the SFRS placement in British Columbia has been carried out using the Meynadier Meyco GM-57 or 60 or Reed Guncrete shotcrete pots. Some contractors have reported a greater rate of wear with the rubber hoses used to convey the shotcrete to the discharge nozzle in the steel fiber shotcrete mixes, compared with plain shotcrete; other than some minor adjustments to wearing plate tolerances, no special procedures are needed to shoot SFRS.

In wet process shotcrete, procedures for batching and mixing SFRS are essentially the same as those used for steel fiber-reinforced concrete (SFRC). Good guidance for batching and mixing SFRC is given in the ACI State-of-the-Art Report on Fiber Reinforced Concrete (11). Henager also gives details of procedures for batching and mixing wet process SFRS as well as information concerning equipment used for placing the material (1). Use of the wet process for applying SFRC in British Columbia has been limited to the rehabilitation of deteriorated concrete bridge abutments.

PHYSICAL PROPERTIES

Plain unreinforced shotcrete, like unreinforced concrete, is a brittle material with little capacity to resist pronounced tensile stresses or strains without cracking and disruption. Steel fibers are incorporated in shotcrete to improve the ductility, energy absorption, fatigue, and impact resistance characteristics of the plain material. Steel fibers perform this role in shotcrete by controlling cracking and holding the material together, even after extensive cracking has occurred. The ability of steel fibers to improve these characteristics of shotcrete is well-demonstrated in studies by Morgan (5,9) and Ramakrishnan (7).

Compressive Strength

As a generalization, the compressive strength of SFRS is governed by the compressive strength of the shotcrete matrix. Increases in compressive strength attributable to the incorporation of fibers are generally small (6,7,9). The useful characteristics of fibers in compression are really only evident in a complete stress-strain curve. The descending portion of the post-peak stress-strain curve is much flatter, characterizing a more ductile material, which is useful in preventing sudden and explosive failure under static loading and in absorbing energy under dynamic loading.

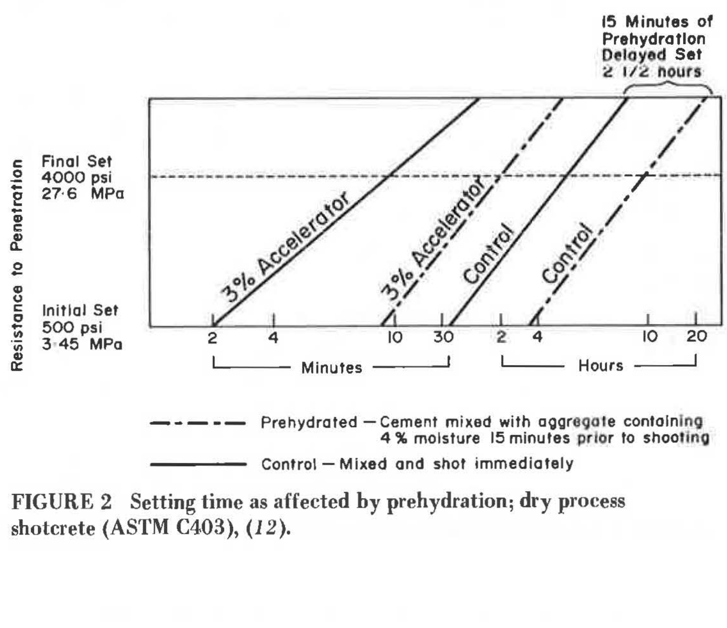

FIGURE 2 Setting time as affected by prehydration; dry process shotcrete (ASTM C403), (*12*).

The compressive strength of well-designed and applied SFRS mixes will usually be in excess of 35 MPa (5,000 psi) at 28 days. The results of tests on 75-mm (3-in.) diameter x 100-mm (4-in.) long cores extracted from SFRS test panels on a British Columbia tunneling project over a 3-month period are given in Table 1. The 28-day compressive strength averaged 43.1 MPa (6,250 psi). The mix contained 445 kg/m³ (750 lb/yd³) cement and 0.75 percent-by-volume of a 30-mm (1.2-in.) long x 0.50-mm (0.02-in.) diameter hooked-end steel fiber.

TABLE 1 Compressive Strength Results for 75 mm Diameter Cores from SFRS Test Panels

	Compressive Strength, MPa					
	7 Days			28 Days		
Date Yr-Mo-Day	a	b	Avg.	a	b	Avg.
82-12-07	26.2	26.2	26.2	37.3	36.5	36.9
82-12-07	43.3	43.1	43.2	52.1	50.2	51.2
82-12-07	44.2	41.6	42.9	46.2	44.0	45.1
83-02-03	30.9	32.8	31.9	45.5	42.8	44.1
83-02-14	44.9	31.4	38.2	42.2	35.0	38.6
83-02-15	34.3	38.1	36.2	44.7	43.8	44.3
83-02-17	31.1	34.2	32.6	43.2	42.2	42.7
83-02-22	31.4	37.1	34.3	45.7	36.4	41.1
83-02-23	42.2	47.2	44.7	45.0	45.0	45.0
83-02-26	36.7	38.7	37.7	47.6	46.6	47.1
83-02-26	41.2	40.0	40.6	43.8	41.9	42.9
83-03-01	39.9	37.7	38.8	45.4	44.9	45.2
83-03-04	29.5	31.5	30.5	39.3	37.4	38.4
83-03-07	31.4	35.2	33.3	44.7	42.8	43.7
83-03-07	29.6	30.5	30.1	47.6	35.9	41.8
83-03-11	39.0	42.8	40.9	42.8	40.5	41.6
Average			36.4			43.1

Flexural Strength

Placement of shotcrete tends to orient the fibers in a plane parallel to the surface being shot. This orientation is beneficial to the properties of the shotcrete layer, particularly when thin sections are being applied. The flexural strength increases with increasing volume concentration and aspect ratio of fibers. This aspect is well demonstrated in studies by Ramakrishnan (7). Two values of flexural strength are generally reported: the first crack flexural strength (the point at which the load versus deformation curve departs from linearity) and the ultimate flexural strength (point of maximum load). For low aspect ratio or low-volume concentrations of fiber, these two strength values may be the same; that is, there may be no increase in strength after the first crack, as shown in Figure 3.

Values of flexural strength for well-designed and applied steel fiber shotcrete mixes are generally in the range of 4.5 to 7.5 MPa (650 to 1,090 psi) at 28 days with values of 6 MPa (870 psi) being commonly achieved (7,9).

Toughness

The addition of steel fibers simply to increase flexural strength is not a good reason for using steel fibers in shotcrete; simple increases in flexural strength alone can be more economically achieved by increasing the strength of the shotcrete matrix (e.g., by the use of higher cement contents). The main reason for adding steel fibers is to increase the toughness of the shotcrete. Toughness may be defined as the work required to cause a specified deformation in a shotcrete beam tested under static flexural loading. The ACI 544 Committee (13) has developed a definition for toughness for flexural testing of 100 x 100 x 355-mm (4 x 4 x 14-in.) beams defined as follows:

Toughness Index = [Area under load-deflection curve to 1.9 mm (0.975 in.) center point deflection]/[Area under load-deflection curve to first crack].

For plain shotcrete, which sustains no post-first-crack load, this value is 1.0. The toughness index of SFRS increases with increasing volume concentration and aspect ratio of fiber. The toughness index is also affected by the aggregate size, tending to decrease as the maximum aggregate size is increased. This is a good reason to avoid using aggregate larger than 10 mm (0.375 in.) in SFRS.

Typical toughness index values for SFRS reported in the literature (5,9) range from about 4 to 10, depending on the volume concentration of fiber and maximum aggregate size, as given in Table 2. Note that the much higher values for toughness index (range of 4 to 23.5) reported by Ramakrishnan (7)

TABLE 2 Toughness Index for SFRS at 28 days (*11*)

Mix No.	Description	Toughness Index
A	Plain control	1.0
B	0.5 percent fiber	3.7
C	1.0 percent fiber	5.9
D	1.5 percent fiber	6.7
E	Sanded, 1.0 percent fiber	10.8

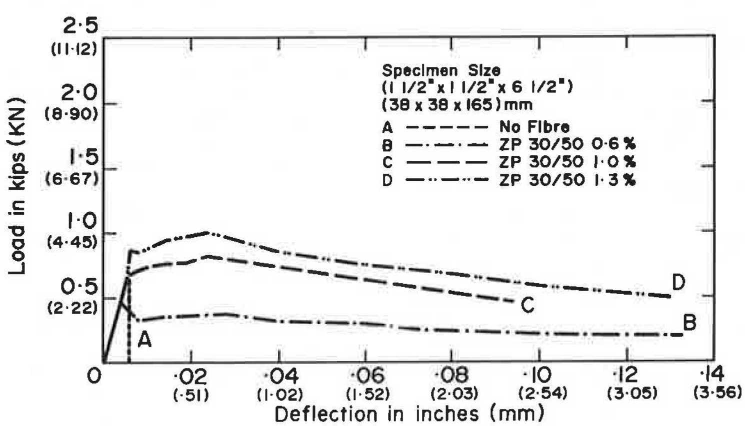

FIGURE 3 Load-deflection curves for static loading at 28 days (*2*).

were based on a different definition than that developed by the ACI 544 Committee (3).

The real benefits of incorporating steel fiber in shotcrete are well-illustrated by this parameter. The substantial load-carrying capacity of SFRS, even after the development of substantial cracking and deformation, gives a good indication of the energy absorbing and ductile characteristics of this material.

Impact Resistance

Some of the earliest SFRS experiments involved the construction of inflated domes for protection of military personnel from exploding missiles and projectiles. In these studies, the excellent impact resistance of SFRS was recognized. The ACI 544 Committee (13) has developed a test procedure for measuring impact resistance. It involves dropping a 4.54-kg (10-lb) hammer 457 mm (18 in.) onto a 64-mm (2.5-in.) diameter ball that rests on a 152-mm (6-in.) diameter by 64-mm (2.5-in.) high shotcrete core. The number of blows to first crack, as well as the number of blows to cause disruption of the specimen are measured. Although the test is basically empirical and the test results do have a high coefficient of variation, it does give a useful indication of the benefits the incorporation of steel fiber has on the impact resistance of shotcrete. Typical test results recorded by Morgan (9) are given in Table 3.

TABLE 3 Impact Resistance of SFRC (*11*)

		Impact Resistance			
		7 Days		28 Days	
Mix No.	Description	Blows to First Crack	Blows to Failure	Blows to First Crack	Blows to Failure
A	Plain control	20	22	39	41
B	0.5 percent fiber	30	68	119	140
C	1.0 percent fiber	66	112	111	211
D	1.5 percent fiber	141	237	218	280
E	Sanded, 1.0 percent fiber	110	223	117	291

Fatigue Strength

There are no reported studies in the literature of the performance of SFRS under fatigue loading conditions. It is reasonable, however, to assume that performance would be similar to that attained in SFRC with similar volume concentrations of fiber. The ACI State-of-the-Art Report on Fiber-Reinforced Concrete (11) has reviewed the results of fatigue testing on SFRC beams. They report that the addition of fibers increases fatigue life and decreases the crack width under fatigue loading. It has also been shown (11) that the fatigue strength of conventionally reinforced beams made with fibrous concrete increases and the resulting deflection caused by fatigue decreases. These are attractive considerations for the use of SFRC for rehabilitation of structures subjected to repetitive flexural loading, such as bridge decks and girders and beams supporting traveling cranes.

Johnston (2) has shown that the greater fatigue endurance of SFRC has resulted in greatly increased pavement life or has alternatively permitted the use of substantially reduced pavement thickness in design of road and airfield pavements and bridge deck overlays. Thickness reductions on the order of 30 to 50 percent or more have been achieved in numerous projects. Morgan (12) has reviewed the performance of SFRC overlays placed on some 20 different bridges in the United States between 1972 and 1983. The major- ity of these overlays were placed to rehabilitate existing deteriorated bridge decks. Nearly all of them have displayed excellent fatigue endurance, with much reduced cracking relative to conventional plain concrete overlays.

Bond Strength

There is little quantitative data in the literature concerning the bond strength of SFRS. Published data (6) indicate that bond strengths in the range of 0.9 to 3.7 MPa (135 to 540 psi) are achievable with SFRS, with the actual bond strength obtained being highly dependent on the condition of the substrate to which the shotcrete is applied. Bond strengths in excess of 1 MPa (145 psi) could reasonably be expected on properly prepared concrete surfaces. Field experience indicates that bond strength is likely to be significantly greater for shotcrete (either plain or SFRS) than for conventional concrete cast up against a surface. Excellent bond has been found in shotcrete applied to surfaces as varied as clay brick masonry, formed concrete, and a wide variety of rock types in tunneling projects.

Durability

The durability of SFRC is governed by the same factors that influence the durability of conventionally reinforced shotcrete or concrete. As long as the matrix retains its inherent alkalinity and remains uncracked, there is no durability problem. It has been shown (2,11) that even when the exposure conditions cause reduced alkalinity, for example, air pollution, de-icing salts, or a marine atmosphere, only the outer 1 to 2 mm (0.04 to 0.08 in.) or so of a good quality, impermeable SFRC are affected over a period of many years. Fibers in the immediate surface layer could rapidly corrode and disappear, but the interior fibers remain totally protected, provided the concrete or shotcrete remains uncracked.

In the event of cracking, the fibers would be exposed to corrosive influences. How long the fibers remain capable of effectively restricting the widening of a crack depends on the crack width, the severity of the corrosive environment, and the type and diameter of fiber used. Some studies have shown (2) that if the crack widths remain in the range of 0.03 to 0.08 mm (0.001 to 0.003 in.) carbon steel fibers will not oxidize even after several years of exposure. Other studies have shown (2) that although corrosion takes place in a moist marine environment when crack widths are in the range of 0.10 to 0.30 mm (0.004 to 0.012 in.), much of the composite strength may be retained because the fibers can tolerate a considerable reduction in diameter by corrosion before failing and permitting unrestricted crack opening. In severe exposure conditions, stainless steel or other nonrusting types of fiber can be used.

In shotcrete applications where surface rusting and staining is aesthetically undesirable, a thin coating of plain shotcrete applied monolithically on top of the SFRS can solve the problem. This procedure has been used with good success in British Columbia in stabilization of rock slopes and embankments adjacent to highways. In pavements and hydraulic structures, any corroded surface fibers are rapidly worn off by traffic or water flow.

SFRC is considered particularly useful for waterfront marine structures, which must have resistance to deterioration at the air-water interface and resist impact loadings. SFRC or SFRS is particularly attractive for construction and rehabilitation of nominally reinforced marine structures such as dolosse, surge breakers, and sewer outfall pipe coatings. These elements have apparently displayed superior performance to conventionally reinforced structures in that there appears to be no mechanism with discreet fibers in a concrete matrix to support the macrocell galvanic corrosion processes that develop in conventional reinforced concrete or shotcrete.

APPLICATION

SFRS has been used in recent years in various innovative types of new construction. It has been used to construct dome and barrel-vault structures, using a process in which an inflated membrane is sprayed with a polyurethane foam that creates the form for application of SFRS. These self-supporting structures have been used for farm storage sheds, commercial offices, industrial warehouses, residential complexes, and military hardened shelters (11).

SFRC has been used to rehabilitate many concrete structures such as bridge decks (12), airfield and road pavements (2), industrial floors, and marine and hydraulic structures (1,2,11). There has been relatively little reported use of SFRS for rehabilitation of concrete structures, however.

Henager (1) reported that SFRS was used to strengthen brick arches under three bridges for British Rail in England. In Sweden, a lighthouse damaged by freeze-thaw conditions was repaired by SFRS, as was the interior of a 50-m (150-ft) tall concrete chimney (1). Reported uses in Australia include repair of an eroded roof in a concrete bunker used for absorbing energy from impacting projectiles, relining a steel bin used for aggregate storage, and lining curved sections of a stormwater drain.

Clearly, there are many concrete structures where SFRS provides a viable alternative to conventional rehabilitation procedures. It is suggested that SFRS may provide an economical and technically viable alternative to conventional rehabilitation procedures in the following situations:

1. Where the use of mesh-reinforced shotcrete was the proposed remedial procedure.
2. Where repair of corrosion induced spalling is required; for example, in bridge deck soffits, girders, and abutments.
3. Repair of impact damage and corrosion-induced spalls in marine structures such as surge breakers, jetties, sea walls, dolosse, and piles.
4. Rehabilitation of deteriorated tank linings, drains, trenches, and electrolytic cell tops in the aggressive chemical environments encountered in the chemical and pulp and paper industries. In such situations, special corrosion-resistant fibers and chemically resistant cements may be required (e.g., stainless steel fiber and Type V sulfate-resisting cement).
5. Refractory shotcrete repair; special SFRS mixes have been used in construction and repair of refractories. Information is contained in a paper by Glassgold (14).

In summary, although there has been relatively little use of SFRS to date for rehabilitation of concrete structures, it is clear that the material has many attributes that make it attractive as an alternative to conventional rehabilitation procedures. SFRS mix design, batching, mixing, and placing has now become routine, and there is sufficient long-term case history performance in a wide variety of applications so that user confidence can be assured. Its potential for use in the rehabilitation of concrete structures is limited only by economic considerations and the imagination of the rehabilitation engineer or contractor.

CONCLUSIONS

Since its first applications in North America in the early 1970s, SFRS has passed from the realm of a new, relatively untried material to one that has achieved considerable success in a variety of applications simply because, despite certain recognized limitations, it can offer both technical and economic advantages over conventional alternatives.

Most SFRS applications have, however, been in either new construction or lining rock slopes and underground openings in mines and tunnels. There has been, to date, relatively little use of this innovative material for rehabilitation of existing concrete structures.

Also reviewed are the physical attributes of SFRS (such as improved flexural strength, toughness, impact and crack resistance, fatigue strength, and durability), which make it attractive as a rehabilitation material.

Current uses of SFRS are summarized and potential applications for rehabilitation of existing concrete structures are presented. These include repair of corrosion and impact-damaged structures such as bridge deck soffits, girders, and abutments and marine structures such as surge breakers, jetties, sea walls, dolosse, and piles. The potential for use of special chemically resistant cements and fibers for rehabilitation of deteriorated structures in the chemical and pulp and paper industries is also discussed. It is suggested that SFRS has many attributes that make it attractive as an alternative to conventional rehabilitation procedures.

REFERENCES

1. C.H. Henager. The Technology and Uses of Steel Fibrous Shotcrete--A State-of-the-Art Report. Battelle Development Corporation, Richland, Wash., 1977.
2. C.D. Johnston. Steel Fibre-Reinforced Concrete--Present and Future in Engineering Construction. Composites, London, England, April 1982.
3. R. van Ryswyk. Tunnel Repairs. Construction West, Canada, Sept. 1979.
4. T. Little. An Evaluation of Steel Fibre-Reinforced Shotcrete. 36th Canadian Geotechnical Conference, Vancouver, British Columbia, June 1983.
5. D.R. Morgan. A Comparative Evaluation of Plain Mesh and Steel Fiber Reinforced Shotcrete. American Concrete Institute, International Symposium on Fiber-Reinforced Concrete, Detroit, Sept. 1982.
6. American Concrete Institute. State-of-the-Art Report on Fiber-Reinforced Shotcrete. American Concrete Institute, Concrete International Design and Construction, Detroit, Mich. (to be published in 1985).
7. V. Ramakrishnan, V.W. Coyle, L.F. Dahl, and E.K. Schrader. A Comparative Evaluation of Fiber Shotcretes. American Concrete Institute, Concrete International Design and Construction, Detroit, Mich., Jan. 1981.

8. American Concrete Institute. Standard Specification for Materials, Proportioning and Application of Shotcrete. ACI Manual of Concrete Practice, Part 5, Detroit, Mich., 1982.
9. D.R. Morgan. Steel Fibre Shotcrete--A Laboratory Study. American Concrete Institute, Concrete International Design and Construction, Detroit, Mich., Jan. 1981.
10. R.J. Schutz. Factors Influencing Dry Process Accelerated Shotcrete. American Concrete Institute, Concrete International Design and Construction, Detroit, Mich., Jan. 1981.
11. American Concrete Institute. State-of-the-Art Report on Fiber-Reinforced Concrete. Concrete International Design and Construction, Detroit, Mich., May 1982.
12. D.R. Morgan. Steel Fibre Concrete for Bridge Rehabilitation--A Review. Roads and Transportation Association of Canada, Annual Conference, Edmonton, Alberta, Sept. 1983.
13. American Concrete Institute. Measurement of Properties of Fiber-Reinforced Concrete. ACI Manual of Concrete Practice, Part 5, 1982.
14. I.L. Glassgold. Refractory Shotcrete--Current State of the Art. American Concrete Institute, Concrete International Design and Construction, Detroit, Mich., Jan. 1981.

Properties of Latex-Modified Shotcrete Beneficial to Concrete Repairs

GARY L. CHYNOWETH

ABSTRACT

The inclusion of a latex into a shotcrete mix imparts a new set of mechanical properties to shotcrete and enhances the benefits of shotcrete when used for the repair of concrete. The effects of the polymer binder on the shotcrete matrix are discussed and then related to the mechanical properties of latex-modified shotcrete. The mechanical properties of latex-modified shotcrete are presented along with a discussion of how they benefit the repair of concrete structures that have experienced corrosion or freeze-thaw damage, particularly in environments subject to chloride exposure. The application of latex-modified shotcrete is discussed and guidelines are provided for preparing the mix proportions and specifications.

Latex-modified shotcrete refers to the inclusion of a latex into a conventional shotcrete mixture of portland cement and aggregate that is conveyed through a hose and pneumatically projected, at high velocity, onto a surface (1). A latex is a form of polymer system, and it generally consists of a water emulsion of a synthetic plastic or natural rubber (2). The most commonly used latex for shotcrete applications utilizes a styrene-butadiene polymer that is the same polymer system used for latex-modified concrete bridge deck overlays. The inclusion of a latex into a shotcrete mixture results in the development of a polymer binder throughout the shotcrete matrix, which imparts a new set of mechanical properties to the shotcrete.

The mechanical properties of the latex-modified shotcrete system are the result of the individual and combined effects of the cement and polymer binders. The proper interaction of these two binders is essential in obtaining the benefits of the latex-modified shotcrete (LMS); this interaction is dependent on the mix proportions and the development of bonds between the binders as the material cures.

The cement in LMS will hydrate and cure in the same manner as in conventional shotcrete and the polymer particles bond to each other as the latex emulsion dries. Bond development between the polymer and cement, however, is dependent on the chemical reactions that take place during the hydration of the cement.

The bond between the polymer and cement appears to occur in the early stages of the cement hydration process with the polymer bonding through the calcium ions present in the cement (3). Once this bond is developed, it is strong and irreversible. As the cement hydration process continues, the polymers will coalesce and bond to form a continuous polymer film. This film formation is the result of loss of water from the latex emulsion, either to evaporation or to the cement hydration, after which the polymer particles are forced together, either by the growth of the cement hydrate or by capillary action created by the water loss. In order to obtain the benefits of LMS, it is important that sufficient polymer particles be present in the mix to develop a continuous polymer film throughout the shotcrete matrix.

As the LMS begins to dry, the cement paste will shrink and microscopic cracks will develop throughout the shotcrete matrix. The polymer binder is capable of undergoing strain and can bridge these cracks and restrain their propagation. The high bond strength of the polymers to the cement paste allows the polymer to sustain the tensile stresses resulting from the restraint of the microscopic cracking and results in an increased tensile capability for

LMS. This increased tensile capability is reflected in improved bond, flexural, and tensile strengths. The ability of the polymer binder to undergo strain while maintaining its bond to the cement paste results in improved flexibility of LMS, which is reflected in a reduced modulus of elasticity and an increased impact resistance. The bridging action of the polymer binder across the micro-cracks in the cement paste coupled with the continuous polymeric film throughout the shotcrete matrix results in a reduced permeability and is reflected in a reduced absorption rate, reduced penetration of chlorides and water, and improved resistance to freeze-thaw and wet-dry cycles.

MECHANICAL PROPERTIES OF LMS

The addition of a latex to a shotcrete mixture imparts a new set of mechanical properties to the shotcrete and improves its performance as a repair material. In general, LMS is more durable than conventional shotcrete and its improved bond and flexibility makes it a more desirable repair material.

Compressive Strength

The addition of a latex to a shotcrete mixture does not improve compressive strength. In fact, tests indicate that variances in the styrene-butadiene ratio or a high polymer-to-cement ratio can cause a decrease in the compressive strength. It has been suggested that the plastic film throughout the shotcrete matrix may act as an internal lubricant that reduces the resistance to compressive stresses; however, the compressive strength of LMS is still in the range of 5,000 to 7,000 psi. Conventional shotcrete with a comparable mix design will have a compressive strength range of 5,000 to 9,000 psi (4-7).

Flexural Strength

The flexural strength of LMS is greater than conventional shotcrete as a result of the capability of the polymer binder to transmit tensile stresses. A normal range of flexural strengths for LMS is 1,300 to 1,600 psi. A comparable range of flexural strengths for conventional shotcrete is 600 to 1,000 psi (4-6).

Tensile Strength

The tensile strength of LMS is increased by 40 to 60 percent over conventional shotcrete because of the polymer binder's capability to transmit tensile stresses. Tensile strength of LMS is in the range of 400 to 700 psi as compared to 200 to 400 psi for conventional shotcrete (5).

Bond Strength

Bond strength capacity of LMS to concrete is 30 to 50 percent greater than conventional shotcrete although both materials will typically exceed the shear and tensile strength of the concrete material to which they are bonded. The primary benefit of LMS is that the polymer binder can undergo strain in addition to transmitting tensile stresses, which makes the bond more resistant to impact or movement. Shear bond strength of LMS to concrete is in the range of 350 to 450 psi and is generally governed by the shear strength of the concrete. Shear bond strength between layers of LMS is in the range of 700 to 900 psi (4,6).

Absorption

A reduced permeability of LMS is reflected in the reduced rate of absorption, which is typically 2 to 4 percent as compared to 6 to 9 percent for conventional shotcrete. The lower absorption of LMS is attributed to the continuous polymer film throughout the shotcrete matrix and the polymer's ability to bridge the micro-cracks that develop in the cement paste (5,6).

Modulus of Elasticity

The high bond strength of the polymer to cement and the ability of the polymer binder to remain elastic results in a modulus of elasticity of approximately one-half that of conventional shotcrete. The modulus of elasticity of LMS is normally in the range of 2.5 million psi.

Freeze-Thaw Resistance

Latex-modified shotcrete's low water-cement ratio, low absorption rate, and high tensile strength combine to provide excellent resistance to freeze-thaw action. An accelerated freeze-thaw test conducted by the U.S. Army Corps of Engineers showed a weight loss of 0.3 to 4.1 percent for LMS after 300 freeze-thaw cycles. Samples of conventional shotcrete tested at the same time showed a weight loss of 41.5 percent after only 105 freeze-thaw cycles (5).

Impact Resistance

The combination of the high bond strength of the polymer to the cement with the polymer's ability to transmit tensile stresses while remaining elastic makes LMS much more flexible and resistant to impact. Impact tests indicate that an average of 250 blows were required to develop the first crack in LMS samples as compared to only 50 blows for conventional shotcrete (5).

BENEFITS OF LMS IN CONCRETE REPAIRS

The primary benefits of using LMS for concrete repairs is its enhanced durability and improved bond. The enhanced durability of LMS improves its performance for repairing concrete that has deteriorated as a result of corrosion of the reinforcing steel or because of freeze-thaw damage. It is particularly useful in repairing damaged concrete that is also exposed to wet-dry cycles. LMS-improved bonding characteristics resulting from the polymer binder's tensile strength and elastic properties make LMS a more compatible repair material than conventional shotcrete by improving the reliability of the bond between the two materials.

Corrosion damage in concrete is initiated when air, moisture, and an electrolyte (usually chlorides) come in contact with the reinforcing steel. Exposure to these combined elements begins the cell action necessary for steel to corrode, and then the resulting corrosion exerts tensile stresses on the surrounding concrete and ultimately causes the concrete cover to spall. Corrosion damage is particularly severe in areas subject to wet-dry cycles, which causes cracking of the concrete cover and increases exposure to water, and also in areas subject to high concentrations of chlorides, which accelerates the penetration of the electrolyte to the steel. Structures subject to severe corrosion damage would include waterfront structures, especially along coastal regions, and bridges that are exposed to de-icing salts.

The normal means of repairing corrosion damage is to remove the surrounding concrete material so that all corrosion can be removed from the steel. When all corroded steel is exposed and cleaned, it is protected by placing a new cover material over it and restoring the structure to its original condition. The improved properties of LMS make it well-suited as a repair material because the low absorption of LMS reduces the penetration of moisture to the steel. In addition, tests have shown that the penetration of chlorides through LMS is insignificant beyond a 0.75-in. depth. If either the chloride or the moisture is prevented from coming into contact with the steel, the recurrence of corrosion is prevented. In areas subject to wet-dry cycles, LMS performance is superior because the low absorption of the material reduces extreme dimensional changes that would cause cracking, and the tensile strength of the polymer binder further inhibits the development of cracks.

Freeze-thaw damage in concrete is caused by the expansion of water within the concrete as the water freezes. The expansion exerts tensile stresses within the concrete matrix and results in cracking of the concrete material. The cracking allows more moisture to accumulate with a greater expansion potential and eventually leads to a complete breakdown of the concrete material. Freeze-thaw damage is greatest in structures exposed to moisture such as waterfront structures, bridge substructures, and retaining type structures.

The normal method of repairing freeze-thaw-damaged concrete is to remove all damaged concrete until sound concrete is exposed. After the removal of all deteriorated concrete, the structure can be rebuilt to its original condition with a new repair material. LMS is extremely durable against freeze-thaw action. The low absorption of LMS inhibits the penetration of moisture and reduces the potential of damage during freezing. The high bond strength of the polymer to cement and the ability of the polymer to transmit tensile stresses while remaining elastic allows it to resist the expansive stresses that may develop during freeze-thaw cycles.

The primary reason for LMS durability against freeze-thaw action is its ability to reduce the penetration of moisture which, upon freezing, causes the damage. This characteristic restricts the use of LMS in repairing strucures, in regions subject to frequent freeze-thaw cycles, which would result in encapsulating a water-saturated concrete substrate. Examples would include lining the exterior of a water tank or completely coating the face of a retaining structure exposed to groundwater. Although the bond between the two materials and the durability of the LMS would not be affected, the substrate concrete would be maintained in a saturated condition because of the LMS lower rate of permeability. If the structure is located in a region that experiences frequent freeze-thaw cycles, the repair would fail because the substrate concrete material would rapidly deteriorate from freeze-thaw actions, resulting in a separation of structure and repair material.

The success of any repair depends on the ability of the repair material to remain bonded to the concrete structure. Many repair failures have occurred because of differential movement between the repair material and concrete surface. These movements may be caused by excessive shrinkage, different thermal expansion coefficients, or a different reaction to flexural movement, all of which develop a concentration of stresses at the bond plane and usually result in delamination.

LMS is compatible with concrete because it is basically a portland cement product. The latex modification of the shotcrete results in a more flexible repair material that will distribute stresses throughout its cross section rather than concentrating the stresses at the bond plane. In addition, the high bond strength of the polymer binder, coupled with its ability to remain elastic, allows the LMS to absorb impact-loading and large deflections without reducing the bond with the concrete.

APPLICATION OF LMS

As with any repair material, the benefits of LMS can be realized only if the material is properly applied. The American Concrete Institute (ACI) report, Specification for Materials, Proportions and Application of Shotcrete (7), can be readily adapted for an LMS application. The general methods of applying LMS are similar to conventional shotcrete and either the wet-mix or dry-mix process may be used. There are, however, special features that must be considered when using LMS.

Mix Design

Latex-modified shotcrete mix proportions are designed for maximum durability rather than strength. The favorable material properties of LMS are dependent on the inclusion of the proper quantity of polymer solids, and on ensuring that an adequate paste content is available in the mixture. There must be enough polymer solids in the mix to allow the formation of a continuous polymer film throughout the shotcrete matrix. The amount of polymer solids required has been determined by testing and is expressed as a polymer-cement ratio of 0.15, by weight, for the styrene-butadiene latex. LMS is normally more effective in richer mixes and experience suggests that a minimum of 750 lb of cement per cubic yard of in-place material be used to ensure adequate paste content.

Most LMS is applied to vertical and overhead surfaces. In order to prevent sloughing, the material is shot relatively dry with a water-cement ratio between 0.26 and 0.35. At this low water-cement ratio, most of the water for cement hydration is provided by the latex emulsion. Accordingly, it is necessary to control the moisture content of the aggregate to ensure that an adequate amount of latex solids can be added during application. The maximum allowable moisture content of the aggregate will vary according to the solids content of the latex used, but is normally around 3 percent.

Quality Control

The addition of latex to a shotcrete mixture does not produce a significant change in compressive strength and, therefore, the commonly specified compressive strength should not be used as a quality control measure for LMS. The changes in mechanical properties that result from the addition of the latex is reflected in an increased tensile capacity and its reduced permeability. More accurate and convenient indicators of the quality of LMS are the flexural strength and absorption tests. Unless a specific project requires more stringent control over the material properties, a minimum flexural strength of 1,300 psi and a maximum absorption of 4 percent can be specified. The samples required for these tests can be cut from the standard shotcrete test panels described in ACI 506.2.

Latex Material

Styrene-butadiene latexes should meet the product specification guidelines suggested by the Federal Highway Administration (8). No other admixtures are recommended for LMS. Air-entraining cement and air-entraining admixtures should not be allowed for LMS because the surfactant used to keep the polymer suspended in the latex emulsion will cause a higher-than-normal entrained air content.

It is desirable for the latex to be delivered with all polymers, water, stabilizers, and additives blended at the point of manufacture. No water or additives should be added to the latex after delivery unless specifically allowed by the specifications. Latex has limited freeze-thaw stability and should be protected against freezing. Latex that has been stored for a long period of time should be stirred or agitated in some manner, before use, to resuspend any latex solids that may have settled during storage.

Proportioning and Preconstruction Testing

Latex-modified shotcrete mix proportions should be selected on the basis of preconstruction testing. The mix proportions selected for use should produce the specified flexural strength, absorption, and other design requirements. Proportions should be selected on the basis of test specimens that are moist-cured for 1 day and dry-cured for the remaining curing period. Three flexural test specimens should be sawed from the test panel no earlier than 5 days after shotcreting and should each measure 3 x 3 x 12 in. Absorption tests can be performed using the broken flexural test specimens.

Batching and Mixing

Batching and mixing of LMS for the wet-mix process is the same as conventional wet-mix shotcrete. The cement, aggregate, and latex are blended, maintaining the proper polymer-cement ratio, and the minimum amount of water is added to provide a pumpable mix with a water-cement ratio that is within the range of 0.26 to 0.35. After mixing, the LMS is conveyed through a hose and pneumatically projected onto the prepared surface.

Batching and mixing of LMS for the dry mix process is the same as for conventional dry mix shotcrete when a pressurized tank or booster pump is used. The cement and aggregate are blended dry and pneumatically conveyed through a hose, and the latex is added through the nozzle body just before projecting the material onto the prepared surface. The latex is normally placed in a tank capable of maintaining sufficient pressure to overcome the latex line losses and to adequately inject the latex through the water ring assembly. Latex that is conveyed or pressurized by pumping should not be pumped with a high shear action pump because of the possible excessive foaming action of the latex. A long nozzle is normally used, which injects latex into the material hose at a point approximately 7 to 15 ft from the nozzle tip. The use of the long nozzle provides the additional time needed to more thoroughly mix the cement, aggregate, and latex. This extra mixing time is desirable because of the lower moisture content of the aggregate and the need to uniformly distribute the polymer solids throughout the shotcrete matrix.

Placement of LMS

The placement of LMS is similar to the placement of conventional shotcrete with the quality of the final product depending largely on the skill of the nozzleman. LMS does, however, require special precautions due to effects of the polymers.

Avoid spilling or spraying latex onto a substrate surface. Latex emulsions are frequently used as bonding agents when applying fresh concrete material onto existing concrete. However, latex that is allowed to dry will form a plastic film that inhibits development of a bond of concrete materials placed over it. To prevent reduced bond and possible delamination of the LMS, any substrate surface contaminated with latex that has been allowed to dry should be sandblasted or waterblasted clean.

The surface of LMS, which has been freshly shot, will develop a surface film of polymer solids and laitance. This film, if not removed, will reduce the bond of succeeding layers of LMS. If the film has not taken its final set, it can be broken by brooming with a stiff broom or cutting back the surface with a trowel. If a final set is established, the film should be removed by sandblasting or waterblasting.

The latexes used in LMS are excellent adhesives and, as a result, rebound and overspray will tend to adhere and build up around the work area rather than blow free of it. Extra precautions must be taken by the workmen to prevent the accumulation of rebound and overspray on the prepared substrate surface and reinforcement. LMS placed over accumulations of rebound and overspray will result in inadequate bond, laminations, and sandpockets, and will produce a nondurable LMS material.

LMS should not be placed at ambient temperatures below the minimum temperature recommended by the manufacturer. At temperatures below the minimum film formation temperature (MFT), the polymer solids become rigid and resist being forced together to form a continuous film. At temperatures above the MFT, the polymers exhibit plastic behavior and thus will coalesce. The MFT will vary between latexes and is normally around 45°F.

Curing

LMS should initially be moist-cured for the first 24 hr by continuous sprinkling or covering with an absorptive mat that is kept continuously wet. After the initial curing period, LMS should be allowed to air cure.

It should be noted that curing applies to all layers, not just to the final surface of the LMS. If the LMS is applied in layers, each layer should be moist-cured for the first 24 hr or until the succeeding layer is placed, whichever is less.

REFERENCES

1. American Concrete Institute. Recommended Practice for Shotcreting. Standard ACI 506-66. Detroit, Mich., 1966.
2. American Concrete Institute. Polymers in Concrete. Standard ACI 548R-77. Detroit, Mich., 1977.

3. R.D. Eash and H.H. Shafer. In Transportation Research Record 542, TRB, National Research Council, Washington, D.C., 1975.
4. Portland Cement Association. Properties of Latex Modified Shotcrete. Construction Technology Laboratories, Skokie, Ill., 1978.
5. Bonneville Second Powerhouse. Report on Tests on Latex Modified Shotcrete and Conventional Shotcrete Panels. North Pacific Division Materials Laboratory, U.S. Army Corps of Engineers, Troutdale, Oreg., 1980.
6. Grand Rapids City--County Parking Garage. Concrete Repair Method Evaluation. Grand Rapids, Mich., 1980.
7. American Concrete Institute. Specifications for Materials, Proportioning and Application of Shotcrete. Standard ACI 506.2-77. Detroit, Mich., 1977.
8. Styrene-Butadiene Latex Modifiers for Bridge Deck Overlay Concrete. FHWA-RD-78-35. FHWA, U.S. Department of Transportation, 1978.

Applications of Permanent Precast Polymer Concrete Forms for Concrete Rehabilitation

DOUGLAS BARNABY and JAMES T. DIKEOU

ABSTRACT

Two case studies are presented of the use of precast polymer concrete stay-in-place forms for rehabilitation of transportation structures. The first study is on precast median barrier shells used by the Pennsylvania Turnpike Commission. The new barrier replaced an obsolete, deteriorated 4-ft-wide concrete island. The shells are 1-in.-thick and come in 20-ft-long sections. They are placed on the roadway, aligned, anchored with anchor bolts, then filled with conventional concrete through holes at the top of each section. The system is easily and rapidly installed, and provides a more impact-resistant and durable barrier than conventional concrete barriers. The second study is on precast bench panels that replaced deteriorated bench walls in Boston's Sumner Tunnel. Polymer concrete panels were selected because of their high strength and high modulus, good impact resistance, and their outstanding resistance to de-icing salts, chemicals, and freeze-thaw. The work, performed during the night, consisted of placing and anchoring panels, sealing off vent openings to prevent backfill concrete from coming out, then placing concrete behind the panels. In addition to improved performance properties, rapid construction time was a major benefit.

The continual use of salts to remove snow and ice and the adverse effects of freeze-thaw cycles and water penetration have combined to accelerate the deterioration of U.S. highways and bridges at an alarming rate. To overcome the deteriorating effects, use of polymer concretes have increased. The high strength-to-weight ratio of polymer concretes and their resistance to freeze-thaw cycles and road salts enable them to be used for rehabilitating and upgrading highway and transportation structures. Because polymer concrete formulations do not include water, the tiny capillaries that remain in conventional cement concrete after the curing water evaporates are not present. Therefore, the material is nonporous and provides a sealing and protective barrier from the elements.

The two case studies included in this report are descriptions of projects completed in the fall of 1983. In both cases, a special formulation of polymer concrete was chosen over other materials because of its ability to decrease life-cycle costs, prevent shear bond failures, and simplify the construction operation while solving particular engineering design requirements that other methods or materials could not accomplish economically.

POLYMER CONCRETE MEDIAN BARRIER--PENNSYLVANIA TURNPIKE

The Pennsylvania Turnpike Commission installed 4,900 linear ft of polymer concrete median barrier on the Susquehanna Bridge as part of a $2.4-million bridge rehabilitation program. The new nonporous and extremely durable material will be more impact-resistant and reflective than traditional precast or poured-in-place concrete barriers.

Located on the Pennsylvania Turnpike between exits 18 and 19, the continuous-span Susquehanna Bridge was built in 1953. Before the bridge rehabilitation, there was a 4-ft concrete island curb with guard rail on top that proved to be unsatisfactory. Figure 1 shows a schematic of the old concrete island. Turnpike engineers investigated precast and poured-in-place barriers but had problems with the precast type because of difficulties with the anchoring system as a result of the condition of the

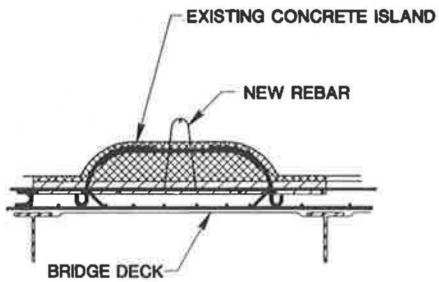

FIGURE 1 Schematic of the old concrete island.

existing concrete median. They were also concerned with environmental factors such as rain, snow, freeze-thaw cycles, and heavy traffic (about 20,000 vehicles per day). Conventional portland cement has a tendency to deteriorate under these conditions, darkening over time and becoming difficult to see on dark rainy nights.

The Commission selected 2-ft-wide x 20-ft-long polymer concrete median barrier shells that are filled on the site with a superplasticized concrete. The shells are placed over new or existing reinforcing steel and anchored to the roadway with 0.375-in.-diameter anchor bolts. Figures 2 and 3 show schematics of the barrier in place and the anchoring system. The barriers are four times stronger than conventional concrete and are impervious to water and freeze-thaw cycles and virtually all acids, salts, corrosive chemicals, and oils. Manufactured in sections for ease of transportation and installation, the barriers were also cast with a smooth white surface to enhance reflectivity. Electrical conduits may also be placed in the shell void, which eliminates the need for excavation or other special details to provide housing for the utilities.

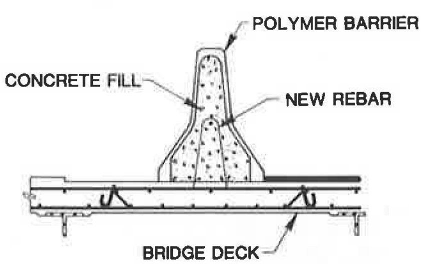

FIGURE 2 Schematic of new barrier in place.

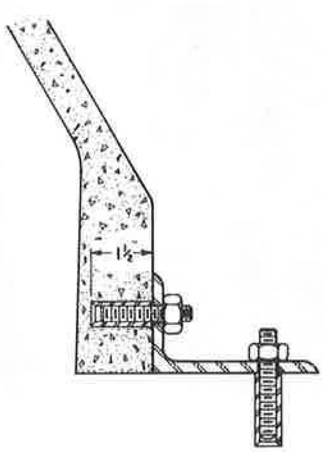

FIGURE 3 Anchoring system for new barrier shell.

Another advantage of the shell concept is its ability to encase existing out-dated medians that are to be upgraded to the new safety shape without the need to demolish the old barrier. The polymer concrete shell can be simply placed over the old barrier or wall and filled with concrete in the usual manner. This feature is especially desirable on those bridges where rehabilitation of the parapet is necessary. A half-shell section is placed alongside the deteriorated parapet wall, anchored in place, and then backed up with concrete (Figure 4). The half-shell prevents further deterioration from splashing salt-laden water and also improves the impact-safety aspect of the parapet. According to the contractor, the median barriers are much easier to install than cast-in-place concrete barriers and they are able to easily set over 500 ft per day with a smaller crew size than would normally be possible with conventional systems.

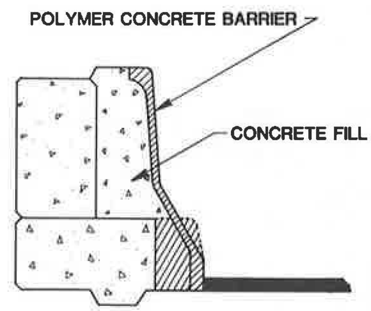

FIGURE 4 Schematic of half-shell used to protect parapet walls.

This was an important feature of the shell concept for the Pennsylvania Turnpike project because work could not begin until after the busy 4th of July weekend and had to be completed before the Labor Day weekend. The tight schedule would have been difficult to meet with conventional methods. Post-finishing operations such as patching were also eliminated.

Erection of the shells began as soon as the trailer load of 12 20-ft sections arrived. (The ability to transport a large number of sections per trailer load minimized the size of the staging area.) The shells were then unloaded by a three-man crew and placed in their approximate location--plus or minus a few inches. After the shells were unloaded, the same crew dropped back to align and anchor them to the roadway with anchor bolts set through clip angles at the base of the sections (Figure 3). After anchoring, they were ready to be filled with 3,000 psi concrete through-holes provided at the top of each section. Figures 5 and 6 show photographs of the erection process.

If unforseen conditions such as the presence of light poles and catch basins had occurred, which would have prevented installation of standard sections, the shells could have been cut with a conventional carborundum saw to suit the required size needed. To complete the operation, polymer concrete plugs were set into the pour-holes.

The $2.4-million contract, including upgrading of the bridge deck surface, began in July 1983. The polymer concrete median-barrier portion and one-half of the deck resurfacing was completed on schedule in early September 1983.

FIGURE 5 Pennsylvania Turnpike: Erection crew unloading polymer concrete shells prior to setting over reinforcing bars.

FIGURE 6 Pennsylvania Turnpike: Polymer concrete shells installed and awaiting placement of infill concrete. (Note the pour holes at the top of the barrier and the splice section to the right).

BOSTON'S SUMNER TUNNEL SIDEWALL PANEL REHABILITATION

Precast bench panels made of a polymer concrete were installed in Boston's Sumner Tunnel (Figure 7). The purpose of the $1.2 million tunnel rehabilitation project was to repair damage caused by years of automobile accidents and concrete deterioration. The engineers in charge of the project evaluated several design alternatives before deciding on polymer concrete panels.

This was the third sidewall rehabilitation project of this 50-year-old tunnel. When first built in 1934, the bench walls of the tunnel were made of concrete and then painted. In the early 1960s, the benches were covered with 4 x 4-in. ceramic tiles. However, the tiles became loose over a period of time because of traffic accidents and concrete and mortar deterioration or both. In 1970 the Authority responsible for the tunnel reconstructed approximately 40 percent of the bench walls with concrete panels and 4 x 4-in. ceramic tiles. The original ceramic tiles continued to deteriorate and fall off the remaining sections of the tunnel. In January 1982, the Authority decided to replace the 2-ft, 6-in. low bench side and the 3 ft, 2-in. high bench side with a more attractive impact-resistant sur-

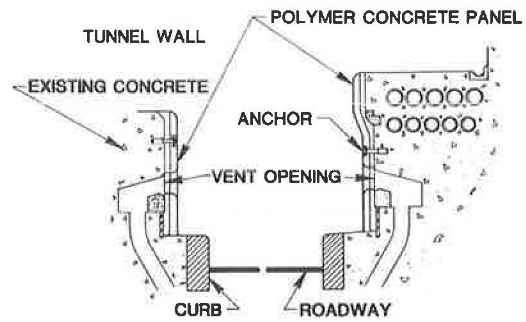

FIGURE 7 Schematic of precast panels in place at Sumner Tunnel.

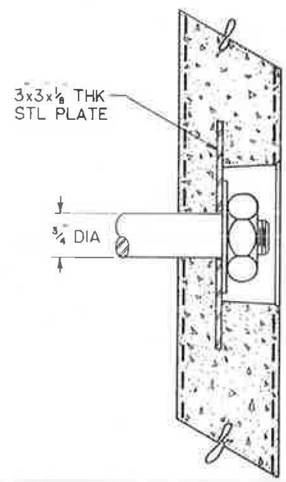

FIGURE 8 Anchoring system for panels.

FIGURE 9 Sumner Tunnel, Boston: Work crew places conventional portland cement concrete with a superplasticizer additive between the polymer panel and the existing sidewall concrete.

face. Because of space constraints, precast concrete was eliminated from consideration. Excessive amounts of existing concrete would have to be removed in order to install new precast barriers. Also, precast sections would have reduced roadway width, would have been too cumbersome to handle in an already tight workside, and would be difficult to modify to unforseen field conditions. Preformed galvanized steel was also rejected because of the concern about deterioration caused by the caustic atmospheric conditions in the tunnel.

Polymer concrete was selected because of a wide range of desirable performance characteristics: a compressive strength of 15,000 psi and a high modulus of elasticity. The panels are unaffected by water, salts, corrosive acids, and chemicals, and are washable. The 3-ft x 15-ft panels were reinforced with fiberglass for greater impact resistance and were manufactured with a precisely located vent opening to conform to existing air vents. The panels were manufactured with a smooth white surface to match the existing tunnel lining and to increase illumination.

Because both lanes of the tunnel must be operational during the day to handle the estimated 80,000 car-per-day volume, construction was begun at midnight and continued through 5:30 a.m. A crew of 12 men placed and anchored approximately 36 15-ft panels per shift. The erection operation on a given shift began by bringing into the tunnel a flatbed trailer with enough panels to be set that evening. The trailer was equipped with a boom device that lifted the panels off the trailer and set them into predrilled holes in the sidewalk to receive anchors that were cast into each panel. Figure 8 shows the anchoring system for the panels. An alignment crew followed up the unloading operation by anchoring the panels to the sidewall. Vent openings were sealed off to prevent backfill concrete from coming out. A modified concrete mix with a superplasticizer was then placed behind the panels (Figure 9). The vertical joints between the panels were sealed and the contractor plugged the anchor holes with a special plastic plug to create a smooth uniform surface. Figure 10 shows the completed bench wall repair. All work had to be completed before the morning rush hour.

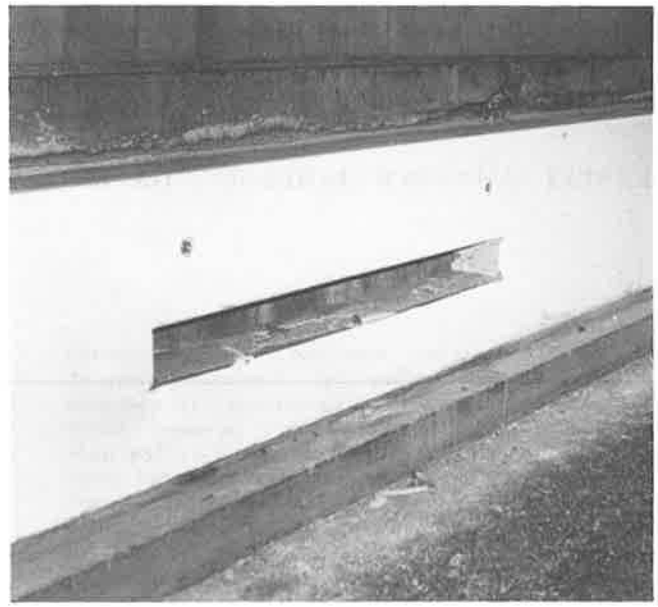

FIGURE 10 Sumner Tunnel, Boston: Completed bench wall repair showing contrast of old and new. Anchor holes were filled with a matching plastic plug to create a uniform smooth surface.

CONCLUSION

Polymer concrete is an advantageous material for use in solving many rehabilitation problems. The design concepts of these two projects combined the advantages of both polymer concrete and conventional portland cement concrete. The polymer concrete was used at the outside surface where deterioration occurs most and portland cement concrete was used as a backup or to give the section mass.

The process of determining how the desirable characteristics of the material can be applied to current engineering needs has made polymer concrete a viable material for solving highway and transportation problems.

Composite Concrete Pavements with Roller-Compacted Concrete

ERNEST SCHRADER, JAMES PAXTON, and V. RAMAKRISHNAN

ABSTRACT

Roller-compacted concrete (RCC) is being used to provide low-cost, low-cement-content mass concrete with marginal-quality unwashed aggregates. Tests show that pavement slabs with moderate flexural strengths can be made at these low cement factors and that high strengths should be attainable with much less cement than used in conventional concrete. Because of the low water content (no slump), shrinkage stresses in RCC pavements are to be decreased and the number of transverse contraction joints can be reduced. By topping the RCC with a thin monolithic layer of steel fiber-reinforced concrete (FRC), a durable, smooth surface with slightly improved static strength results. Tests also indicate that a fatigue life much better than conventional concrete develops, but the tests are limited. This improvement may be a result of better strength gain with maturity in the RCC or a result of the excellent fatigue properties of the fibrous concrete. By sandwiching the RCC between thin layers of FRC, an effective "structural" slab with good dimensional stability and low shrinkage can be made.

Roller-compacted concrete (RCC) has demonstrated tremendous savings in time, money, and resources when used in mass applications (1-3). It has potential for similar savings in large airfield and highway pavements, and has already been used effectively to provide pavements for log-handling facilities, port terminals, heavy-duty storage areas, and hardstands.

Recent tests indicate that RCC can be incorporated into composite paving and large slab construction with judicious use of a high-quality material such as fiber-reinforced concrete (FRC) to provide an efficient "sandwich" section. This combination can give economy, high fatigue endurance, a tough wearing surface within standard grade tolerances, minimal shrinkage and reduced jointing, reduced or eliminated corner and edge curling, and other advantages. It appears that a sizable project is necessary to realize the greatest potential in savings, and the benefits may be reduced for pavements that must be put into service soon after placement.

ROLLER-COMPACTED CONCRETE (RCC)

In simple terms, RCC can be considered as an upgraded cement-treated base (CTB) or a cement-treated base for which the engineering and material properties have been determined and are being used to advantage. After placing and curing, RCC is a concrete that can have strength properties similar to those of conventionally placed more expensive pavement mixes.

Although there are no set limits, RCC has generally been made with cement factors ranging from less than 100 to more than 500 lb of cement per yd^3 (2 to 13 percent by weight) and with maximum size aggregates ranging from 0.75 to 9 in. Fly ash or other pozzolans can be used as a substitute for a portion of the cement in RCC or as a mineral filler. Both cement factors and compressive strengths of RCC mixes have a wide range of values, but strengths can easily be the same as for conventional concrete while typically using less cement (Figures 1 and 2).

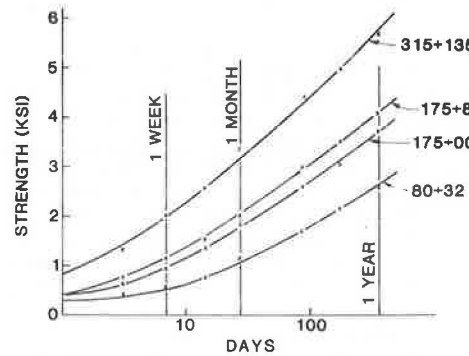

FIGURE 1 Fatigue test results.

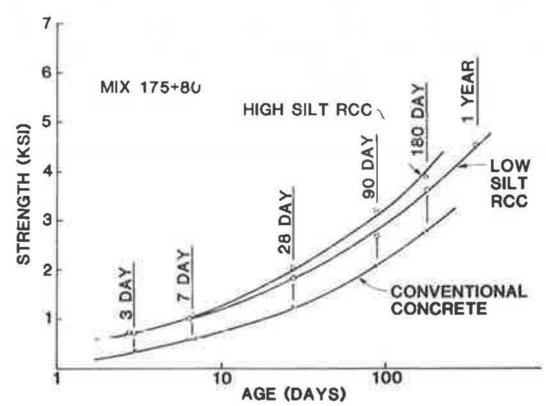

FIGURE 2 Curl results.

Figure 3 shows a general band for gradations that most airfield and highway base and top courses fall into. Also shown on the same figure are the gradings of two RCC mixes. It is apparent that RCC can be made with most highway base materials. Higher strength, better density, and more efficient use of cement is probable if the aggregate contains a normally unacceptable amount of nonplastic fines. In most cases, this should consist of 4 to 11 percent of the total aggregate weight. It can be advantageous to not spend time and money washing the aggregates and maintaining a clean gradation. Additionally, it may be possible to use large aggregate material instead of the relatively small maximum

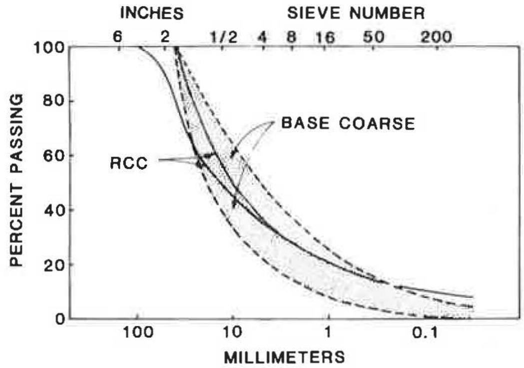

FIGURE 3 Compressive strength versus time for various RCC mixes.

aggregate sizes generally used in conventionally placed pavement concretes and base materials.

Figure 2 shows the effect of making concrete with an RCC aggregate having a typical base course gradation but with a top size of 3 in. and without removing the silt. As long as the silt and clay-size particles are relatively nonplastic, they are generally beneficial. Also shown on the same figure is the strength gain with time when the concrete is made to normal high-quality standards using conventional concrete practices; that is, aggregate manufactured to a closely controlled ideal grading, fines removed, low slump but wet-mix consistency, chemical admixtures used, and so forth. The surprising result is that this extra effort and expense resulted in significantly less strength. It also required a higher water content which, in turn, develops more shrinkage.

A major advantage in pavements of RCC's no-slump consistency is the reduced water content. Along with low cement factors, the reduced water causes theoretical drying shrinkage to be significantly less than for conventional concrete with a measured slump. An indication of what can be expected for drying shrinkage with mixes that might be used in pavements is shown in Figure 4. The figure also shows a range of strain capacities that can be expected in concrete before cracking. The lower shrinkage of RCC is obvious from this figure. In paving applications, this can directly translate into greater joint-spacing. Fewer joints and less movement in turn means lower construction costs, reduced maintenance costs, and probably less internal stress due to shrinkage.

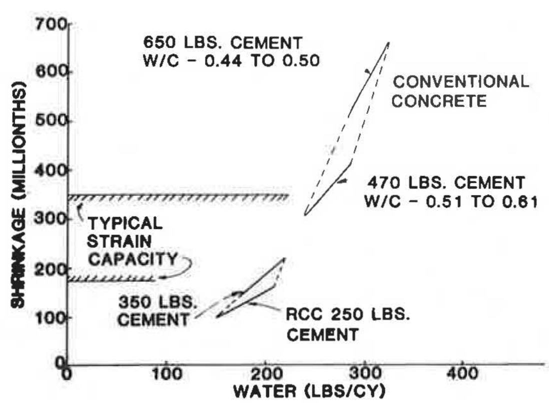

FIGURE 4 Comparison of RCC and conventional concrete strengths.

Depending on cement factor, the water-to-cement ratio (w/c) for RCC can vary considerably. When cement factors are very low, high w/c values on the order of 1.0 to 2.0 can result; yet, these mixes can have minimal shrinkage and good strengths. Conversely, because little water is used in RCC, higher cement factor mixes can have low w/c values in the range of 0.3 to 0.5.

Experience has shown that visual observation in the field can easily control and properly maintain the moisture content at a level that is just low enough to prevent the roller from sinking or pumping the mix. This is essentially the optimum moisture regardless of the resulting theoretical w/c, and it provides enough water for compaction and hydration without causing internal pore pressure during compaction because of excess water. It is important to recognize that Abram's Law (which is the basis for the long-standing emphasis on decreasing the w/c to improve quality and strength) is applicable to slumpable mixes of workable consistency--RCC is not slumpable. From a variability standpoint, theoreticians must also recognize that with low cement factor mixes, w/c ratios may vary by 0.10 throughout a workday just from changes in ambient conditions. The desire for close control of w/c ratios, which is appropriate for slumpable conventional mixes, should be greatly relaxed or ignored in properly designed lean RCC mixes.

Flexural strengths of RCC can be surprisingly high and consistent for its relatively low cement factors and no-slump consistency. Data also suggest that the long-term strengths can increase substantially. Typical flexural strengths for large beams are given in Table 1 for some RCC mixes.

TABLE 1 Flexural Strength of RCC

Identification	Maximum Aggregate (in.)	Cement (lb/yd^3)	Fly Ash (lb/yd^3)	Age (days)	Strength (psi)
Z-100	3	100	0	90	155
Z-100	3	100	0	7	55
Z-200	3	200	0	90	275
Z-200	3	200	0	7	165
E-94F	3	94	38	90	150
W-80F	3	80	32	90	200
W-175	3	175	0	90	330
W-175F	3	175	80	90	340
W-315	3	315	135	90	500

Complementing the flexural strength of RCC is its relatively high creep rate and typically low modulus of elasticity. High static flexural strengths achieved in conventional concrete by using high cement factors can result in pavements with higher internal stresses due to both drying shrinkage and thermal cooling associated with dissipation of heat from hydration. These mixes typically also have low creep rates and a high modulus of elasticity, leading to a more brittle material with little ability to relieve internally developed stresses. Designers often are unaware that although beam strengths from unrestrained test specimens are high, the actual usable strength available in a restrained pavement to carry externally applied loads may be hundreds of psi less when subtracting out the internal stresses. With RCC, the lower modulus and higher creep rate minimize development of internal stresses that already have lower potential because of the reduced water and cement contents. Typical modulus and creep data are shown in Figure 5 for RCC and conventional concretes.

Unfortunately, RCC by itself has drawbacks if used as a paving material. These are uncertain long-

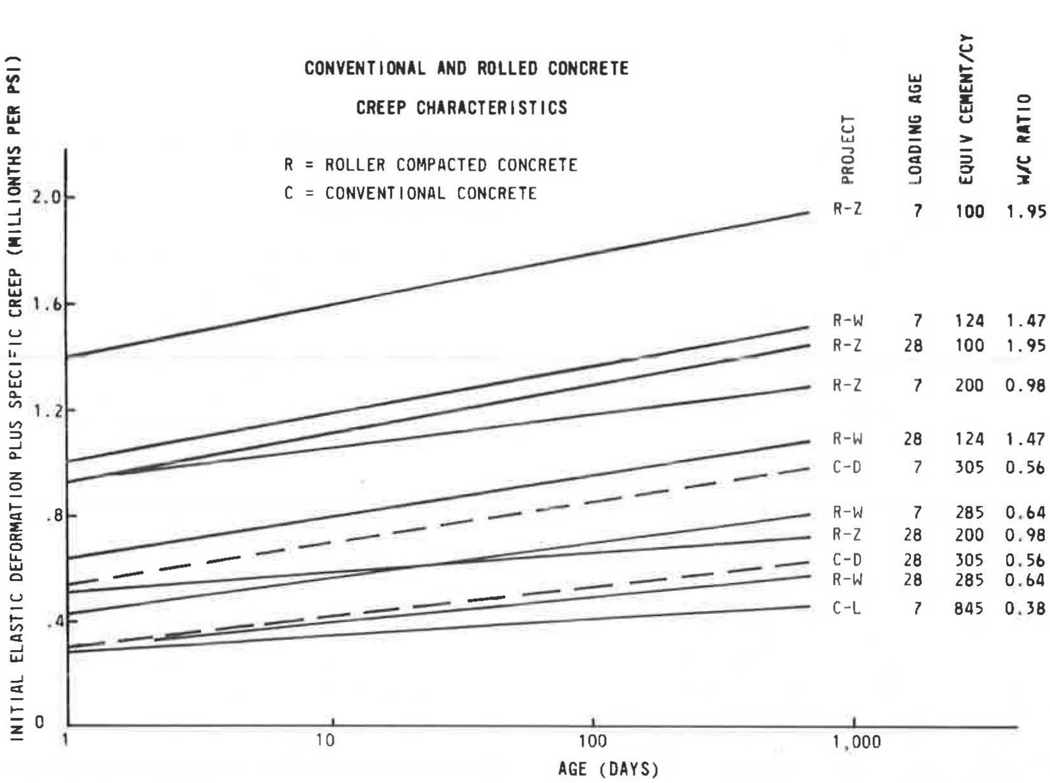

FIGURE 5 RCC and base course gradations.

term freeze-thaw durability and control of surface tolerances during high production placement. These concerns have not restricted the use of RCC for heavy-duty pavement facilities and applications such as haul roads and handling lots at port facilities or log handling yards. These concerns have, however, prevented applications of RCC to airfield pavements and highways.

Spreading and rolling equipment as well as the consistency of the mix need close attention if a flat surface is to be achieved. Without the use of a spreader box or paving machine such as is used in asphalt construction, gradual undulations of the surface of about 0.1 ft per 10 ft can be expected. With laser-controlled blades on spreading equipment, quite accurate control can be achieved before rolling, but even then, roller marks and dips where the roller reverses can be expected.

Durability of RCC in freeze-thaw environments can correctly be described as anything from excellent to terrible, depending on which data are used. When subjected to rapid freeze-thaw conditions while saturated (such as in the ASTM C666 test), RCC deteriorates rapidly. Also, when large blocks of RCC containing 200 lb of cement per yd^3 were subjected to alternating freezing and thawing concurrent with wetting and drying in a salt water tidal zone, they disintegrated.

On the other hand, RCC tested in environments simulating freezing and thawing from typical frost action and intermittent rain (surface damp but not thoroughly saturated conditions) with subfreezing internal temperatures to depths of 0.25 and 1 in., showed that it could withstand 1,000 cycles of freezing and thawing with only minimal loss to less than 1 in. deep. Also, large slabs of RCC left exposed for years in the natural environment near Portland, Oregon, have shown excellent performance. The slabs have rough irregular horizontal surfaces that puddle water. The area gets many cycles of freezing and thawing, but few hard and continuous freezing periods. The slabs show no apparent change from their condition when first placed outside. Even more notable is the excellent performance of hundreds of thousands of square yards of unprotected RCC pavements used in various log handling and shipping terminal facilities around the area of Vancouver, British Columbia, Canada. Most of these pavements have been in service for about 1 to 5 yr.

RCC pavements can be given the close surface tolerances and the durability desired by topping them with a thin layer of conventional concrete placed with conventional equipment. The idea is similar to the concept used for toppings of bridge decks or "super flat" industrial floors. The practicality of doing this on a large scale for miles of pavement has been investigated. Concrete paving equipment to accomplish this is used in highway or airfield construction and is currently available with only minor modifications. On a smaller scale, a demonstration project conducted without paving machines has shown excellent results for more confined and specialized flooring applications.

A variety of topping materials could be used ranging from latex-modified concrete, to dense concrete (Iowa system), to fiber-reinforced concrete. The topping mix needs to have minimal shrinkage and good bond as well as "finishability" and durability. It should also closely approximate most of the hardened physical properties of the RCC.

Bond can be achieved relatively easily for several reasons. The RCC surface will not be smooth, but will have a substantial roughness when examined closely. Also, because there should be little or no excess free moisture in the RCC mix, bleeding and the resulting problem of laitance at the surface is generally nonexistent or insignificant. Consequently, expensive and time-consuming surface-cleaning and abrading is not necessary. In most cases, the topping mix is expected to consist of a thin (1 to 2 in.) layer of relatively high-strength high-cement factor concrete with corresponding high paste and mortar. This combination lends itself automatically to good bond.

Because the RCC has minimal shrinkage and the topping will be bonded to it, a similar low value of shrinkage should be designed into the surface mixture. This can be accomplished with high-range water reducers, latex modifiers, no-slump dense mixes, or vacuum dewatering.

FIBER-REINFORCED CONCRETE

Fiber-reinforced concrete (FRC) is ideally suited for pavement because of its high static flexural strengths and, more important, because of its improved fatigue performance. Unfortunately, it is expensive unless a reduction in design thickness is achieved, and it may develop other concerns in thin pavement sections.

There are hundreds of publications concerning FRC, but perhaps the best overview is the American Concrete Institute's state-of-the-art report (4). Airfield pavement thicknesses of about 5 to 10 in. are achievable with FRC as compared to about 8 to 20 in. for conventional concrete.

When taking into account the static strength and rate of strength gain for paving concrete and then subtracting the loss of strength for service conditions (fatigue and less than ideal cure), the usable working stress can be plotted (5). Figure 6 shows the results of this type of analysis for an actual airfield paving project that compared conventional concrete to fibrous concrete. The graph clearly shows that under the fatigue of service conditions, conventional concrete continually loses load-carrying capacity with time whereas fibrous concrete improves with time after a slight initial reduction at the start of its service life. The FRC is simply gaining strength with maturity faster than it is losing it because of fatigue.

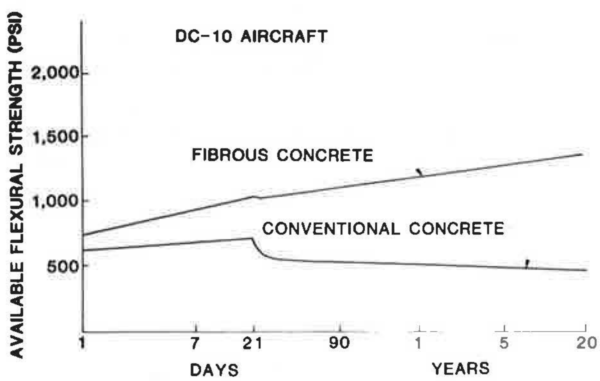

FIGURE 6 Shrinkage and strain capacity for RCC and conventional concrete.

However, this example does not take into account curl and shrinkage stresses due to drying and dissipation of internal heat. These should be included in the analysis for both fiber and conventional concrete. Without special provisions such as high-range water reducers or cooled mixes, the fiber material typically uses high water and cement contents and will have higher internal shrinkage stresses. Depending on thickness, it may or may not have higher adiabatic thermal stresses than the thicker but lower cement factor conventional mix.

Because of the thinner pavement sections achieved with FRC, corner curling and related stresses are of more concern than with deeper conventional pavements (6). This can limit the benefits of FRC when used by itself in a full pavement thickness.

From an engineering standpoint, FRC has improved fatigue endurance, higher flexural and tensile strength, greater strain capacity and crack resistance, high toughness and energy absorbing properties, and extraordinary resistance to damage by impact. With proper entrained air and mix proportioning, it has excellent resistance to freeze-thaw and wet-dry damage.

In pavement applications, steel fibers are typically used, but because they are discrete and nonconnected elements, they have not shown the internal corrosion problems of conventionally reinforced concrete in salted environments.

From a practical standpoint, conventional equipment can be used to mix and place FRC in thick or thin pavements and slab sections. The typical close surface tolerance controls desired in highway, industrial floor, and airfield pavements can be achieved.

FRC mixes normally have fairly high cement factors and higher sand contents, and often use smaller maximum size aggregates. These characteristics make them well-suited for latex modifiers, high-range water reducers, and placement in thin sections.

RCC PAVEMENTS WITH FRC

When used in combination, FRC and RCC complement each other and can provide a remarkable paving material. FRC is an ideal topping for RCC slabs and can also be used with them to create a "sandwich panel" pavement.

A series of tests was conducted to establish whether the RCC and FRC could be placed with compatibly; to determine the hardened physical properties

FATIGUE TEST RESULTS

BEAM		CEMENT + ASH (LBS/CY)	% STATIC STRENGTH* (UPPER TO LOWER LOAD)	CYCLES TO FAILURE
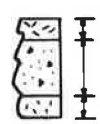	2"	585+249		
	9"	315+135	10% - 80%	455,700
	2"	585+249		
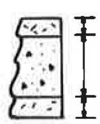	2"	902+0		
	9"	175+0	92% - 100%	100
	2"	902+0		
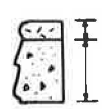	2"	585+249		
	9"	315+135	10% - 80%	1,076,820
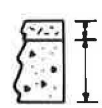	2"	902+0		
	9"	175+0	10% - 80%	615,170

* BASED ON 28 DAY STRENGTH. ACTUAL AGE AT THE TIME OF FAILURE FOR EACH TEST WAS GREATER. STORAGE AFTER 28 DAYS WAS COOL AND DRY CONDITIONS.

FIGURE 7 Conventional and roller-compacted concrete creep characteristics.

of deep pavement sections made with the FRC as a topping and with RCC sandwiched between FRC layers; and to obtain an indication of what the long-term performance of the composite material might be in service. The dimensions of the sections and the cement factors used for the RCC and FRC mixes are shown in Figures 7-10. The beams were a nominal 4 ft long and were obtained by sawing them out of slabs made with different design sections, as shown in Figures 11-13.

Aggregates and mix designs for the RCC were identical to those used in more than 400,000 yd³ of

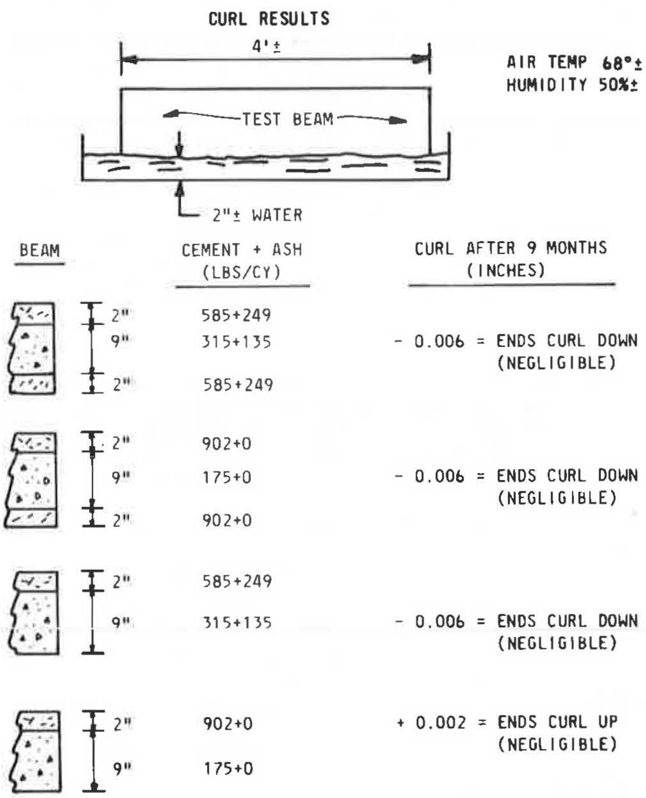

FIGURE 8 Usable design stresses in an airfield pavement.

RCC placement on the Willow Creek Project (1). Although that work was for a dam, the contractor was an experienced road builder, and the method of mixing, placing, spreading, and compacting used paving procedures. In essence, the dam consists of 12-in. pavement slabs stacked on top of each other. A dual-drum low-profile pavement plant mixed the material, scrapers and bottom dumps hauled it, a bulldozer spread it, and a vibratory roller compacted it. The in-place cost of the RCC was approximately \$19 to \$20 per yd³.

The RCC aggregate quality, grading, and production are discussed by Schrader (1) and Schrader and McKinnon (3). The aggregate basically consisted of 70 percent basalt from a quarry; the basalt was crushed simultaneously with the silty sandy gravel overburden composing the other 30 percent of the aggregate. The RCC mixes used both 3-in. maximum size aggregate (mix 175+0) and 1.5-in. maximum size aggregate (mix 315+135). There was no washing of the aggregate. It would not have met normal road base criteria and would not have begun to approach normal conventional concrete aggregate specifications. Typically, the total aggregate contained about 8 percent material passing the No. 200 sieve. When separated into two piles on the 0.75-in. sieve, approximately 17 percent of the 0.75 minus product passed the No. 200 sieve.

The FRC aggregate was manufactured by processing and washing of the RCC aggregate so that it had a maximum size of 0.5 in. and a typical conventional concrete gradation. It is generally prudent to use the same basic aggregate source or similar materials for both the FRC and RCC so that thermal and elastic similarity is achieved.

From a materials standpoint, the test slabs and beams were designed by:

1. Using the previously established RCC mixes and their required water content for compaction by vibratory rolling;
2. Assuming that a w/c of 0.26 provided adequate water to hydrate the cement;
3. Determining the quantity of water added to the RCC that was above the amount necessary for cement hydration;
4. Establishing topping mix proportions (in this case, fiber-reinforced concrete) using enough water to hydrate the cement at a w/c of 0.26 and provide

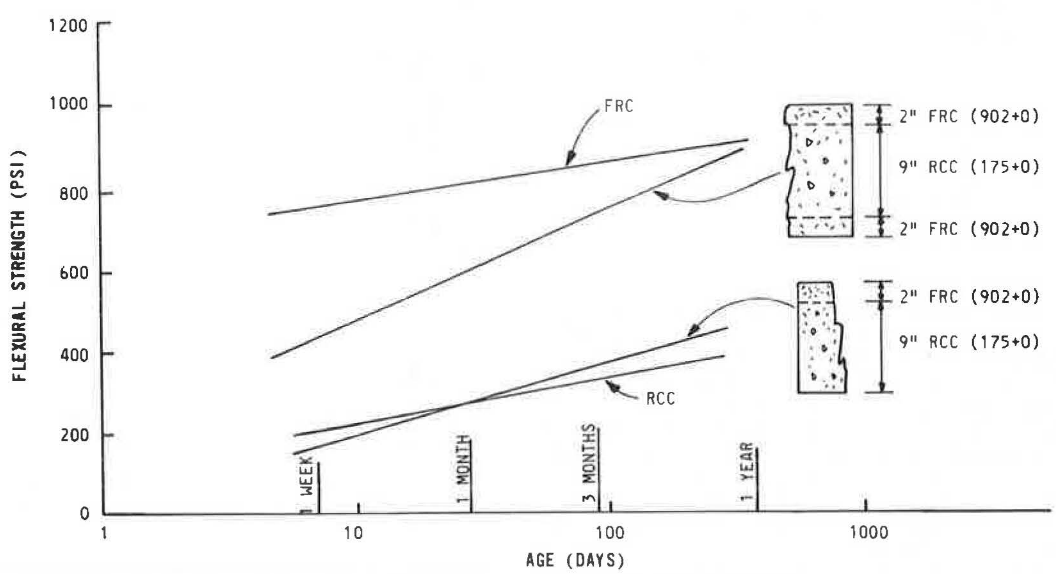

FIGURE 9 Static flexural strengths of RCC-FRC composite pavement (no fly ash).

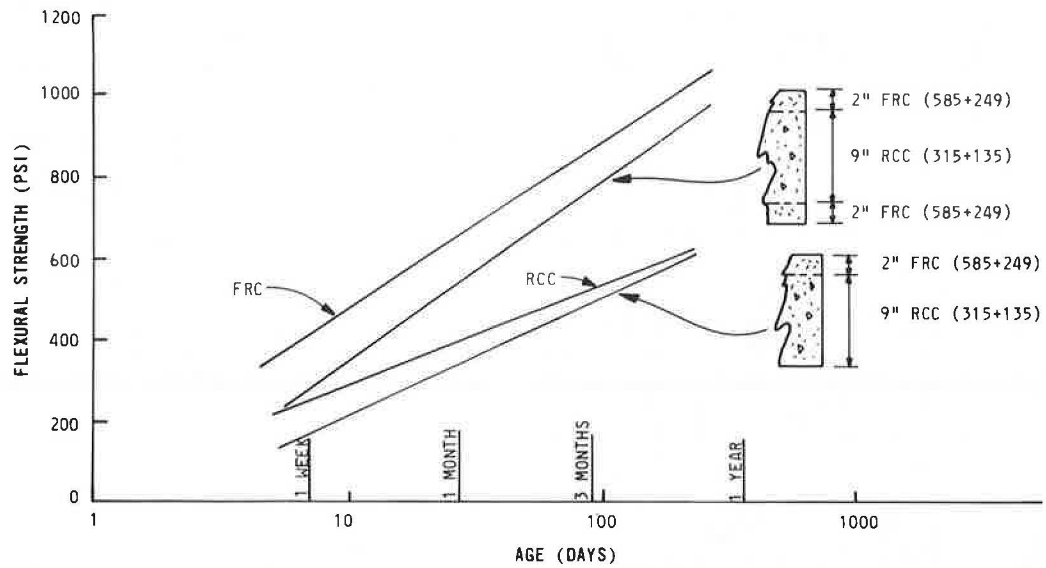

FIGURE 10 Static flexural strengths of RCC-FRC composite pavement (fly ash).

FIGURE 11 RCC topped with FRC (close up view).

the same amount of total excess water per cubic yard as found for the RCC mix; and

5. Using a high-range water reducer and air entraining additive to provide approximately 5 percent entrained air and a workable topping mix with a slump that allowed it to be placed with conventional equipment.

The slabs were constructed in a manner that simulated an anticipated practical large-scale construction schedule for the system. A vibratory roller compacted the RCC and the FRC was placed with a vibrating screed. The RCC had been compacted for about 4 hr when the top lift of FRC was placed. No cleaning, bonding, or special treatment was performed except for keeping the lift surface damp as would be

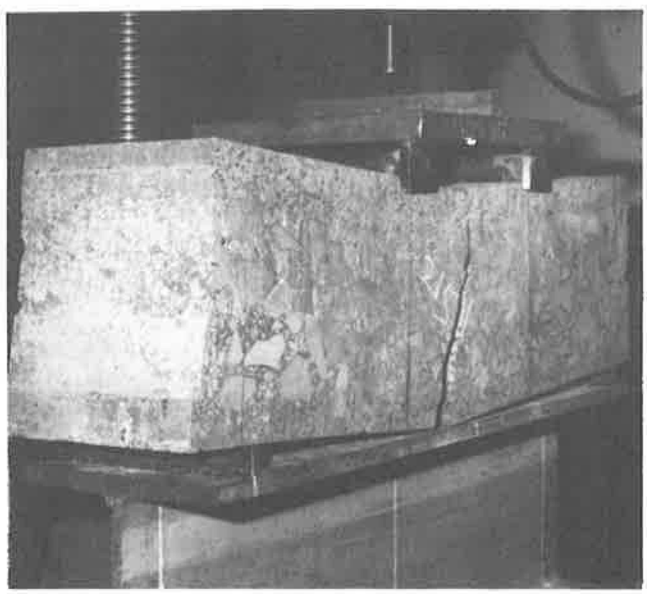

FIGURE 12 RCC topped with FRC (long view).

accomplished with a standard water truck during construction. In practice, the FRC could be placed immediately after rolling the RCC or probably as late as 6 hr, depending on temperature.

The sandwich panel section with top and bottom lifts of FRC requires an additional pass of the vibrating screed to place it. Paving equipment already exists that has demonstrated excellent ability to place thin FRC sections in a production situation. Because of the high-range, water-reducing admixture, a suitable initial slump with a desired rapid rate of slump loss can easily be achieved. The interlocking effect of the fibers and the rapid slump loss (without affecting the final set time) allows dumping and spreading of the FRC over the RCC during a practical working time from about 0.5-5.5 hr after placing. This time can be adjusted with the admixture chemistry.

The sequence and timing for the different concrete mixes dictates a moving series of two or three paving operations. The same mix plant could make

FIGURE 13 RCC sandwiched between FRC.

both the RCC and FRC mixes, although in anticipated high production application, two separate plants may be necessary just to provide the material quantities. Discussions with equipment manufacturers indicate that modifications to existing paving equipment to combine the operations into an efficient single pass system handling both mixes is feasible.

A major part of the test program was concerned with potential delamination of the two mixes. This never occurred nor was it possible to force a delamination. The pavement section acted as a composite monolithic mass. Testing included flexural bending to ultimate failure, fatigue testing at a high range of loading, and long-term curl tests with the bottom of the slabs maintained in ponded water while the top dried.

Figures 5 and 6 show results of static flexure tests for the different composite paving sections and for the individual mixes. Simply topping to RCC with FRC logically did little or nothing to improve flexural strengths. However, when bending is in the opposite direction (not tested), such as would occur at the cantilevered edges and corners of pavements, a major increase in load-carrying capacity similar to that shown for the sandwich panel section could be expected. The sandwich panels showed a marked improvement in static flexural strength--almost to the point of achieving as much strength at later ages as could be expected if the expensive FRC were placed to the full depth. In reality, if it were placed in a very deep section, high internal thermal stresses due to the high cement factor may have made the usable strength of an all-FRC pavement less than that of the sandwich section.

The fatigue results shown in Figure 7 are limited, but they point toward very good fatigue endurance properties beyond those of conventional concrete pavements. Additional testing to better define the improvement and to identify whether it is the result of the FRC or if RCC by itself has good fatigue endurance should be pursued.

The curl test results shown in Figure 8 indicate no movement of any significance. The measured curl was less than 0.007 in. over a span of 4 ft in all cases and probably was within the accuracy of the test. For comparison, it is not unusual to have conventional pavement slabs curl 0.125 to 0.250 in. Occasionally, curl as much as 0.500 to 0.750 in. has been recorded. It should be noted that these values are for spans 3 to 10 times as great as those tested and involve temperature changes as well as moisture differences. The deep section and low cement factors of FRC/RCC pavements of similar spans should provide the stiffness and material properties that result in negligible field curl even at the greater spans.

CONCLUSIONS

RCC can provide an economical and rapidly placed pavement. The drawbacks to its use in airfield and highway applications can be overcome by judicious use of an integral high-strength specialized concrete such as FRC. Aggregate materials typically used for base support under a pavement can be made to less stringent requirements, mixed with a relatively small amount of cement, and used to produce a structural RCC section. A very efficient sandwich panel pavement can also be constructed with RCC and FRC, but it appears that its practicality is limited to heavy-duty pavements, large projects, and jobs having inherently poor subgrade support that would otherwise require a deep section or expensive upgrading of the subgrade.

ACKNOWLEDGMENTS

The U.S. Army Corps of Engineers' North Pacific Division Laboratory facilities were used for fabrication and most of the testing. Fatigue testing was performed at the South Dakota School of Mines and Technology. Funds for careful transportation and testing of the fatigue beams were provided by the Bekaert Steel Wire Corporation.

REFERENCES

1. E.K. Schrader. World's First All-Rollcrete Dam. Civil Engineering, American Society of Civil Engineers, April 1982, pp. 45-48.
2. E.K. Schrader. Roller Compacted Concrete. The Military Engineer, Society of American Military Engineers, Vol. 69, No. 451, Sept.-Oct. 1977, pp. 314-317.
3. E.K. Schrader and R. McKinnon. Construction and Initial Operation of Willow Creek Dam. Concrete International Design and Construction, American Concrete Institute, Detroit, Mich., June 1984.
4. American Concrete Institute. State-of-the-Art Report on Fiber Reinforced Concrete. Concrete International Design and Construction, Detroit, Mich., May 1982, pp. 9-30.
5. E.K. Schrader. Design Methods for Pavements with Special Concretes. Proc., 1982 International Symposium on Fiber-Reinforced Concrete, American Concrete Institute, Detroit, Mich., 1983.
6. E.K. Schrader and D.R. Lankard. Inspection and Analysis of Curl in Steel Fiber Reinforced Concrete Airfield Pavements. Bekaert Steel Wire Corporation, Irving, Tex., April 1983.